Syracuse University

SURFACE

Dissertations - ALL SURFACE

December 2015

AN EXPERIMENTAL STUDY ON THERMAL STABILITY OF FAEE BIODIESEL FUEL WITH ETHANOL

Yujie Shen
Syracuse University

Follow this and additional works at: https://surface.syr.edu/etd

 Part of the Engineering Commons

Recommended Citation

Shen, Yujie, "AN EXPERIMENTAL STUDY ON THERMAL STABILITY OF FAEE BIODIESEL FUEL WITH ETHANOL" (2015). *Dissertations - ALL*. 371.
https://surface.syr.edu/etd/371

This Thesis is brought to you for free and open access by the SURFACE at SURFACE. It has been accepted for inclusion in Dissertations - ALL by an authorized administrator of SURFACE. For more information, please contact surface@syr.edu.

ABSTRACT

Biodiesel fuel is usually synthesized from vegetable oil and animal fat, and now it has been widely used in tractors, trucks, buses and ships. Unlike traditional fossil fuels, biodiesel is more environment-friendly and it is renewable, which can help people solve the energy crisis to some extent (Huang, Chen, Wei, Zhang, & Chen, 2010).

Nowadays, supercritical esterification has become a novel way to produce biodiesel, but high temperature may cause the decomposition of biodiesel. Researchers mainly focus on studying the properties of fatty acid methyl ester (FAME), however, fatty acid ethyl ester (FAEE) biodiesel has only been slightly explored. So in this study, ethanol was used to synthesize biodiesel instead of methanol. Also, the thermal decomposition of FAEE biodiesel with excess ethanol was also studied.

In the synthesis studies of FAEE biodiesel, the conditions evaluated were: molar ratio of ethanol to oil of 9:1, potassium hydroxide is chosen as the catalyst, and the reaction is kept at 75˚C (±1˚C) and 1 atm for 2 hours. In order to study the decomposition of biodiesel, the thermal decomposition experiments were performed in stainless steel coils at the temperature from 250˚C to 425˚C for residence time from 3 to 63 minutes. When ethanol was added, the volume ratio of ethanol to biodiesel was 1:1. All the products were analyzed by GC-FID and GC-MS.

There are mainly three kinds of reactions observed in the thermal decomposition of biodiesel: isomerization, polymerization and pyrolysis. They occurred at the following temperature range respectively: ≥ 275 ˚C, ≥ 300 ˚C and ≥ 350 ˚C. When the temperature is below 275 ˚C, the decomposition ratio is less than 5%, which suggests that FAEE biodiesel is stable

below 275 ˚C. It is also found that at a given temperature, longer residence time results in higher decomposition ratio.

A first-order reversible reaction model was proposed to represent the thermal decomposition of FAEE biodiesel, this model fits the experimental data very well from 250 ˚C to 400 ˚C. At 425 ˚C, the first-order irreversible reaction model is better, which suggests that the main reaction is pyrolysis at 425 ˚C. The reaction rate constants were calculated using these two models.

Kinetic analysis was also conducted. The Arrhenius equation and van't Hoff equation were used to define the kinetic parameters. For the forward reaction, the pre-exponential factor (A) is 2.54×10^9 min^{-1} and the activation energy (E_a) is 128.2 kJ/mol. For the reverse reaction, A is 7.98 min^{-1} and E_a is 29.6 kJ/mol. For the entire reaction, the standard enthalpy (ΔH^0) is 98.6 kJ/mol. In fitting the data, the high coefficient of determination of higher than 0.97 was obtained, which supports the hypothesis that the first-order reversible reaction model was reasonable over the range of conditions studied.

AN EXPERIMENTAL STUDY ON THERMAL STABILITY OF FAEE BIODIESEL FUEL WITH ETHANOL

by

Yujie Shen

THESIS

Submitted in partial fulfillment of the requirements for the degree of Master of Science in Chemical Engineering in the Graduate School of Syracuse University

December 2015

Copyright ©2015

Yujie Shen

All Rights Reserved

ACKNOWLEDGEMENTS

I wish to express my sincere thanks to my advisor, Prof. Lawrence L. Tavlarides, for his continuous support of my study and research, for his patience, enthusiasm, and immense knowledge. Whenever I have a problem, he is willing to help me. He will be my role model in my future study and work.

I am grateful to all the faculty members in the Department of Biomedical and Chemical Engineering for giving me excellent courses and help. I also want to take this opportunity to thank my labmates: Mr. Jiuxu Liu and Mr. Yue Nan for their help through all my work. They taught me how to use the equipment and they gave me valuable advice.

I would like to thank Prof. Jesse Bond for allowing me to use the GC-MSD in his laboratory, without his help, I cannot analyze the biodiesel samples. Special thanks are also given to Prof. Philip A. Rice, he gives me many valuable suggestions.

I am highly indebted to Professors Benjamin Akih-Kumgeh, Dacheng Ren and Jesse Bond for serving on my defense committee and thank them for their valuable time and comments.

Finally, my sincere thanks go to my parents and my friends for they not only gave me financial support but also mental support during my two years studying abroad.

TABLE OF CONTENTS

LIST OF FIGURES

LIST OF TABLES

Chapter 1: Introduction

Biodiesel refers to the fatty acid monoalkyl esters which are synthesized through the transesterification reaction of vegetable oils or animal fats with alcohol. The main fatty acid groups in biodiesel is palmitic acid (C16:0), stearic acid (C18:0), oleic acid (C18:1), linoleic acid (C18:2) and linolenic acid (C18:3). Biodiesel also has few shorter or longer chain fatty acid groups, like lauric acid (C12:0), myristic acid (C14:0), gondoic acid (C20:1), and many others (Hoekman, Broch, Robbins, Ceniceros, & Natarajan, 2012).

Biodiesel can be produced from various kinds of feedstock, such as soybean oil, sunflower oil, rapeseed oil and even waste cooking oil (Zhang, 2003). Alcohol can also be changed using methanol, ethanol or 1-butanol (Demirbaş, 2003). When compared with diesel, biodiesel has the following advantages: (1) Biodiesel has less sulfur and aromatic alkanes than diesel, it produces less harmful gases to the environment after combustion, so it is more eco-friendly; (2) Biodiesel is a renewable source of energy. Unlike petroleum and coal, biodiesel will not be exhausted, which can help people to solve the energy crisis; (3) The typical flash point of biodiesel is 93˚C, it is about 25˚C higher than the flash point of traditional biodiesel, so biodiesel is much safer in usage, storage and transportation (Bajpai & Tyagi, 2006). However, biodiesel also has some disadvantages: (1) Biodiesel has a lower cold filter plugging point (Bozbas, 2008), so it will freeze easily in cold weather; (2) Biodiesel fuel is less stable, it will degrade if stored for a long time period (Bozbas, 2008); (3) Biodiesel has a higher cost than diesel, and it is only competitive when tax is not included (Carraretto, 2004).

Besides the advantages and disadvantages mentioned above, biodiesel has similar density, viscosity and combustion heating value with diesel (Miao & Wu, 2006), so it is always used directly or blended with diesel in the diesel engine. Up to now, people mainly use and study the FAME (fatty acid methyl ester) biodiesel, FAEE (fatty acid ethyl ester) biodiesel is seldom mentioned, probably because it costs more to produce FAEE than FAME. However, when compared with FAME, FAEE has higher heating value, higher cetane number and lower pour point (Sun et al., 2014). So with the same amount of biodiesel, FAEE biodiesel can provide more energy. The higher cetane number indicates that FAEE biodiesel emits less undesirable exhaust gases to the environment due to the shorter ignition delay (Ladommatos, Parsi, & Knowles, 1996). And the lower pour point makes FAEE biodiesel more suitable to be used under low temperature. In addition, the raw material methanol is very toxic to humans, it may cause permanent blindness.

According to the above issues mentioned, in this study, ethanol is used to synthesize biodiesel instead of methanol. People usually use the following four ways to produce biodiesel: direct use and blending, thermal cracking (pyrolysis), transesterification (alcoholysis) and microemulsions (Ma & Hanna, 1999), among which transesterification is the most widely used method recently. Depending on the reaction conditions, different catalysts can be used in the transesterification reaction, for example, acid catalysts, alkali catalysts and enzymes (Fukuda, Kondo, & Noda, 2001). When catalysts are used, reactions can occur under lower temperature and reaction time can be also decreased. However, after the reaction, it requires additional processing to remove the remaining catalysts from the final products.

Recently, the novel method supercritical transesterification was developed, in which there is no catalyst needed. Under supercritical condition, oil and alcohol can be mixed more efficiently. The reaction only takes several minutes under very high temperature and pressure (>240˚C and >80bar), which are above the critical points of alcohol. Because there is no catalyst used, the purification process can be much simpler and more eco-friendly (Saka & Kusdiana, 2001). But it also has its own shortages, it needs more energy to provide such high temperature and pressure and the equipment must be strong enough to satisfy the reaction condition.

Nan's work shows that the yield of biodiesel in supercritical ethanol is not very high, which is only 87.8% under 340˚C and 170 bar (Nan, Liu, Lin, & Tavlarides, 2015), it may be due to the thermal decomposition under high temperature, so in this study, the catalytic esterification is chosen to produce the FAEE biodiesel. In order to get a higher yield and better quality biodiesel from the supercritical esterification reaction, people have researched the thermal stability of FAME biodiesel for a long time, however, the research on FAEE biodiesel is still inadequate. Therefore, the thermal stability of FAEE biodiesel is studied here, which could help people to find an optimal condition to produce FAEE biodiesel under supercritical conditions and also to produce more stable FAEE biodiesel.

The effect of excess ethanol on the thermal decomposition of FAEE biodiesel is also investigated in this study, due to the observation that decomposition of biodiesel decreases with the increasing molar ratio of ethanol to oil (Bertoldi et al., 2009). Also, Olivares-Carrillo's work (Olivares-Carrillo & Quesada-Medina, 2012) shows that when raising the molar ratio of methanol to oil, methanol can protect the decomposition of polyunsaturated methyl esters. However, these phenomena are only mentioned in their work, and there is no deeper study on it.

So the importance of this work is to understand the mechanism and kinetics of the ethanol effect on the decomposition of FAEE biodiesel. With the mechanism and kinetic model, the decomposition of FAEE biodiesel under high temperature can be better understood, and a better method can be found to protect the decomposition of biodiesel, thus more stable and reliable biodiesel fuel can be produced to meet the requirements of the market.

In this work, the reaction conditions in the synthesis of FAEE biodiesel employed potassium hydroxide as the catalyst and the reaction was conducted at 75 ℃ for 2 hours using vegetable oil and ethanol as the feed stock. The reaction is repeated (at the same conditions) to get a higher yield. The thermal decomposition of biodiesel was performed in stainless steel coils in a fluidized temperature sand bath at the temperatures ranging from 250˚C to 425˚C for residence times from 3 to 63 minutes. The volume ratio of ethanol to biodiesel is 1:1. All the final products were analyzed by the GC-FID. Based on the decomposition ratio of biodiesel, the mechanism and kinetic model can be constructed to explain the ethanol effect on the thermal decomposition of FAEE biodiesel.

Chapter 2: Literature Review

2.1 The production of biodiesel

Biodiesel is regarded as a renewable and eco-friendly fuel, it is now widely used in vehicles and machines. People started to use biodiesel as fuel since 1980, at that time, people just directly used the vegetable oil or blended it with diesel in the diesel engine; there was no pretreatment for the vegetable oil (Ma & Hanna, 1999). The engines worked very well for a short time period. But if the time is longer than 10 hours, due to the disadvantages of vegetable oil (high viscosity, low vapor pressure and the reactive unsaturated hydrocarbon), problems started to appear. These included (1) carbon deposits; (2) oil control rings sticking; (3) lubricating oil thickening and gelling; (4) fuel injectors plugging and other problems (Pryde, 1983). Despite these problems, people started to pay attention to this new kind of energy, and this has developed very fast in recent decades.

In order to solve the problems caused by the high viscosity of vegetable oil, the method of microemulsions formation was discovered later. The spray characteristics of vegetable oil can be improved, because of the explosive vaporization of the low boiling point components in the micelles (Pryde, 1984). Qi, et al. (Qi, Chen, Matthews, & Bian, 2010) used a microemulsion of ethanol–biodiesel–water in a diesel engine. After testing under different engine loads, the microemulsion improved the combustion efficiency, so it had less energy consumption. And when compared with biodiesel, it had higher hydrocarbon and carbon monoxide emissions, lower NO_x emissions, and huge reduction of smoke emissions. In the work of Dantas Neto et al. (Dantas Neto, Fernandes, Barros Neto, Castro Dantas, & Moura, 2014), a diesel/biodiesel

microemulsion was used in a diesel engine, and NP5EO (nonylphenol ethoxylate with five oxyethylene units) was used as surfactant. Compared with pure diesel, there was a reduction in CO, NO_x and smoke emissions, but the unburned hydrocarbon was increased because of the decreasing of gas temperature in the cylinder.

Thermal cracking (pyrolysis) of vegetable oil and animal fats is another way to synthesize biodiesel, and it has been studied for a long time. In 1947, Chinese scientists used the thermal cracking of tung oil to produce motor fuels (Chang & Wan, 1947), the yield of gasoline content in the crude oil is 20% by volume. Cinara M.R. Prado's work (Prado & Antoniosi Filho, 2009) shows that after the thermal cracking of soy bean oil, the biodiesel mainly consists of C_6-C_{30} compounds and a small fraction of C_4-C_{14} compounds, which has similar properties with the petroleum derivatives. In Yan Luo et al.'s work, the canola oil based feedstock leads to a higher yield than the soybean oil based feedstock (Luo et al., 2010). However, the temperature is very high in thermal cracking, the decomposition of biodiesel is inevitable, therefore the yield is still not desirable.

The most commonly used method to produce biodiesel is transesterification, also known as alcoholysis. The main reaction in transesterification is shown in Fig. 1. Catalysts can be used to lower the reaction conditions and increase the reaction rate. There are many choices of catalyst, such as acid catalysts, alkali catalysts, enzyme and so on. The research shows that the alkali-catalyzed transesterification is much faster than using the acid catalysts (Canakci & Van Gerpen, 1999). The quality and yield of final products can be influenced by the following factors: molar ratio of oil to alcohol, reaction temperature and time, initial amount of free fatty acid and amount of catalysts (Marchetti & Errazu, 2008). After the transesterification reaction, purification of

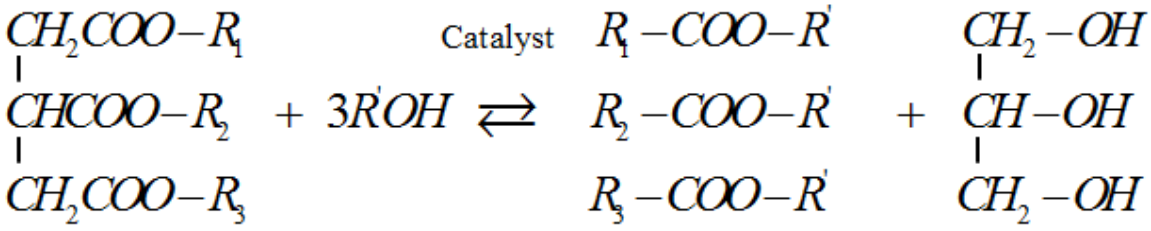

Fig. 1 The main reaction in transesterification.

produced biodiesel is also a problem, because the use of alkali catalysts may cause saponification, soap needs to be eliminated, as well as the remaining catalysts (Predojević, 2008). In order to simplify the purification process, homogeneous catalysts are used in the biodiesel production (Bournay, Casanave, Delfort, Hillion, & Chodorge, 2005). Their results showed that the yield of methyl esters were above 95% and the high purity of glycerin was also obtained.

Recently, a catalyst-free transesterification, supercritical transesterification is being developed. The reaction temperature and pressure are higher than the critical point of alcohols, it is usually over 240˚C and 80 bar, and the reaction time is much shorter, which is less than 10 minutes. In Liu's work (Liu, Lin, Nan, & Tavlarides, 2015), it shows that when the reaction condition is 300-400 ˚C , 200 bar, reaction time is 0.5-10 min and methanol to oil molar ratio is 9:1, all the feedstock is in a homogeneous state, and the mass transfer rate is so fast that it increases the conversion rate. The process is also simpler than the catalytic transesterification, only unreacted alcohols have to be removed after reaction. Demirbas's work (Demirbas, 2002) shows that the biodiesel fuel from six different kinds of vegetable oil all have good quality, the viscosity is only slightly higher than the No. 2 Diesel fuel. He et al. (He, Wang, & Zhu, 2007) pointed out that the yield can be improved by increasing the molar ratio of methanol to oil, reaction pressure and temperature, however, if these parameters exceed a certain value, the yield will decrease, due to some side reactions of unsaturated fatty acid methyl esters.

2.2 Thermal stability of biodiesel

Recently, supercritical transesterification process has been widely used to produce biodiesel, however, the temperature and pressure are very high, which may result in the degradation of biodiesel, and the yield is not very high. Therefore, the thermal stability of

biodiesel should be studied, which is helpful to find an optimal condition for biodiesel production.

Imahara et al. (Imahara, Minami, Hari, & Saka, 2008) studied the thermal stability of biodiesel in the presence of supercritical methanol. Four kinds of FAMEs (C18:0, C18:1, C18:2, C18:3) were used to represent the biodiesel, because they are the main constituents in biodiesel. Temperature was raised from 270 ˚C to 380 ˚C and pressure was between 17 MPa and 56 MPa. It was found that monounsaturated fatty acids are more stable than the polyunsaturated ones, and with higher degree of unsaturation, decomposition is more likely to happen. In the thermal decomposition, polyunsaturated fatty acids were partly isomerized into trans-type polyunsaturated fatty acids. However, all the FAMEs are very stable when the temperature is under 300 ˚C. Also there was no obvious change on the cold flow properties (cloud point and pour point) of biodiesel after thermal stressing.

Shin et al. (Shin, Lim, Bae, & Oh, 2011) conducted further studies on the thermal stability of FAME biodiesel. Their result shows that biodiesel is stable at the temperature of 325 ˚C, and it starts to decompose at 330 ˚C. Methyl linoleate (18:2) and methyl linolenate (18:3) will degrade dramatically when the temperature is over 350 ˚C. It is also found that the thermal decomposition of biodiesel mainly involves three kinds of reactions: isomerization, hydrogenation and pyrolysis. By analyzing the recovered methyl esters, they discovered that shorter chain or more saturated FAME has higher thermal stability in the supercritical methanol. They also suggested the supercritical transesterification should occur at less than 325 ˚C (23 MPa) and 20 min, so that a high yield biodiesel can be produced.

In the fuel and lubricant industries, there are three more methods to measure the thermal stability of biodiesel: Rancimat method, ASTM method and TGA/DTA method (Jain & Sharma, 2011). (1) The Rancimat method is carried out at 110 ˚C for at least 6 hours. During the test, the conductivity of biodiesel is recorded, so plots of conductivity versus time can be drawn. From the plots, the induction period can be obtained, which is the period of sudden increase of conductivity. Then plots of induction period versus temperature can be also drawn, if it is a straight line, it indicates that biodiesel is stable over that temperature range. The Rancimat method has become a significant method to test the thermal stability of biodiesel. (2) In the ASTM method, biodiesel is heated at 150 ˚C for 90 to 180 min in the presence of air. After cooling, the product is filtered using a filter paper with pores of 11 μm, so that the insoluble components can be weighed, and it provides a more intuitive way to observe the thermal decomposition of biodiesel. (3) The TGA method, also known as thermogravimetric analysis, can also be used to study the thermal stability of biodiesel. It is very accurate and sensitive using only a small amount of sample. Using this method, activation energy and reaction order can be calculated, so that the thermal stability of biodiesel under certain temperature can be estimated. However, the relationship among these three methods is still not discovered, more work needs to be done in the future.

2.3 Mechanism in the thermal decomposition of biodiesel

Since thermal decomposition of biodiesel is inevitable in the supercritical transesterification process, the mechanism of the thermal decomposition of biodiesel has been studied to show what happens in the thermal decomposition. By knowing the mechanism, the

thermal decomposition of biodiesel can be reduced and the yield can be increased. Researches on this topic will be reviewed in the following text.

Quesada-Medina and Olivares-Carrillo first showed the evidence of the thermal decomposition of biodiesel under supercritical conditions (Quesada-Medina & Olivares-Carrillo, 2011). After comparing the GC chromatograms of all the final products, an unexpected peak was found, and the peak was higher, when the temperature and residence time increased. They indicated that it might be the thermal decomposition of biodiesel, and the peak was the decomposition products. Another method, mass balance, was also used to examine the thermal decomposition of biodiesel. The total weight of reactants and products were calculated, and it was found that at high temperature the weight of reactants was higher than the weight of products, which demonstrated that some side reactions happened. These two methods both proved the thermal decomposition of biodiesel under supercritical conditions.

Lin et al. (Lin, Zhu, & Tavlarides, 2013) studied the thermal decomposition of FAME biodiesel at 250-425 ˚C, a six-lump model was proposed to explain the mechanism in thermal decomposition. When the temperature is below 275 ˚C, biodiesel is stable. During the decomposition of biodiesel, there are three main reactions: isomerization, polymerization and pyrolysis, and they occur at the following temperature ranges: 275 - 400 ˚C, 300 - 425 ˚C and >350 ˚C, respectively. It is found that saturated FAME is much more stable than the unsaturated FAME, C16:0 does not decompose until 375 ˚C. In the isomerization reaction, two types of reactions will happen: cis-type isomerization and trans-type isomerization. When temperature is higher, polymerization reactions will happen, which is also known as Diels–Alder reaction, two unsaturated chains can react to form a longer chain, so dimers and polymers are

produced. Pyrolysis reactions will occur when the temperature is higher than 350 ˚C, it can produce small molecular FAMEs, hydrocarbons and gases. Besides the above reactions, hydrogenation and dehydrogenation reactions may be also involved.

Biodiesel viscosity and cold flow properties after thermal decomposition have also been studied (Lin, Zhu, & Tavlarides, 2014). Biodiesel viscosity increased first and then reduced with the increasing temperature, because dimers and polymers produced in polymerization reactions increased the biodiesel viscosity; small molecular weight components produced in pyrolysis reduced the viscosity. The isomerization reactions also increased the viscosity, but it could be negligible when compared to the effect of polymerization reactions. Thermal stressing also affected the crystallization temperature of biodiesel, it had the similar change as viscosity, the crystallization temperature increased first and then decreased. When there was only 20% decomposition of biodiesel, the effect on the crystallization temperature can be neglected. The reason of increasing was not mentioned, but it was found that the small molecular weight components formed in pyrolysis could lower the crystallization temperature.

The pyrolysis reaction in the thermal decomposition was comprehensively studied by Huynh and Violi (Huynh & Violi, 2008). In their study, methyl butanoate was used to represent the common biodiesel, because they both have the similar ester chemical structures. During the pyrolysis reaction, many reactive radicals will form, and they will react with methyl butanoate, it is also called hydrogen abstraction reaction. The reaction between H• and methyl butanoate is the main reaction to breakdown biodiesel. The pyrolysis reactions produce many small molecule compounds and gases. It is also found that CO produced in pyrolysis mostly comes from the breakdown of $C(O)OCH_3$.

In summary, the thermal decomposition of biodiesel involves many different kinds of reactions, and mechanisms only shows the conceptual contents in the thermal decomposition. In order to obtain the reaction rate, activation energy and other parameters, the kinetics in the thermal decomposition of biodiesel should be analyzed.

2.4 Kinetic models for thermal decomposition of biodiesel

As previously mentioned, the thermal decomposition of biodiesel is very complicated. There are many reactions (isomerization, polymerization, pyrolysis etc.) in the thermal stressing of biodiesel, these reactions are not independent, they will affect each other. Moreover, biodiesel contains numerous kinds of compounds, and a large amount of products will be produced in different reactions, so it is impossible to study the reactions one by one. A simplified model should be built and some proper assumptions should be made to analyze the kinetics in the degradation of biodiesel.

Lin et al. (Lin et al., 2013) built a simplified model to study the kinetics in the thermal decomposition of biodiesel. They simplified all the reactions to the following one:

$$A \underset{k_2}{\overset{k_1}{\rightleftharpoons}} P$$

where A is biodiesel, P is all the decomposition products, k_1 and k_2 are the reaction rate constants. The concentration of P can be obtained using the GC-FID.

Due to the complexity of thermal decomposition and limitation of equipment, it is very difficult to obtain the concentrations of all the products, so they assumed that this reaction is a first-order reversible reaction, and this model is a simple one to represent that biodiesel is

thermally decomposed into other compounds. Reaction rate constants k_1 and k_2 can be calculated using the following differential equation:

$$-\frac{dC_A}{dt} = k_1 C_A - k_2 C_p \quad (1)$$

Then a fitting line can be drawn using software, and it was found that the line fitted the experimental data very well. The researchers also used a first-order irreversible model and they repeated the above steps, and results showed that it did not quite fit the experimental data. Therefore, they concluded that the thermal decomposition of biodiesel can be well represented by a one-step first-order reversible reaction. Furthermore, they calculated the pre-exponential factor, activation energy and enthalpy of the reaction using the Arrhenius equation and the van't Hoff equation:

$$k = Ae^{-E_a/(RT)} \quad (2)$$

$$\ln K = -\frac{\Delta H^0}{RT} + \frac{\Delta S^0}{R} \quad (3)$$

These parameters can be used to calculate decomposition rate at different temperatures and they also can be employed for a quantitative analysis of thermal decomposition of biodiesel.

Though this model is very simple and shows much information in the thermal stressing, it has its own disadvantages (Widegren & Bruno, 2008). These authors studied the thermal decomposition of jet fuel using a similar model. They suggested that the reaction rate constants, activation energy and enthalpy mentioned above are not only affected by reaction temperature, but they are also influenced by the materials of reactors, so if different kinds of materials are

used as the reactors, different value of those parameters may be obtained. Because different materials have their own surface properties, this will change any surface-catalyzed decomposition and can also change decomposition rate constants. In order to understand its effect on the reaction, the thermal decomposition was carried out in several reactors with varying ages. It was found that errors in the data were not very large, therefore these data can be accepted and the effect of material is not very great.

In this study, a similar kinetic model will be used to analyze the kinetics in thermal decomposition of biodiesel. Using GC-FID and first-order reaction model, some typical parameters can be obtained.

Chapter 3: Experiments

3.1 Materials

In this work, fatty acid ethyl ester (FAEE) biodiesel fuel is mainly studied, because FAEE biodiesel fuel is seldom explored and it has better performance in some aspects than fatty acid methyl ester (FAME) biodiesel fuel. However, only few companies in North America provide FAEE biodiesel and it is very expensive, so FAEE biodiesel is first synthesized in this laboratory.

In the biodiesel production process, vegetable oil was chosen as the feedstock. The vegetable oil was purchased from Walong Marketing, Inc. Its main ingredient is soybean oil and it has 10% saturated fat. The density of this vegetable oil is 0.904 g/cm^3. Ethanol was another feedstock and it was also used to be mixed with biodiesel in the thermal stressing experiment. Ethanol was provided by Decon Laboratories, Inc. It is named as ethanol 200 proof and it is 100% pure (undenatured) ethanol.

Glycerol (≥99.5%) was purchased from Sigma-Aldrich, Inc. It was used to separate biodiesel from the final products. Ethyl esters are insoluble in glycerol, but unreacted glycerides, glycerin, excess ethanol, base catalysts and the soaps produced in the reaction are all soluble in the glycerol (Encinar, Gonzalez, Rodriguez, & Tejedor, 2002). Therefore, glycerol is an ideal chemical in the purification of biodiesel.

Heptane (≥99.5%) was supplied by Fisher Scientific, Inc. It was used to clear reactors after reaction and it was also used as solvent in the GC-FID analysis. Because heptane is highly volatile, it can be easily removed by heating, and it will not affect the subsequent reactions.

Another reason for heptane use is that there are no more solvent peaks after 2 min on the GC chromatograms, so it will not interfere with other peaks.

In the GC-FID analysis, 4 types of gases were used. They are ultra high purity Helium (carrier gas), ultra high purity Nitrogen (makeup gas), ultra zero air and ultra high purity Hydrogen (flame gases). They are all purchased from Airgas, Inc.

Standard samples were not needed to calibrate chromatograms since previous results were employed (Lin et al., 2013).

3.2 Experimental setup

There are three main components in this study: (1) Biodiesel production process in which FAEE biodiesel can be produced; (2) Biodiesel thermal stressing experiments where biodiesel can be heated to desired temperature; (3) GC-FID experiments can be used to analyze the composition of biodiesel after thermal decomposition. These three components will be explained in the following text.

In the production of biodiesel, a 1000 mL volumetric flask was used as the reactor, because it has a small mouth which can be easily sealed to prevent the evaporation of ethanol during the reaction. A magnetic stirrer from Fisher Scientific, Inc. was also used in the reaction to stir and heat the reactants. This stirrer contributes energy of mixing and assists to raise the temperature up to 540 ˚C during heating and its speed can be up to 1200 rpm, which meets the needs of the experiment.

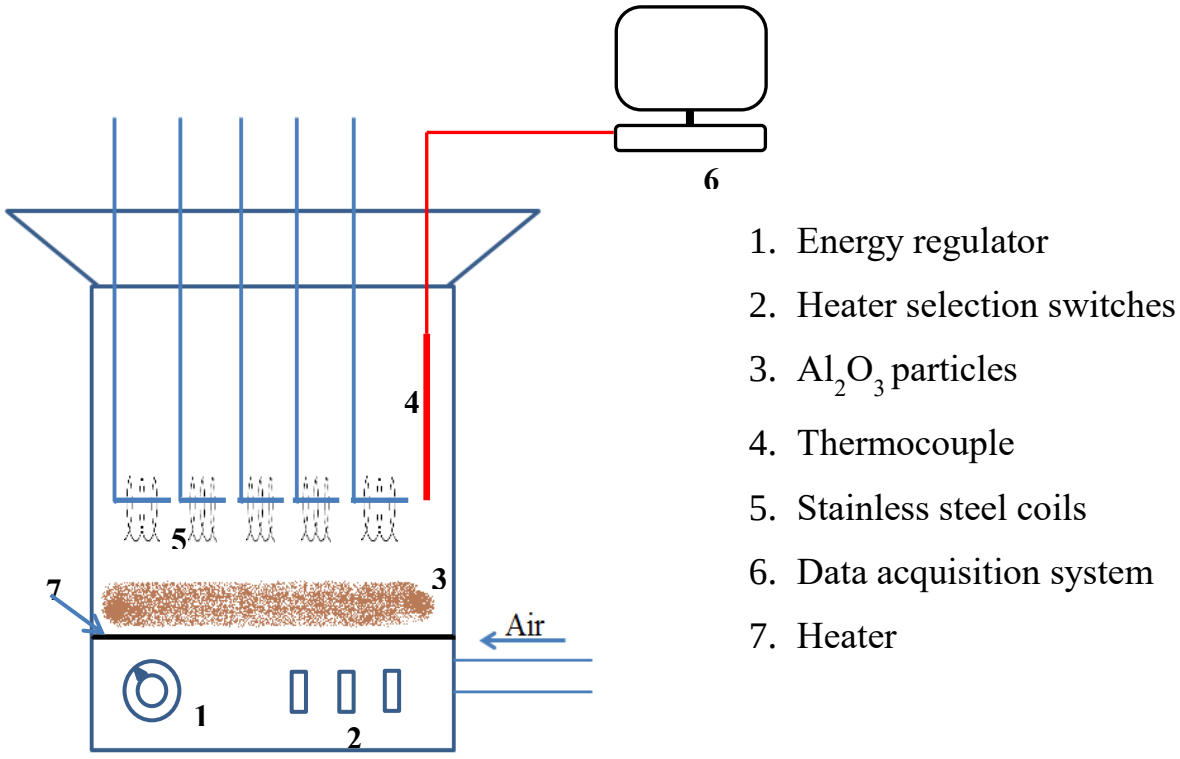

Fig. 2 A schematic diagram of the Fluidized Temperature Sand Bath.

Fig. 3 A photograph of the stainless steel coil with hex-head caps.

In the thermal stressing experiments, a Fluidized Temperature Sand Bath (Techne SBL-2) was used as the heating source. Its schematic diagram is shown in Fig. 2. This fluidized sand bath has 3 heater selection switches: low, medium and high, which represent 1kW, 2kW and 3kW heating power, respectively. It also has an energy regulator from 0 to 10, which can control the heating power more precisely. The real-time temperature was measured by a thermocouple connected to the data acquisition system, the temperature curve showed the trend of temperature, so heating power can be adjusted to maintain the temperature at a certain value. The temperature can be raised up to 600 ˚C, and the fluctuation is less than 3˚C.

The "sand" used here was the Al_2O_3 particles. When compared with traditional oil bath, the sand bath is much easier to clean after reaction, a brush is enough to remove Al_2O_3 particles on the reactor. The sand bath was also connected to low pressure dry and clean air. Air entered the sand bath through a porous plate (diffuser) which ensured the direction of air flow and also supported the sand. At proper air flow rate, the Al_2O_3 particles appeared at a "boiling" state, which indicated that these particles were fluidized. In this situation, heat transfer was very fast and uniform, therefore all the reactors could be kept at the same temperature.

The thermal stressing experiments were carried out in several stainless steel coils (Fig. 3), the length was 200 mm and the internal diameter was 1.524 mm. Biodiesel was injected in these steel coils using syringes and hex head caps were used to seal up the reactors. During the experiments, sand bath was heated to a certain temperature first, and then the reactors were immersed into the sand bath for different time periods. The thermocouple was put at the same horizontal level with these steel coils, so it could detect the temperature of reactors accurately.

In analyzing the samples, a gas chromatograph with a flame ionization detector (GC-FID) was used to measure the concentration of organic components in biodiesel and its decomposition products. The GC-FID used here was the Hewlett Packard 5890 Series II. It was equipped with a Restek Biodiesel TG column, it was designed to analyze biodiesel. The column was 10 m long, the I.D. was 0.32 mm and the film thickness was 0.10 μm. The GC-FID was connected to a data acquisition system, so the data can be collected and analyzed. The gases used here were helium, nitrogen, hydrogen and air, they were carrier gas, makeup gas and flame gases, respectively.

3.3 Experimental details

3.3.1 The production of biodiesel

In order to produce FAEE biodiesel, vegetable oil and ethanol were chosen as the feedstock, three different kinds of catalysts: NaOH (sodium hydroxide), KOH (potassium hydroxide) and H_2SO_4 (sulfuric acid) were selected to see which one had the best performance. When different catalysts were used, the reaction condition was also different, especially the reaction time, it was only 2 hours for base catalysts, but it took 24 hours for acid catalysts, because the base-catalyzed reaction is much faster than the acid-catalyzed reaction (Lotero et al., 2005). The reaction conditions are shown in Table 1. All the reaction conditions are the optimized conditions for biodiesel production for these catalysts (Leung & Guo, 2006; Marchetti & Errazu, 2008). The concentration of catalyst was based on the weight of vegetable oil.

Though different kinds of catalysts were used, the experimental procedure was almost the same. First, 300 mL vegetable oil was measured into a volumetric flask, and the flask was put on a stirrer to be preheated to the reaction temperature. Then, proper amount of ethanol and

Table 1 Reaction conditions for different catalysts

Catalyst	Reaction Temperature/ ˚C	Reaction Time/h	Molar Ratio (Ethanol to Oil)	Catalyst wt% (Based on Oil)
NaOH	75	2	9:1	1
KOH	75	2	9:1	1.5
H_2SO_4	65	24	6:1	2.2

catalysts were measured according to the reaction condition. Ethanol and catalysts should be added into the oil simultaneously, and in order to simplify the process, catalysts could be dissolved in the ethanol first. After that, the flask was sealed using a plastic paraffin film and the heater was adjusted to maintain the reaction temperature. After the reaction and products cooled down, 25% glycerin by volume (based on the volume of vegetable oil) was added into the flask and the mixture was settled overnight. The products separated into two layers, the upper layer was ethyl esters and the bottom layer contained ethanol, catalyst, unreacted reactants, soap and glycerin.

In order to get a nearly 100% yield, which means there are essentially only long chain ethyl esters in biodiesel, the upper layer was taken out and treated as vegetable oil, and all the above steps were repeated again, including adding the glycerin. But this time, the molar ratio of ethanol to oil was reduced to 5:1, the weight percent of catalyst was kept the same. Then the upper layer was washed by water to remove the remaining catalyst and ethanol. Finally, the final product was put into an oven and heated for 12 hours at 60 ˚C to remove water and ethanol. When the products became clear and transparent, GC-MSD was used to test the samples. The result (Fig. 6) shows that main components are all long chain esters, so it indicates that the final products are 100% biodiesel. Then the biodiesel can be used to do the following experiments.

3.3.2 Thermal stressing experiments

First, in order to simulate condition in supercritical transesterification, the sample was prepared by blending biodiesel and ethanol at the volume ratio of 1:1, which is 17:1 in molar ratio (ethanol to biodiesel), this molar ratio is close to the molar ratio used in supercritical

Table 2 Settings for Fluidized Sand Bath at some temperature

Temperature/ ˚C	Heater Switches	Energy Regulator Setting
200	Low	5~6
250	Low	8~9
300	Medium	2~3
400	Medium	7~8
500	High	2~3

Table 3 Reaction conditions of thermal stressing experiments

T, ˚C	250	275	300	325	350	375	400	425
Residence time								
3	×	×	×	×	×	×	×	×
5							×	×
8	×	×	×	×	×	×	×	×
10							×	×
13						×	×	×
18	×	×	×	×	×	×		
23					×	×		
33	×	×	×	×	×			
63	×	×	×	×				

× -- Experiment was conducted under this reaction condition

transesterification (Cao, Han, & Zhang, 2005). All the samples were prepared before the thermal stressing experiments to minimize the volatilization of ethanol. Five stainless steel coils were used as the reactors, they were all washed by heptane to remove the decomposition products in them, because heptane is a good solvent and it has a high volatility, it can be easily removed by heating. The mouth of steel coils was very small, so a syringe was needed to inject the samples into the coil and a pipette was used to get samples out of the coil reactor. The volume of the coil was only 0.9 mL. After injecting the samples, hex head caps were used to seal up the reactors.

Before the steel coils were put into the sand bath, the sand bath was heated slightly higher than the desired temperature, so when five reactors were put into the sand bath, the temperature would drop to the desired temperature. Table 2 shows the settings for sand bath at various temperatures. During the thermal decomposition experiments, the energy regulator should be adjusted frequently to maintain the temperature at a desired value.

The critical temperature of ethanol is 241 ℃ (Gude & Teja, 1995), so in the supercritical transesterification process, the temperature is always higher than that. However, the temperature cannot be too high, the decomposition of biodiesel will decrease the yield. The supercritical transesterification experiments are usually conducted at 250-425 ˚C (Anitescu, Deshpande, & Tavlarides, 2008). Therefore, in this study, in order to study the thermal decomposition of biodiesel, the temperature was also selected from 250 ˚C to 425 ˚C; every 25 ˚C there was a data point, including 250 ˚C and 425 ˚C. The time period that reactors stayed in the sand bath is denoted as the residence time. The residence time was chosen from 3 to 63 min. However, the residence time was shortened when the temperature increased, because at high temperature, the pyrolysis reaction became the main reaction, it produced many gases which made it very difficult

to collect the samples. For example, at 425˚C the longest residence time was only 13 min. Table 3 shows the detailed reaction conditions. There were 8 different temperatures and each had 5 different residence time points, "×" means that the experiment was done under that temperature and that residence time. All the experiments were duplicated to reduce the error.

Thermal stressing experiments can be started when all the preparation was done. Five stainless steel coils were hung on five steel hooks, separately. These hooks had the same length, so all the steel coils were at the same horizontal level in the sand bath, and they can be kept at the same temperature. Five coils were put into the sand bath simultaneously, and they were taken out one after another when different residence time was achieved. As soon as the coil was taken out, it was washed by cold water to lower the temperature to room temperature which only took several seconds, hence the thermal decomposition can be stopped, and the thermal stressing time was the determined residence time. During the experiments, temperature of the sand bath was monitored by the thermocouple and data acquisition system, and the energy regulator was adjusted to keep the temperature at desired value (±1 ˚C). After each experiment, all the reactors were washed by heptane to remove the decomposition products and then heptane was evaporated by heating in the oven.

After thermal stressing experiments, the decomposition products were taken out of the steel coils using pipettes and they were all washed by deionized water to remove ethanol. Then all the samples were stored in the glass vials for GC-FID tests.

3.4 Analytic methods

In this study, two gas chromatography methods were used: GC-FID and GC-MSD. The gas chromatography with a flame ionization detector (GC-FID) (Hewlett Packard 5890 Series II) was used to measure the concentration of organic components in the fresh biodiesel and its decomposition products. Due to its high sensitivity to hydrocarbons, only a small amount of samples (less than 5 μL) were needed in the analysis. A calibration curve of fresh biodiesel was built first, then the decomposition ratio of biodiesel can be calculated by comparing with the calibration curve. The gas chromatography with mass spectrometer detector (GC-MSD) was used to determine the chemical structure of each component in the samples. By comparing the GC-MSD plots, the decomposition products can be identified at each thermal stressing temperature.

3.4.1 Sample preparation for GC analysis

I. Prepare standard samples

In order to build a calibration curve of fresh biodiesel, five different concentrations of biodiesel were prepared: 500, 1000, 1500, 2000, 3000 ppm (volume fraction). All the GC samples were prepared and stored in the 2.0 mL glass vials. First, 1.0 mL heptane was injected into the vial as solvent. Then, 0.5, 1.0, 1.5, 2.0, 3.0 μL fresh biodiesel was injected into the vial, respectively. After the vial was enclosed by the short screw cap, it was shaken up. There were two samples prepared at each concentration to reduce the experimental error.

II. Prepare experimental samples

Table 4 Gas pressure and gas flow rate in GC-FID

	He	Air	H_2	N_2
P (psi)	50	40	7-10	40
Flow rate (mL/min)	2	400	30	28

Table 5 Settings of GC-FID

Initial oven temperature	60 ˚C
Detector temperature	350 ˚C
Injector temperature	350 ˚C
Injection volume	1 μL
Injector mode	Splitless
Equilibrium time	1 min
Oven temperature program	60-150 ˚C at 6 ˚C/min, hold for 10 min; 150-350 ˚C at 10 ˚C/min, hold for 1 min

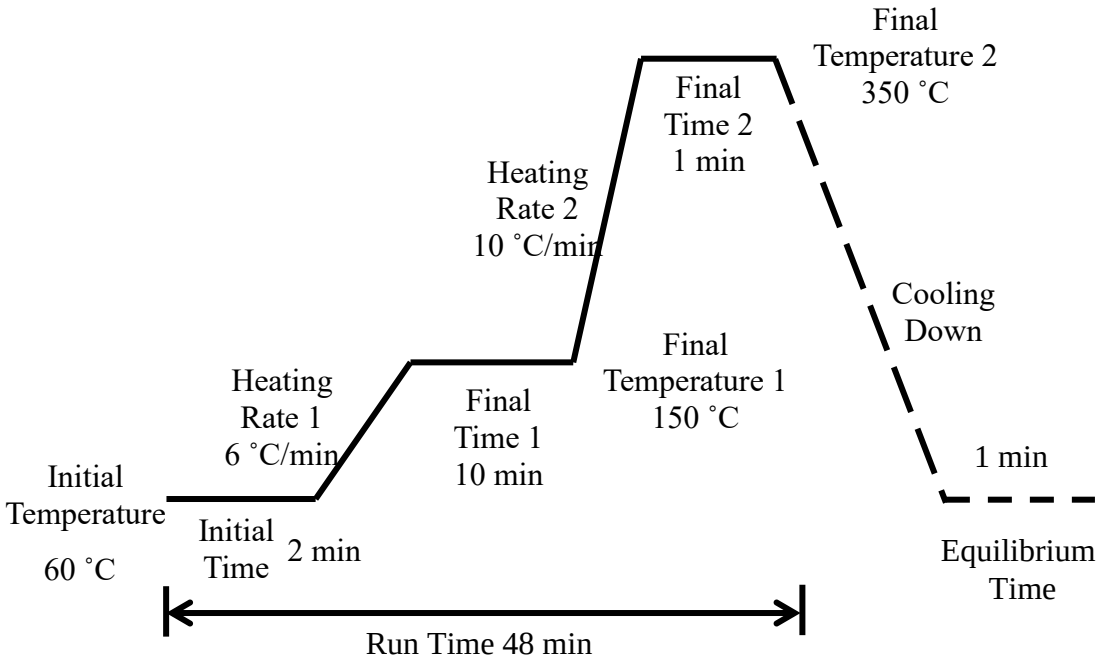

Fig. 4 A schematic diagram of the two-ramp model for GC-FID oven temperature program.

The sample preparation for GC analysis of thermal stressed biodiesel was very similar. But here, 3.0 μL thermal stressed biodiesel was added into 1.0 mL heptane. Due to the high volatility of heptane, all the samples were prepared just before the GC analysis. During the GC analysis, all the glass vials were put on an automatic injector, so that the samples can be injected in to the GC-FID automatically.

3.4.2 GC-FID analysis

In operating GC-FID, it is important to set a proper gas pressure and gas flow rate. If gas flow rate is too high, the baseline on the GC plot will also be very high, so some small peaks may be covered by the baseline and it will affect the result. However, if gas flow rate is low, it is difficult to ignite the flame gases. Table 4 shows the proper gas pressure and gas flow rate used in the experiments.

In order to have a good separation of peaks, settings of GC-FID and oven heating program are also important. In this study, different settings were tried, the optimal settings of GC-FID are shown in Table 5 and the oven heating program is shown in Fig. 4. In the analysis, the temperature of detector and injector were both set to 350 ˚C, the initial oven temperature was set to 60 ˚C. The injection volume was 1 μL, which means that only 1 μL sample was injected into GC-FID in one run. The injector mode was splitless.

The oven heating program here was a two-ramp model. The initial temperature of oven was set to 60 ˚C and it stayed at 60 ˚C for 2 minutes. Then the oven was heated to 150 ˚C at a heating rate of 6 ˚C/min and it was held there for 10 minutes. After that, the oven was heated again to 350 ˚C at a heating rate of 10 ˚C/min, it stayed there for only 1 minute this time. At last,

the oven was cooled down to the initial temperature, 60 ˚C. The GC-FID was then ready for the next sample. At 150 ˚C, the components with high volatility will be separated; at 350 ˚C, the compounds with low volatility will be separated.

3.4.3 GC-MSD analysis

While using GC-MSD to analyze the decomposed samples, more information can be obtained, especially the composition of samples, which can be used to conjecture the reactions at different temperature.

In this work, a Gas Chromatography Agilent Technologies 7890A with 5975C Mass Spectrometer Detector was used. It had a longer and thinner column (HP-INNOWAX) than the one in the GC-FID. The length was 10 m, the I.D. was 0.25 mm and the film thickness was 0.25 μm.

Settings for GC-MSD were different from GC-FID settings. It used a one-ramp heating program. The initial oven temperature was 50 ˚C and it was held there for 1 min. Then it was heated at a heating rate of 3 ˚C/min to 250 ˚C and it was held at 250 ˚C for 10 min. More details will be shown in Table 6.

Table 6 Settings of GC-MSD

Initial oven temperature	50 ˚C
Interface temperature	250 ˚C
Injector temperature	250 ˚C
Injection volume	5 μL
Split ratio	20:1
Oven heating program	50-250 ˚C at 3 ˚C/min, hold for 10 min

Chapter 4: Results and discussion

4.1 The production of biodiesel

In producing biodiesel, three kinds of catalysts were chosen and they had totally different performance. Following the experimental procedure mentioned in Chapter 3, biodiesel fuels were synthesized and stored in glass bottles which are shown in Fig. 5. From left to right, these three bottles were final products of using NaOH, KOH and H_2SO_4 as catalysts, respectively.

In the left bottle, the final product is shown after water was added to wash away the remaining catalysts and ethanol. This liquid was so turbid that it was quite difficult to separate biodiesel from it, and only small amount of separated biodiesel on the surface of the emulsion was produced. Because when NaOH was added into the vegetable oil, the main reaction became the saponification reaction instead of transesterification reaction. A lot of sodium soaps were produced which resulted in this product.

Saponification reaction would also occur when KOH was used, however, in the middle bottle, the final product was much better, its color was close to the purchased biodiesel. These results because potassium soap was softer than sodium soap (Leung & Guo, 2006); potassium soap would suspend in the final products instead of sinking in the bottom. After glycerol was added, the potassium soap would dissolve in the glycerol and it could be separated from biodiesel easily by just flowing out the upper layer.

The biodiesel in the right bottle had a darker color compared to the middle one. This may be due to the high oxidizability of sulfuric acid, some components were oxidized in the reaction.

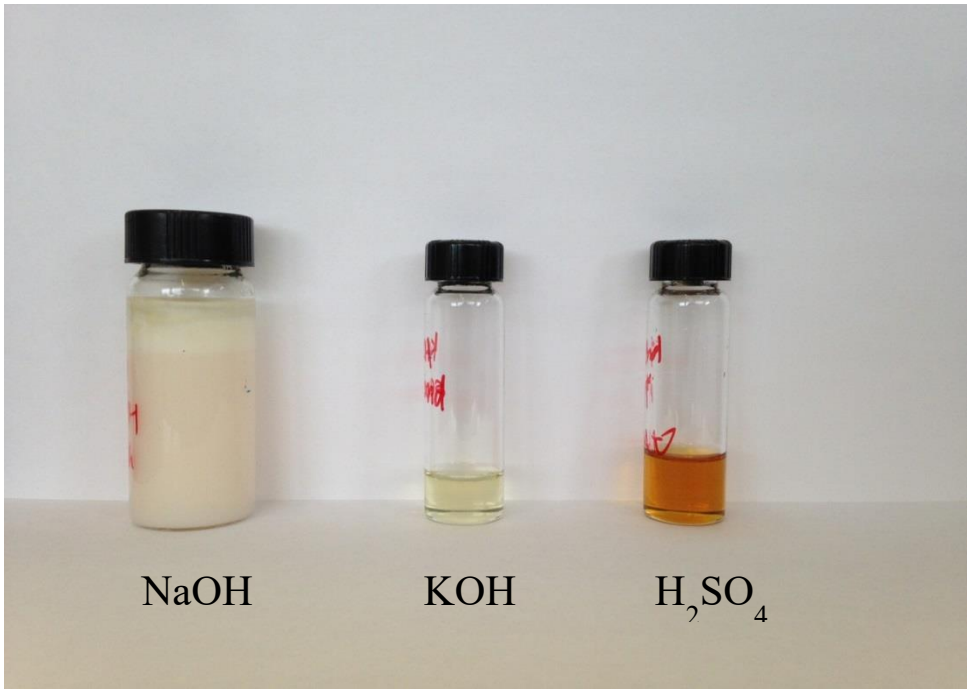

Fig. 5 A photograph of the final products using three different catalysts.

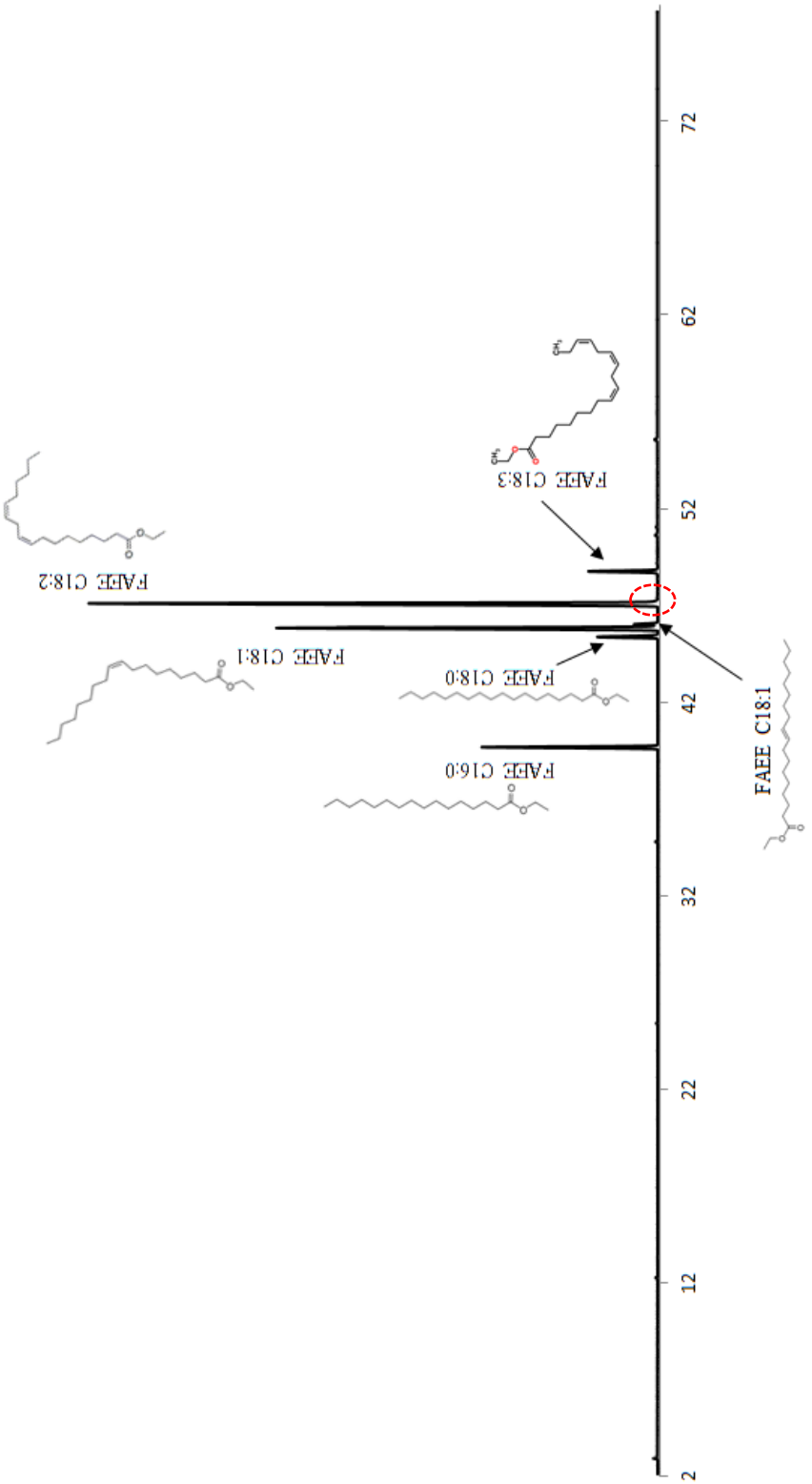

Fig. 6 The GC-MSD plot of produced biodiesel. (Red circle indicates no compound present immediately after the C18:2 FAEE peak)

Longer reaction time was also required, it took much more time than using base catalysts, and so more energy was needed in producing biodiesel. It is also not a good choice.

According to the reaction conditions and performance mentioned above, KOH is the best catalyst among these three catalysts. The GC-MSD plot (Fig. 6) shows that the main components of produced biodiesel are C16:0, C18:0, C18:1, C18:2 and C18:3, which indicates that there is nearly 100% biodiesel in the final products, so the two-step reaction process worked. KOH was used as the catalyst in producing biodiesel in the rest of the study.

4.2 Visual observation of thermal decomposition of biodiesel

After FAEE biodiesel was thermal stressed at 250-425 ˚C for residence times of 3-63 min, all the samples were collected in glass vials. Figures 7 (a) - 7 (c) show the photographs of thermal stressed biodiesel. Basic information can be obtained through visual observation, like color change, volume change and gas generation. Each photograph represents a thermal stressing temperature, from left to right, the residence time of each sample increases.

In Fig 7 (b) - (3) and Fig 7 (c), color change is very obvious. When temperature and residence time increased, color of samples became darker. As the temperature below 350 ˚C, there was only slight change in color, the color changed from colorless to light yellow. After temperature reached above 350 ˚C, color change was more distinct and it took less time for that change. Especially, when the temperature was 425 ˚C and the residence time was 13 min, the color even became brown.

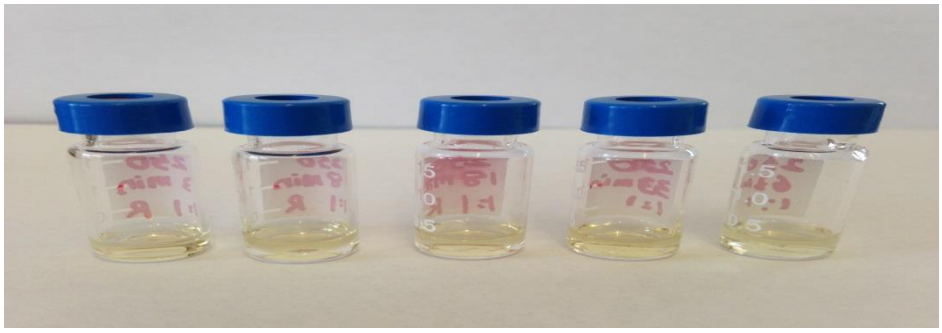

(1) T=250 ˚C; τ=3, 8, 18, 33, 63 min (from left to right)

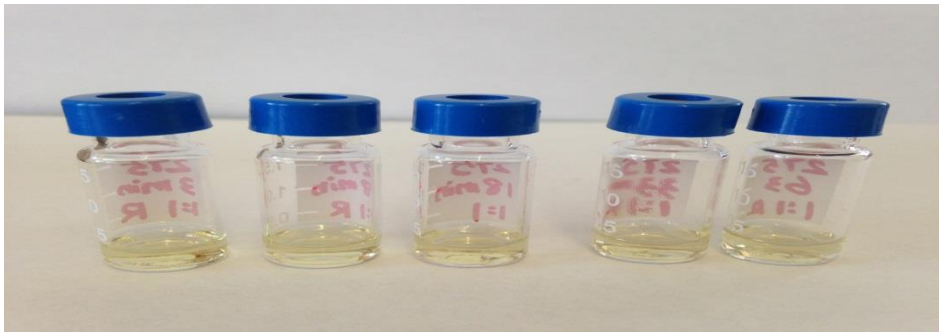

(2) T=275 ˚C; τ=3, 8, 18, 33, 63 min (from left to right)

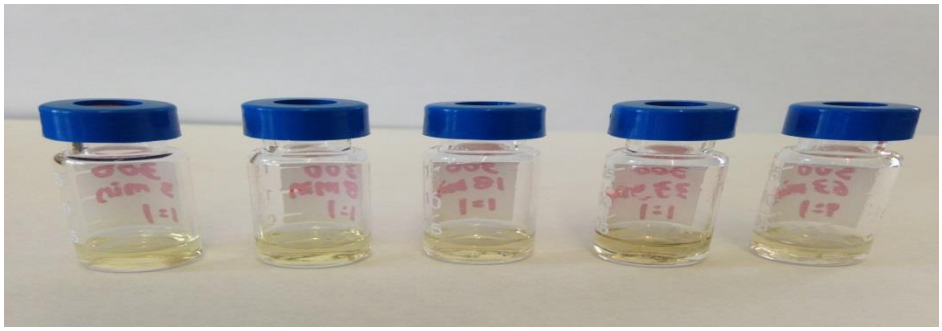

(3) T=300 ˚C; τ=3, 8, 18, 33, 63 min (from left to right)

Fig. 7 (a) Photographs of thermal stressed biodiesel samples in glass vials. (T is the thermal stressing temperature, τ is the residence time)

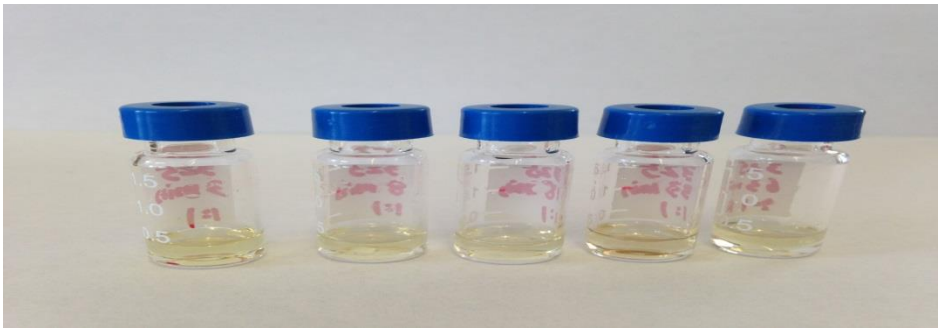

(1) T=325 ˚C; τ=3, 8, 18, 33, 63 min (from left to right)

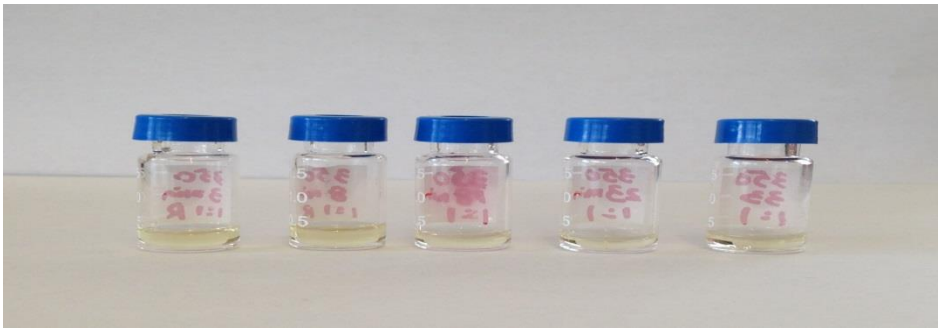

(2) T=350 ˚C; τ=3, 8, 18, 23, 33 min (from left to right)

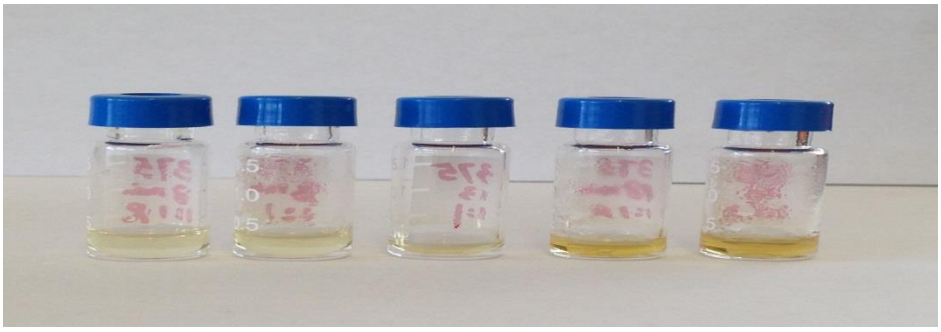

(3) T=375 ˚C; τ=3, 8, 13, 18, 23 min (from left to right)

Fig. 7 (b) Photographs of thermal stressed biodiesel samples in glass vials. (T is the thermal stressing temperature, τ is the residence time)

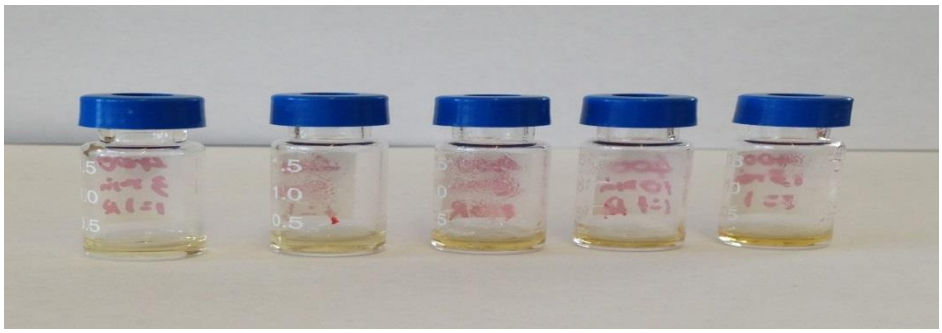

(1) T=400 ˚C; τ=3, 5, 8, 10, 13 min (from left to right)

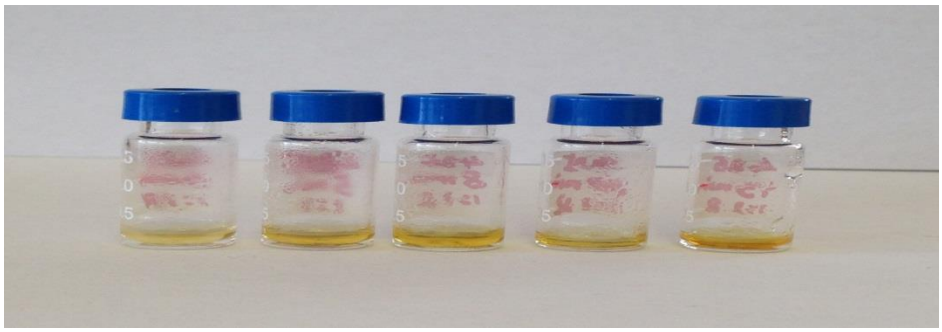

(2) T=425 ˚C; τ=3, 5, 8, 10, 13 min (from left to right)

Fig. 7 (c) Photographs of thermal stressed biodiesel samples in glass vials. (T is the thermal stressing temperature, τ is the residence time)

Besides color change, gas generation was observed in the thermal stressing experiments, and it was also accompanied by the volume decrease. Gas started to generate at 350 ˚C and 18 min, since then, gas products were observed in all the following experiments. When temperature and residence time increased, the volume of samples decreased and gas products increased. There were two reasons for the decrease of sample volume: (1) some components became gases during the thermal stressing experiments; (2) gas products made it difficult to collect the samples, because when the reactor was opened, samples were sprayed out from the reactor coil by the gases.

According to all these phenomena, it can be concluded that the higher temperature and longer residence time are, the higher is the decomposition ratio of FAEE biodiesel. Gas started to be produced at 350 ˚C, which suggests that pyrolysis reaction of FAEE biodiesel occurs at 350 ˚C. But all these conclusions are approximate, accurate results can be obtained through the GC-FID and GC-MSD analysis.

4.3 Calibration curve of FAEE biodiesel

In building a calibration curve for pure FAEE biodiesel produced in our experiments, five samples of different concentrations were prepared and analyzed by GC-FID. The GC plots (Fig. 8) showed that the total peak area is proportional to the concentration of pure biodiesel samples, and the total peak area increased with increasing concentration. Here the total peak area refers to the peak area of C16:0, C18:0, C18:1, C18:2 and C18:3 peaks, because these compounds are the main components in FAEE biodiesel. The peak area can be measured by using the software in the data acquisition system.

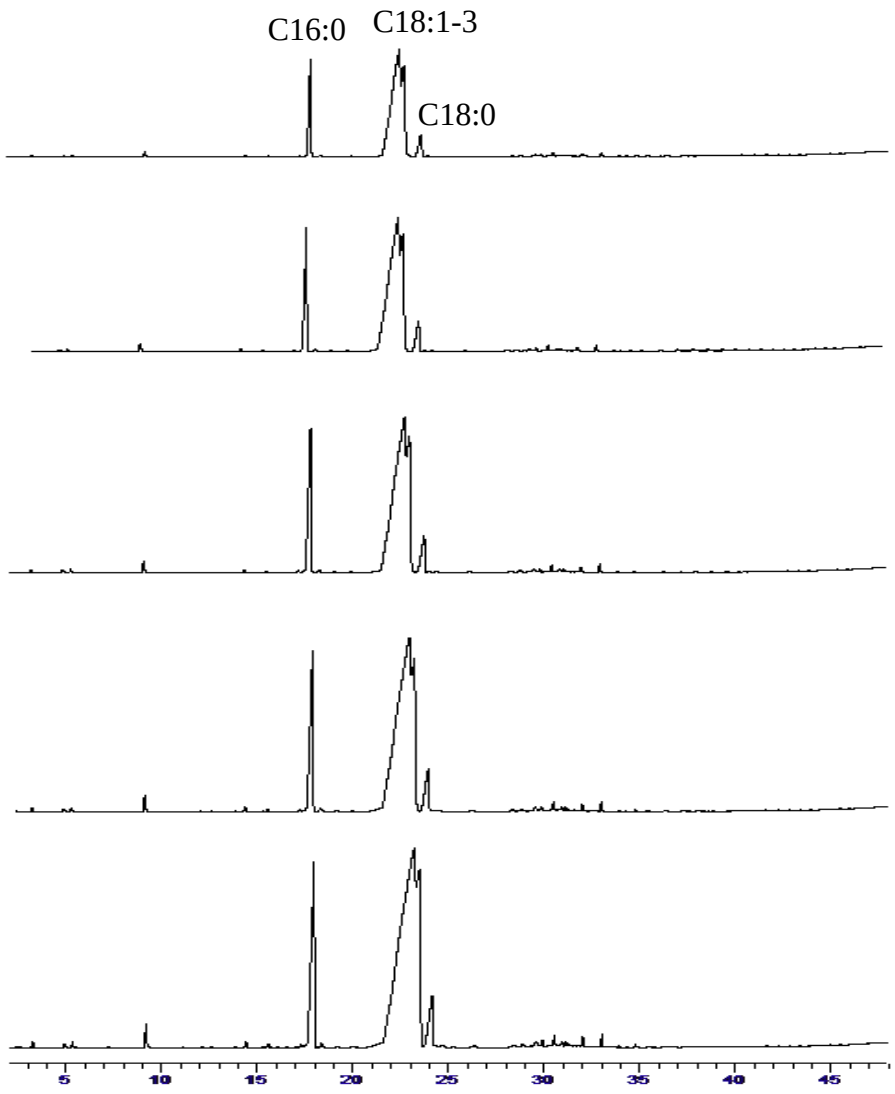

Fig. 8 GC plots of different concentration FAEE biodiesel. (From top to bottom, the concentration is 500, 1000, 1500, 2000, 3000 ppm)

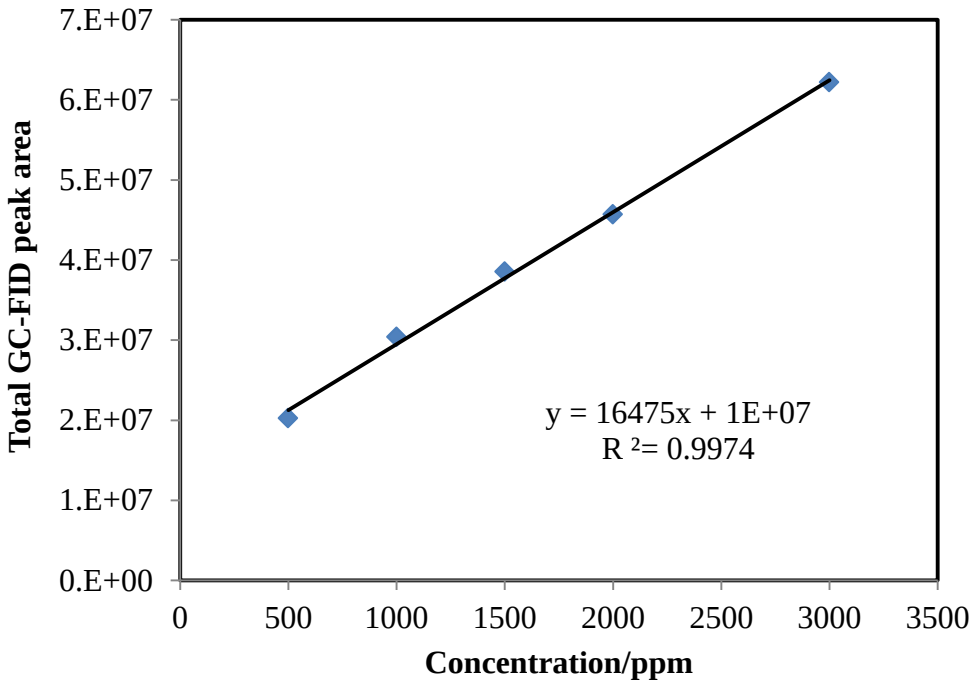

Fig. 9 GC-FID calibration curve of pure FAEE biodiesel.

In order to obtain the relationship between the sample concentration and the total peak area, a chart was made in Fig. 9. X-axis is the concentration of biodiesel samples (by volume), y-axis is the peak area measured by the software, five blue dots are the experimental data and black line is the fitting data.

From the chart, the relationship between sample concentration and peak area is shown as a straight line, so it can be represented by the following linear equation:

$$A=1.65\times10^{4}C+1.31\times10^{7} \quad (4)$$

where A is the peak area, C is the concentration of FAEE biodiesel in ppm. Here R^2 equals 0.9974, which represents that this linear equation fits the data very well. Therefore, in the thermal stressing experiments, once the peak area was measured by the software, the concentration of undecomposed biodiesel can be calculated.

4.4 GC-FID and GC-MSD analysis of thermal stressed biodiesel

In order to get more details in the thermal stressing of biodiesel, samples were analyzed in the GC-FID. Fig. 10 to Fig. 17 are the final results from GC-FID at different thermal stressing temperatures (SMWC means small molecular weight compounds). The mechanism in the thermal decomposition of FAEE biodiesel can be concluded by observing the peak change and comparing it with our previous study (Lin et al., 2013). The appearance of new peaks and decrease of peak area indicate that new components were produced and some compounds were decomposed. In analyzing the GC-FID plots, there are three main reactions observed in the thermal decomposition of biodiesel: isomerization reactions , polymerization reactions and pyrolysis reactions.

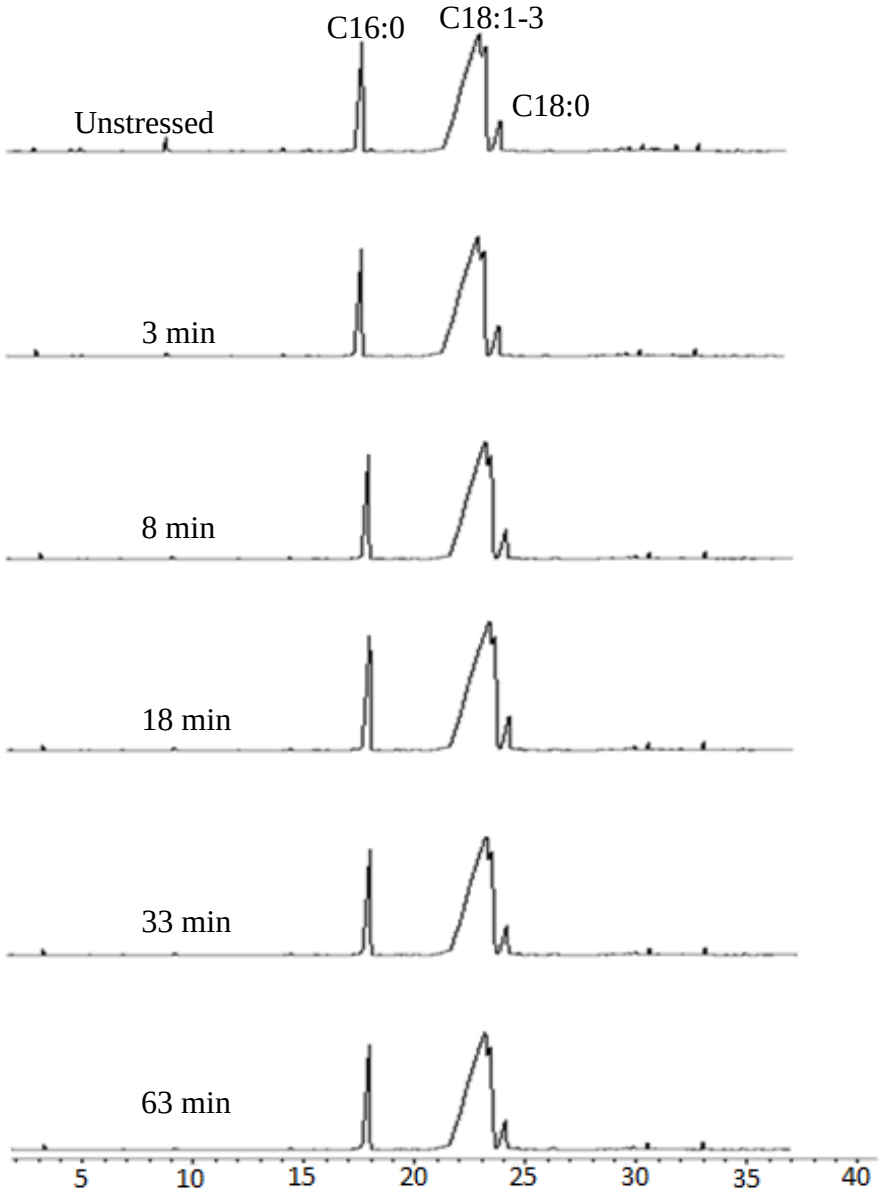

Fig. 10 GC-FID plots of thermal stressed biodiesel at 250 ˚C. (Note that the time specified in this and subsequent GC-FID plots is the thermal stressing time)

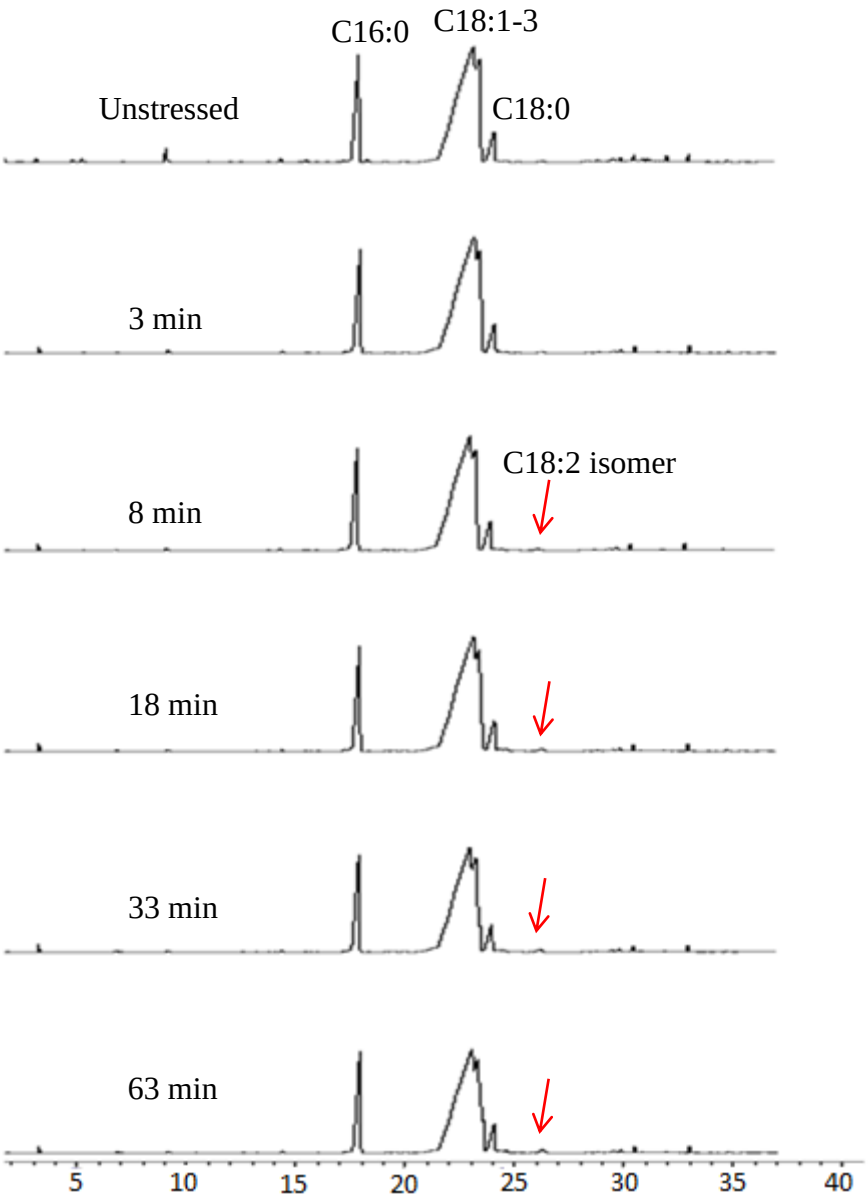

Fig. 11 GC-FID plots of thermal stressed biodiesel at 275 ˚C.

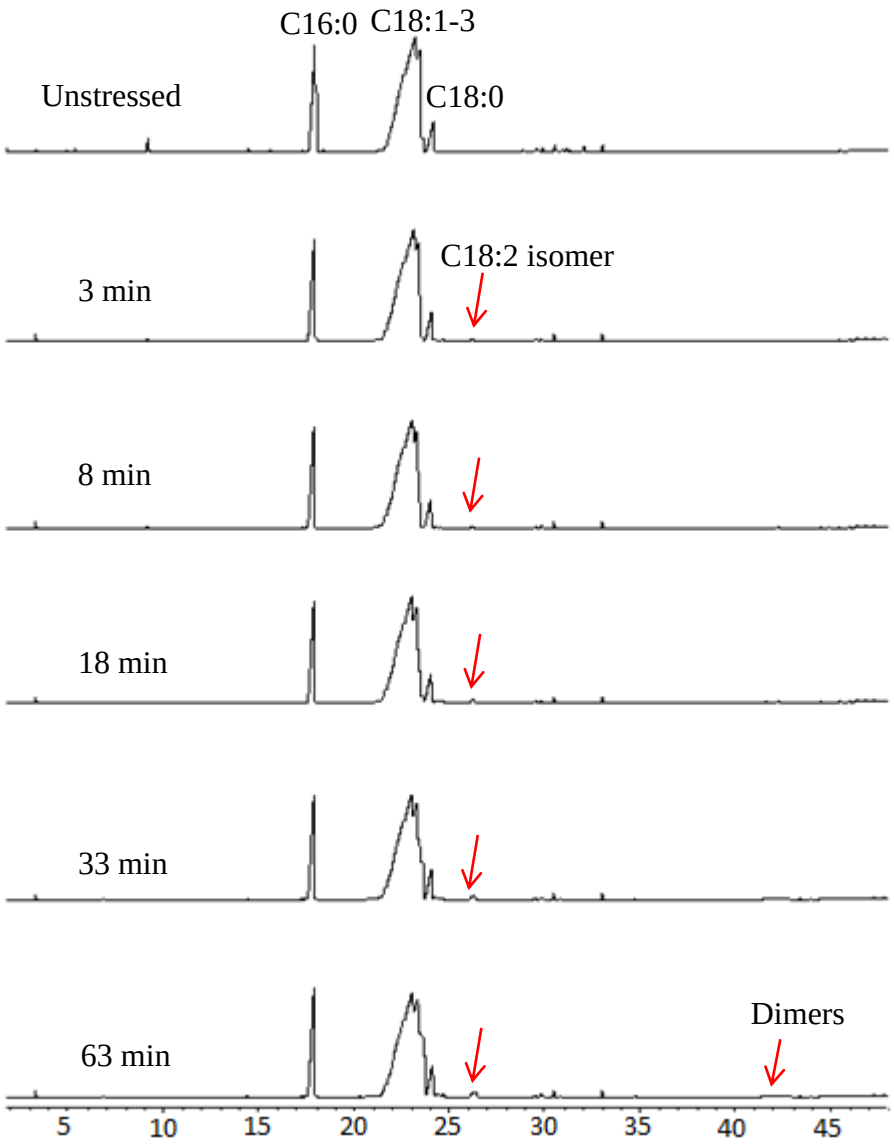

Fig. 12 GC-FID plots of thermal stressed biodiesel at 300 ˚C.

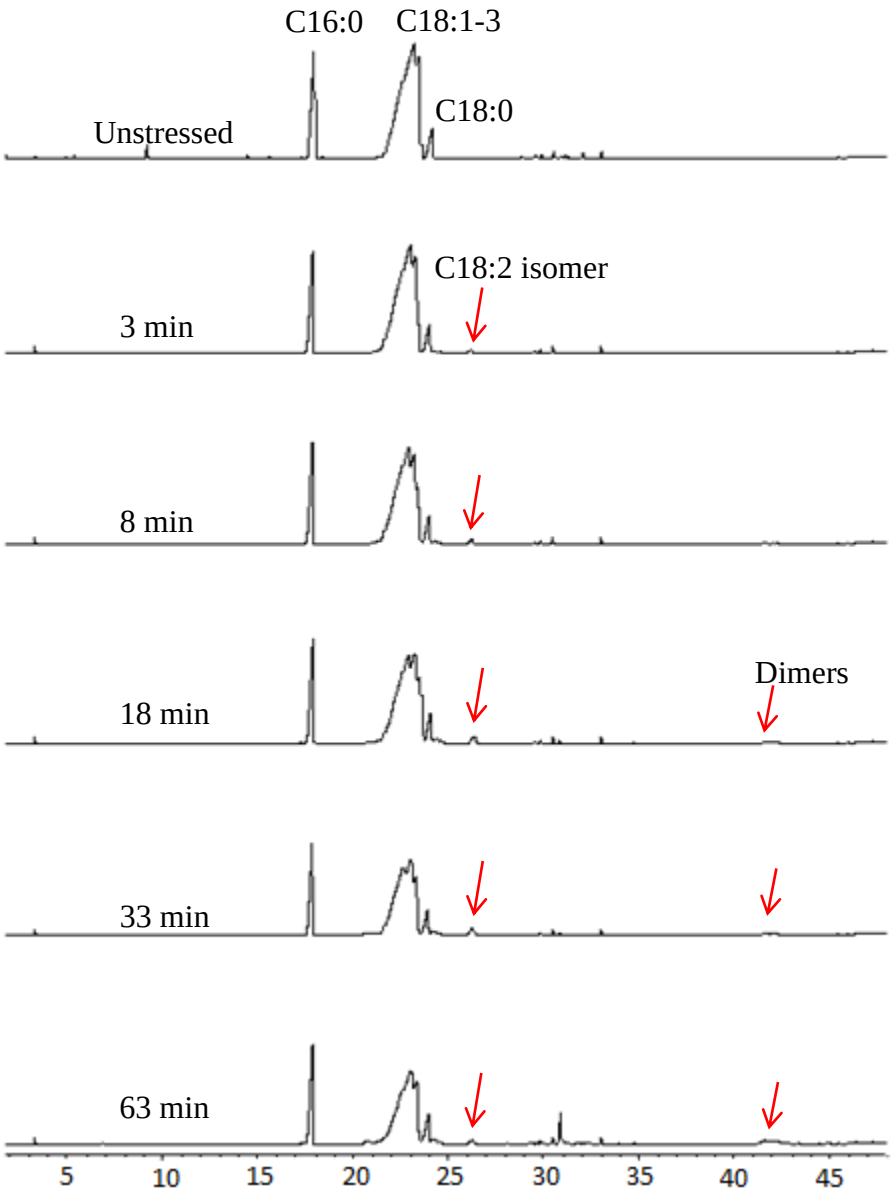

Fig. 13 GC-FID plots of thermal stressed biodiesel at 325 ˚C.

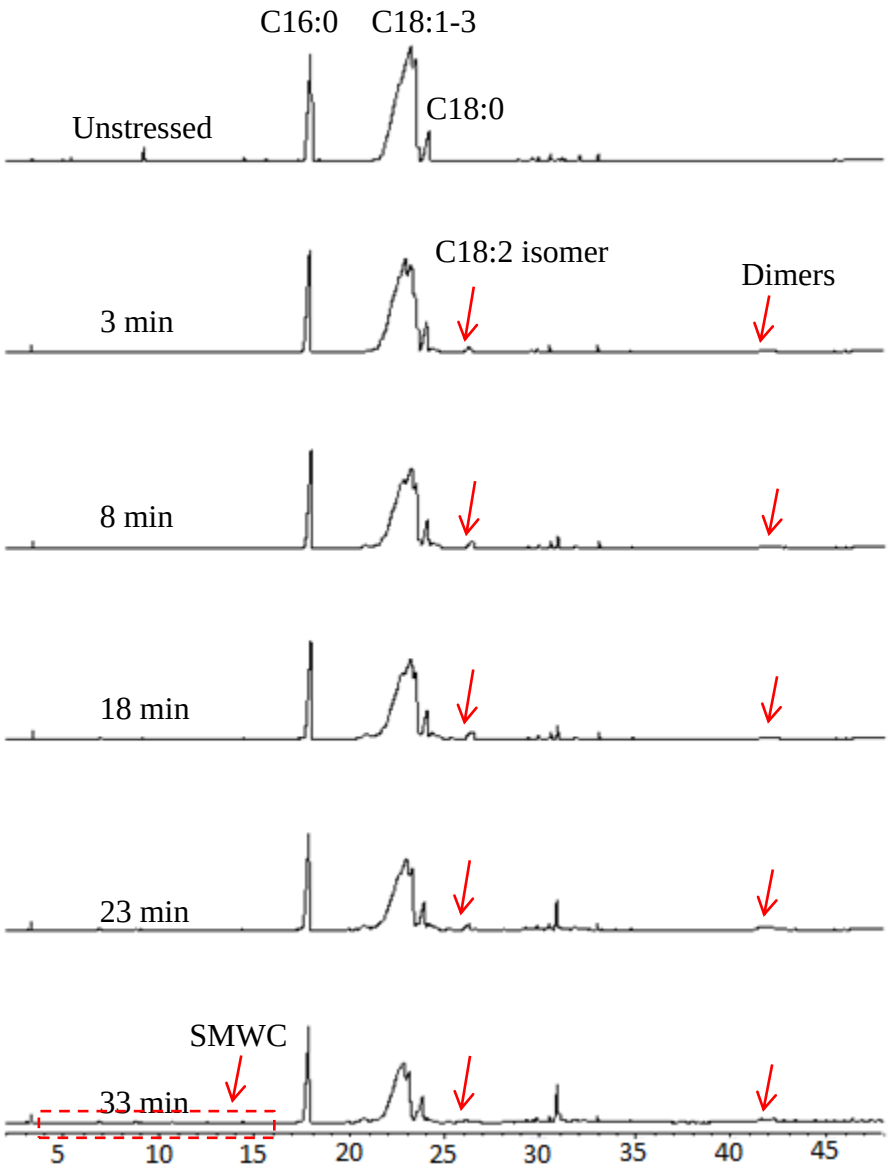

Fig. 14 GC-FID plots of thermal stressed biodiesel at 350 ˚C.

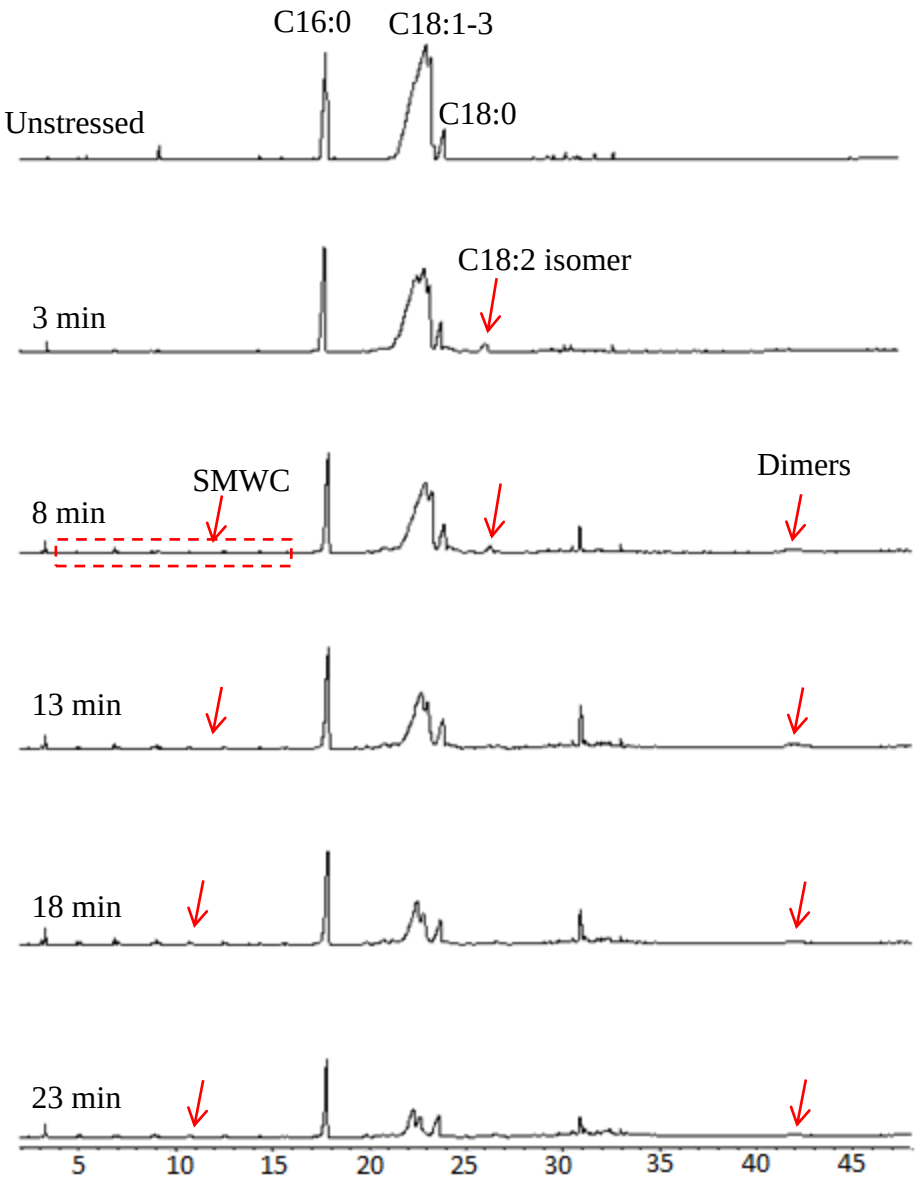

Fig. 15 GC-FID plots of thermal stressed biodiesel at 375 ˚C.

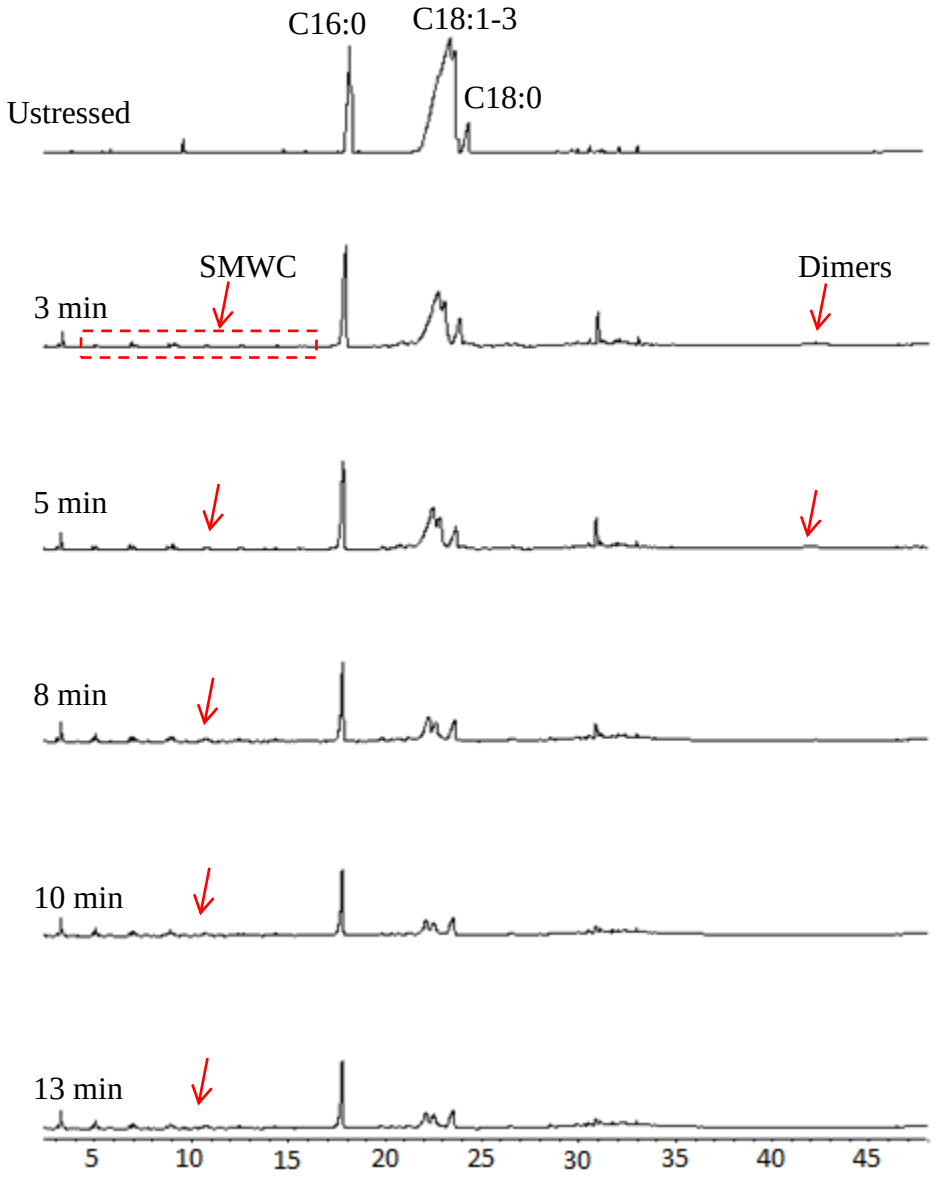

Fig. 16 GC-FID plots of thermal stressed biodiesel at 400 ˚C.

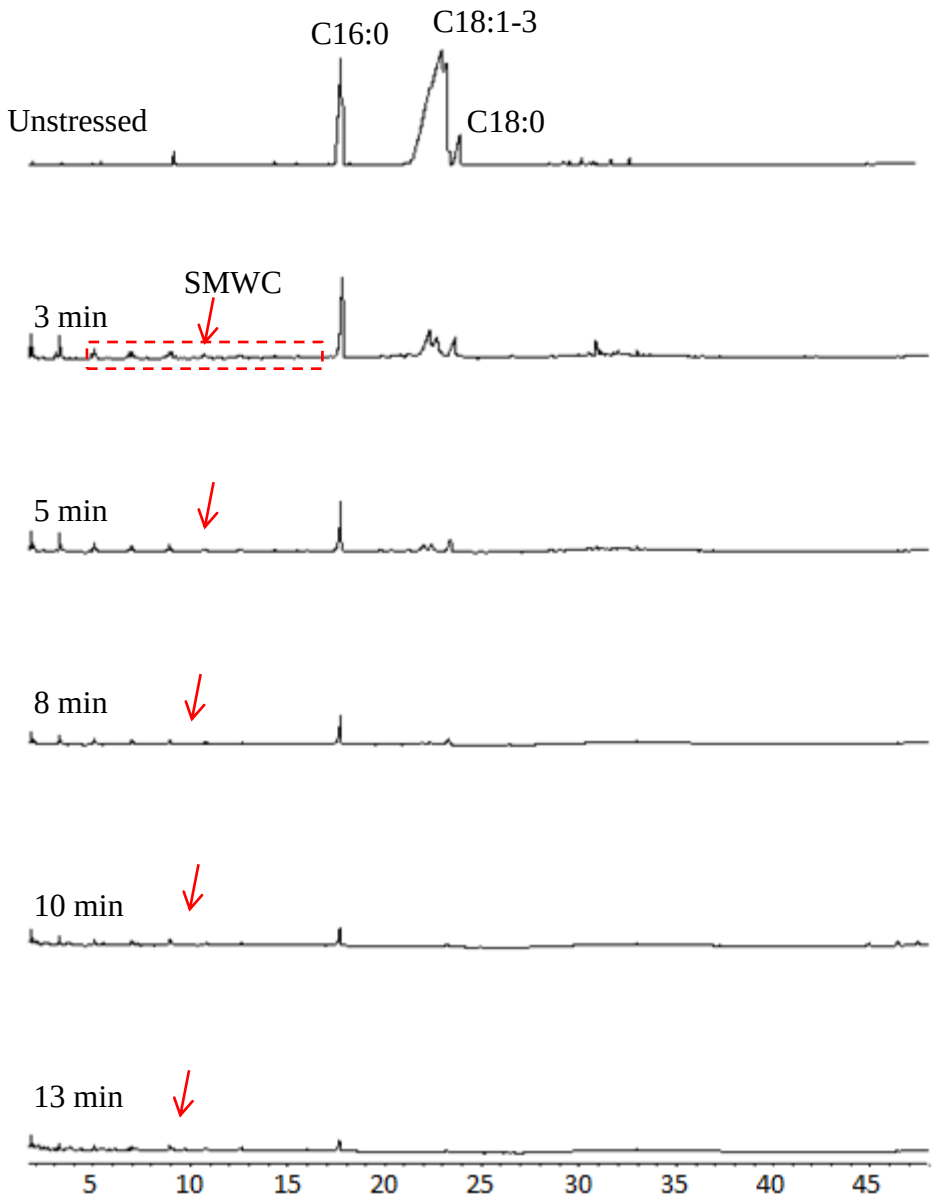

Fig. 17 GC-FID plots of thermal stressed biodiesel at 425 ˚C.

4.4.1 Isomerization reactions

In each figure, there is a GC-FID plot of unstressed biodiesel on the top, which can be used to compare with the other GC-FID plots of thermal stressed biodiesel, so peak change can be easily identified. When the thermal stressing experiments were conducted at 250 ˚C, there was no difference observed in the GC-FID plots as shown in Fig. 10, which suggests that biodiesel is stable at or under 250˚C.

When temperature was raised to 275 ˚C and residence time was 8 min, a new peak was observed (Fig. 11 around 26.5 min). In order to obtain the chemical structure of the new peaks, GC-MSD was used. In Fig. 18, the GC-MSD plot shows that there is also a new peak and the new peak is C18:2 9-cis 11-trans FAEE, but in the GC-MSD plot of pure biodiesel (Fig. 6) there is no trans-type FAEE detected, which suggests that this new peak is C18:2 isomer. In Fig. 11 and Fig. 19, same tendency was observed, these new peaks both increased with the increasing residence time, which is another evidence to prove that the new peak is C18:2 isomer. Therefore, it can be concluded that this new peak is C18:2 isomer and isomerization reactions occur from 275 ˚C.

In Fig.11 to Fig. 13, the peak area of C18:2 peaks (around 26.5 min) increased with the increasing temperature and residence time, which meant that more and more cis-type C18:2 compounds were converted to trans-type ones. However, when temperature was 350 and 375 ˚C, the peak area of C18:2 isomer peak began to decrease during the thermal stressing experiments. This might be due to the decomposition of trans-type C18:2 isomers. And isomerization reactions are believed to occur at the temperature above 275 ˚C.

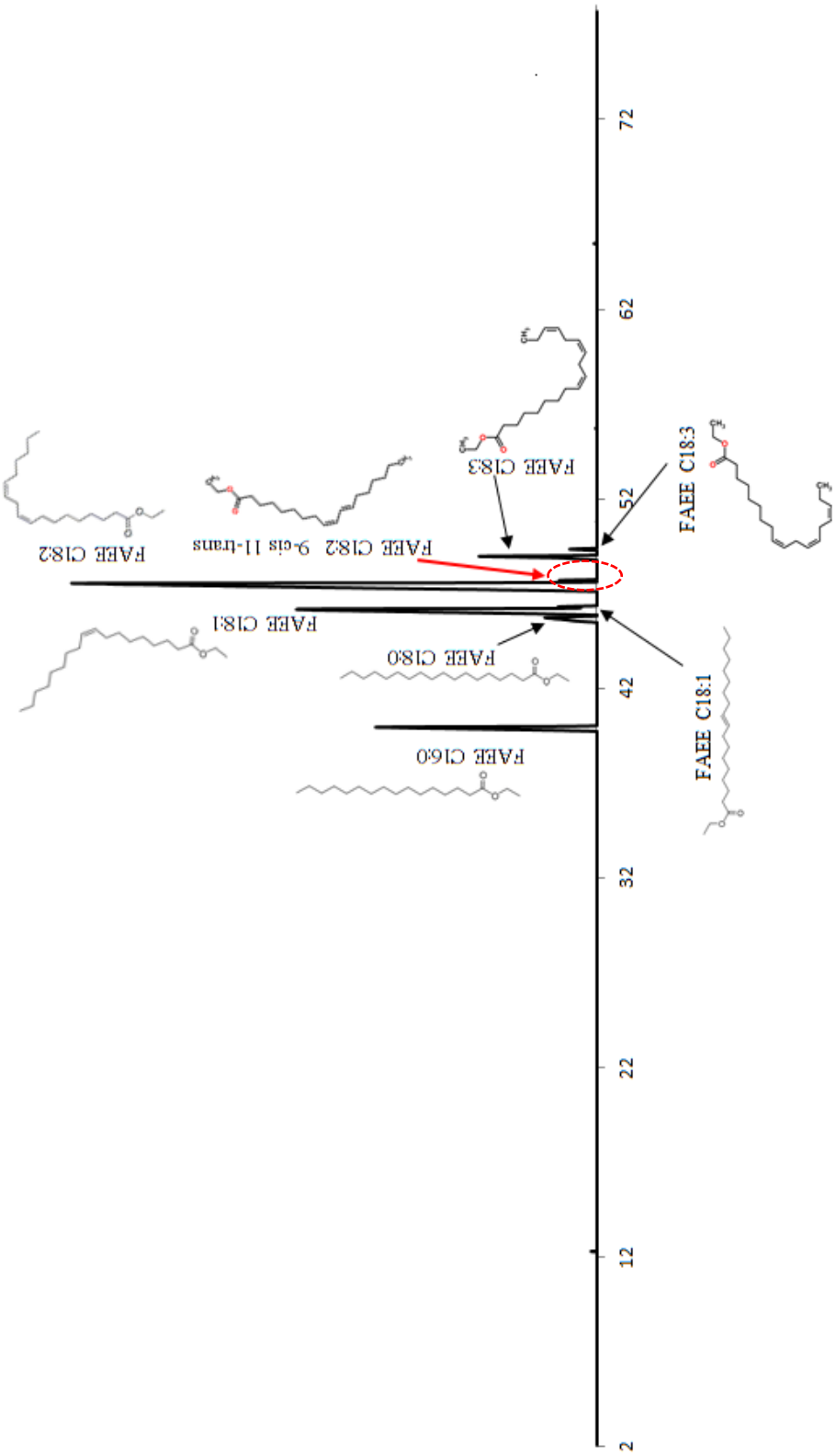

Fig. 18 GC-MSD chromatogram of thermal stressed biodiesel at 275 ˚C for 8 min. (Notice emergence of the C18:2 9-cis, 11-trans FAEE peak after the FAEE C18:2 peak)

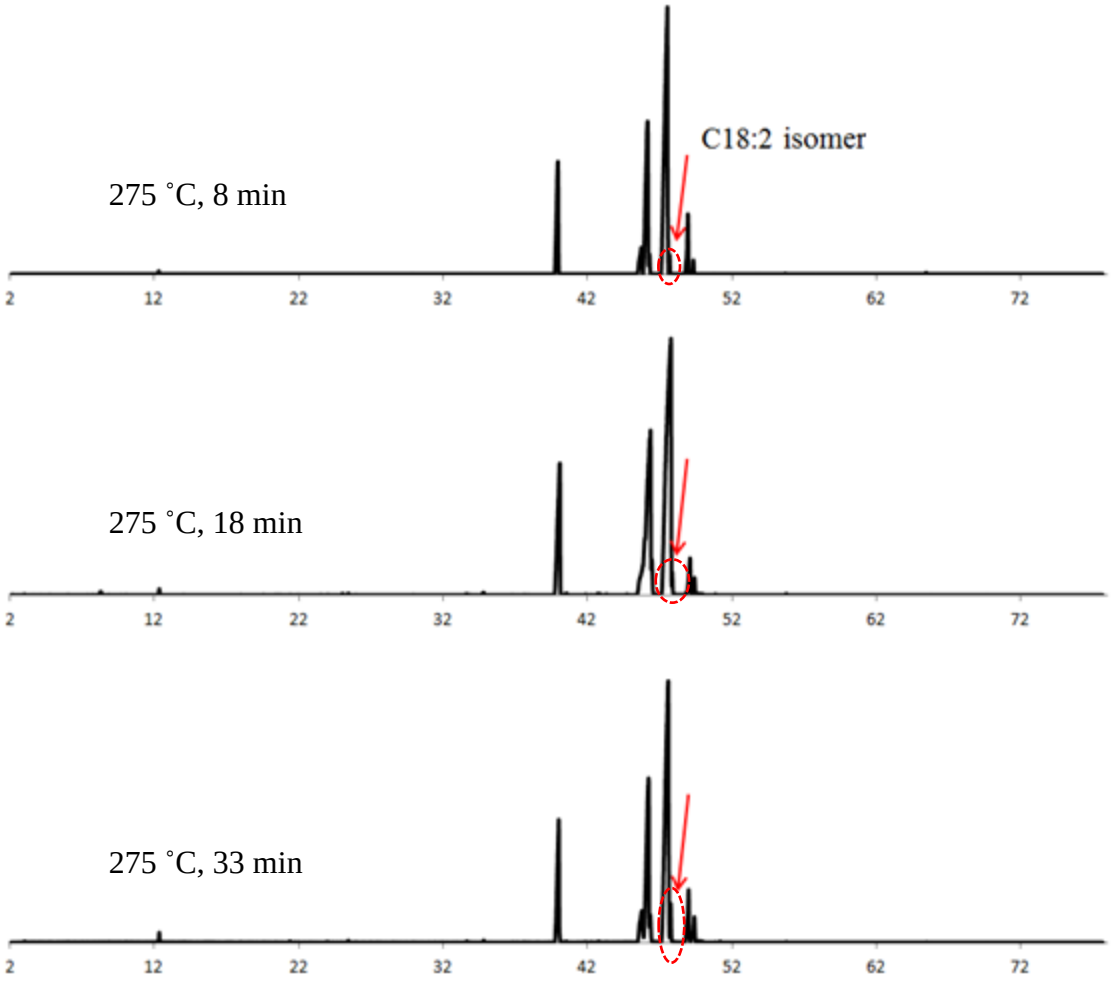

Fig. 19 GC-MSD chromatogram of thermal stressed biodiesel at 275 ˚C for 8 to 33 min. (Notice emergence of the C18:2 9-cis, 11-trans FAEE peak after the FAEE C18:2 peak)

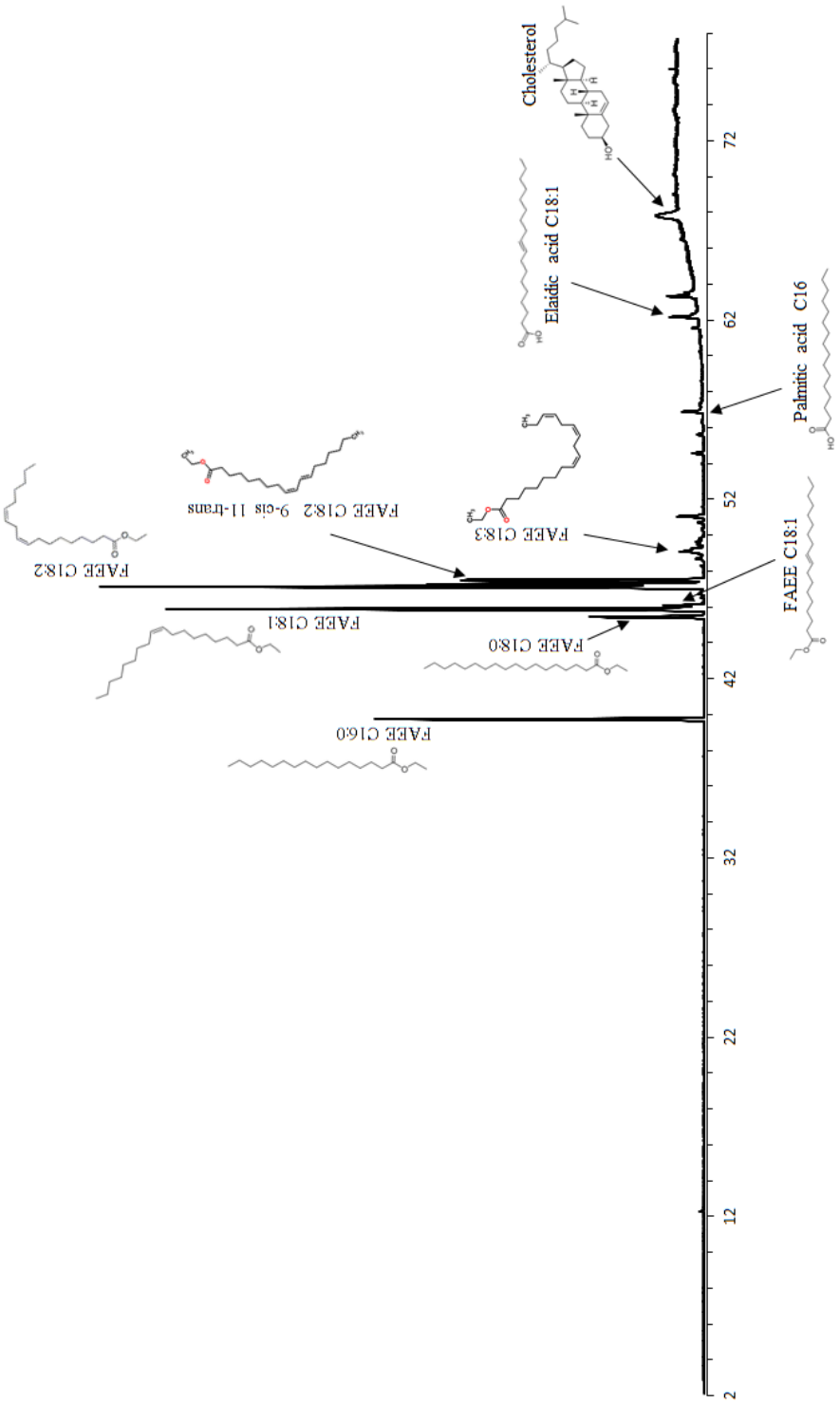

Fig. 20 GC-MSD chromatogram of thermal stressed biodiesel at 300 ˚C for 63 min

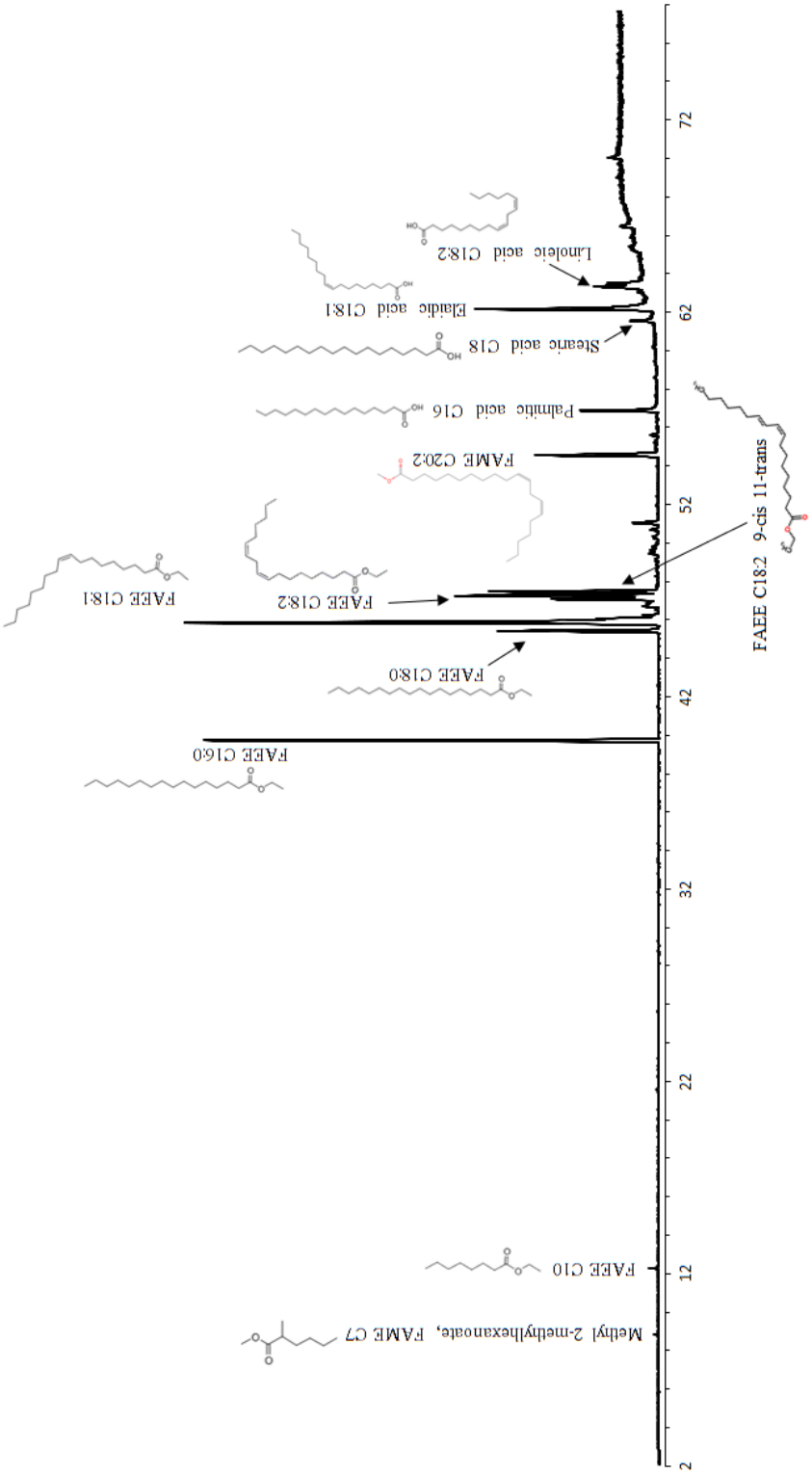

Fig. 21 GC-MSD chromatogram of thermal stressed biodiesel at 350 ˚C for 33 min

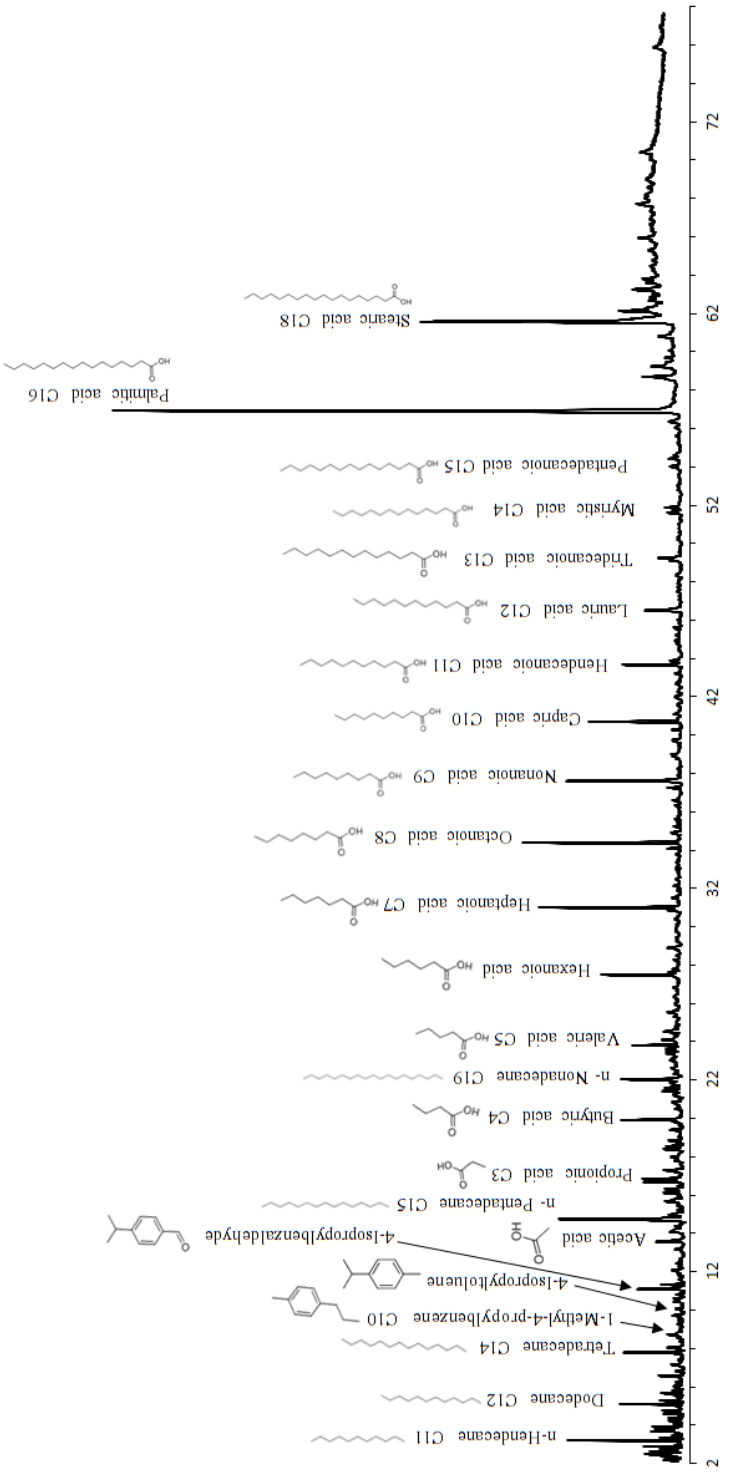

Fig. 22 GC-MSD chromatogram of thermal stressed biodiesel at 425 ˚C for 13 min

In Fig.14, the peak area of C18:2 peaks increased up to 18 min first and then decreased as the residence time increased, which meant that isomers were produced first and then decomposed. Therefore, it also suggested that the isomerization reaction was a reversible reaction as well as having subsequent decomposition of products.

4.4.2 Polymerization reactions

Besides the two peaks mentioned above, a hump appeared around 45 min in Fig. 12 to Fig. 16, in which the temperature was from 300 to 400 ˚C. These peaks were first observed at 300 ˚C and the residence time was 63 min (Fig. 12). Then with the increasing temperature and residence time, the peak area of these two peaks also increased. It is worth to mention that accompanied by the enlargement of these peaks, the C18:1-3 peaks began to shrink. Due to the Diels–Alder reaction mentioned in Chapter 2 and some high molecular weight compounds are detected in Fig. 20, these new peaks were believed to indicate the formation of dimers and polymers.

In Fig. 15 and Fig.16, it could be observed that these peaks (around 45 min) enlarged first and then shrunk as the residence time increased. It might suggest that polymerization reaction was a reversible reaction, the reaction went forward first, so the concentration of dimers and polymers increased; then the reaction went backward, so the concentration of products decreased. When the temperature was raised up to 400 ˚C, these dimer peaks disappeared after 10 min thermal stressing experiments, which might be due to the decomposition of dimers and polymers. Hence, it can be concluded that polymerization reactions occur at the temperature above 300 ˚C.

4.4.3 Pyrolysis reactions

In the thermal stressing experiments, gases were first observed at 350 ˚C when the residence time was 18 min, the production of gases was a signal of pyrolysis reaction, so it was believed that pyrolysis reaction started from 350 ˚C. In Fig. 21, the GC-MSD plot shows that small molecular weight compounds (C7 and C10 FAEE) were produced at 350 ˚C for 33 min. This was another signal of pyrolysis reaction, and these peaks kept appearing and became more and more in the following temperatures, so pyrolysis reaction occurred when temperature was over 350 ˚C. The thermal stressed biodiesel sample which was treated at 425 ˚C for 13 min was also analyzed by the GC-MSD, the results were shown in Fig. 22. It is found that nearly all the biodiesel decomposed and the final products are C11-C19 alkanes and C3-C15 acids.

It was also found that C18:1-3 peaks shrunk very fast when temperature was over 325 ˚C, and especially at 400 and 425 ˚C, they nearly disappeared. However, C16:0 and C18:0 peaks shrunk at a much slower rate, which indicated that unsaturated FAEEs decomposed faster than saturated FAEEs, in other words, saturated FAEEs were much more stable than unsaturated FAEEs at high temperature. This conclusion is similar to Hee-Yong Shin's study (Shin et al., 2011).

4.5 Kinetics in the thermal decomposition of biodiesel

4.5.1 Quantitative analysis of thermal decomposition of biodiesel

As mentioned in previous sections, C16:0, C18:0 and C18:1-3 FAEEs are the main components in biodiesel and the concentration of undecomposed biodiesel has a linear

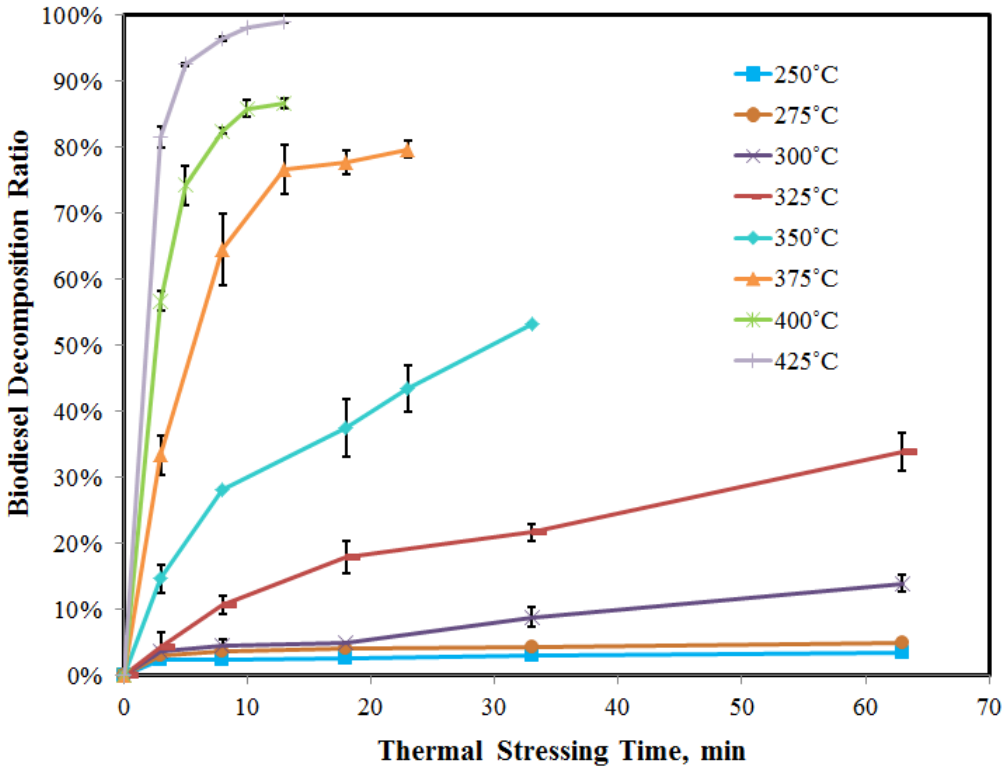

Fig. 23 Experimental data of thermal decomposition ratio at different temperatures and different residence times.

relationship with the peak area of C16:0 and C18:1-3 peaks. Therefore, once the peak area of C16:0, C18:0 and C18:1-3 peaks are measured, the concentration of undecomposed biodiesel can be calculated using the calibration curve equation (in Section 4.3). Then, the thermal decomposition ratio of biodiesel can be obtained by the following equation:

$$\omega = 1 - \frac{C}{C_0} \tag{5}$$

where, ω represents the thermal decomposition ratio of biodiesel, C is the calculated concentration of remaining FAEE biodiesel, and C_0 is the concentration of pure biodiesel, which is 3000 ppm (3 μL biodiesel was combined with 1 mL heptane).

Fig. 23 shows the calculated thermal decomposition ratio as a function of temperature and residence time. From this figure, same conclusions can be obtained as analyzing the GC-FID plots. At the same thermal stressing time, higher temperature resulted in higher thermal decomposition ratio, and at a certain temperature, longer residence time had the same effects, especially at 425 ˚C, nearly 100 % FAEE biodiesel was decomposed when the residence time was 13 min.

Temperature played an important role in the thermal decomposition of biodiesel. In Fig. 23, it can be observed that when the temperature was below 275 ˚C, the decomposition ratio was less than 5 % according to Eqn. 5, almost no decomposition occurred. However, when temperature was raised to 300 ˚C, the thermal decomposition ratio suddenly increased, which could be considered as the signal of thermal decomposition of biodiesel, this temperature might not be the decomposition starting temperature, but it can be concluded that FAEE biodiesel was stable at the temperature below 275 ˚C. This conclusion was the same as what was obtained in the

analysis of GC-FID plots. When biodiesel was heated to higher temperature, the decomposition ratio increased very fast. For example, from 325 ˚C to 375 ˚C, the thermal decomposition ratio of biodiesel raised from 30 % to almost 50 % and then to near 80 %.

Thermal stressing time also affected the thermal decomposition considerably. In Fig. 23, the trend showed that at a certain temperature, the thermal decomposition ratio became higher with the increasing thermal stressing time. It was also observed that the thermal decomposition ratio increased very fast at the first 3 min, the concentration of biodiesel was much higher than the decomposed biodiesel, so the reactions went forward to make biodiesel break down; later, the concentration of decomposed products increased, therefore, the reactions reached equilibrium, , this phenomenon might indicate that the reactions in the thermal stressing experiments were reversible reactions, which may explain why horizontal lines were observed at longer residence time in Fig. 23.

The error bars on each curve showed the errors under each experimental condition. These error bars were obtained according to the GC-FID tests. Each sample was tested in GC-FID twice, so each sample had two different data, when comparing the real data with the average data, the error bars can be obtained. There were many factors that would affect the accuracy of this study. (1) While measuring the volume of samples, because of the errors in operating pipettes, the measured volume was not accurate, it was more or less than the desired volume, then it would affect the GC-FID results; (2) In the thermal stressing experiments, the sand bath was not able to be set at a certain temperature, there were fluctuations (±1 ˚C) during the experiments, which affected the thermal decomposition ratio; (3) GC-FID had its own errors while analyzing

samples, for example, some impurities in the machine and errors of detectors, which would change the peak area and then have some effects on the final results.

4.5.2 Kinetic models in thermal decomposition of biodiesel

In analyzing kinetics of thermal decomposition of FAEE biodiesel, more information can be obtained, like reaction rate constants, activation energy and etc. However, there is no research on this topic now, so this work may provide a better understanding of the thermal decomposition of FAEE biodiesel.

As mentioned in the previous sections, the thermal decomposition of biodiesel is very complicated, many kinds of reactions are involved in the thermal decomposition. Several reactions occurred simultaneously and many products were produced, so it took great effort to analyze them one by one, a simplified kinetic model was needed to represent the thermal decomposition of biodiesel. In Lin's work (Lin et al., 2013), a first order reversible reaction was used to study the thermal decomposition of FAME biodiesel. In this work, a similar model will be used, and a first order irreversible reaction will also be used to see which one fits the data better.

4.5.2.1 First-order reversible kinetic model

The first-order reversible model is an assumption here. It assumes that the thermal decomposition of biodiesel is a first-order reversible reaction, which can be represented by the following reaction:

$$B \underset{k_2}{\overset{k_1}{\rightleftharpoons}} P$$

Table 7 Reaction rate constants (k_1 and k_2) and equilibrium constant (K) for the first-order reversible reaction model

T/ ˚C	k_1/ min^{-1}	k_2/ min^{-1}	K
250	0.0006	0.0082	0.0669
275	0.0014	0.0110	0.1299
300	0.0036	0.0181	0.1975
325	0.0124	0.0211	0.5906
350	0.0393	0.0281	1.4007
375	0.1537	0.0347	4.4269
400	0.3118	0.0424	7.3594
425	0.6927	0.0404	17.1460

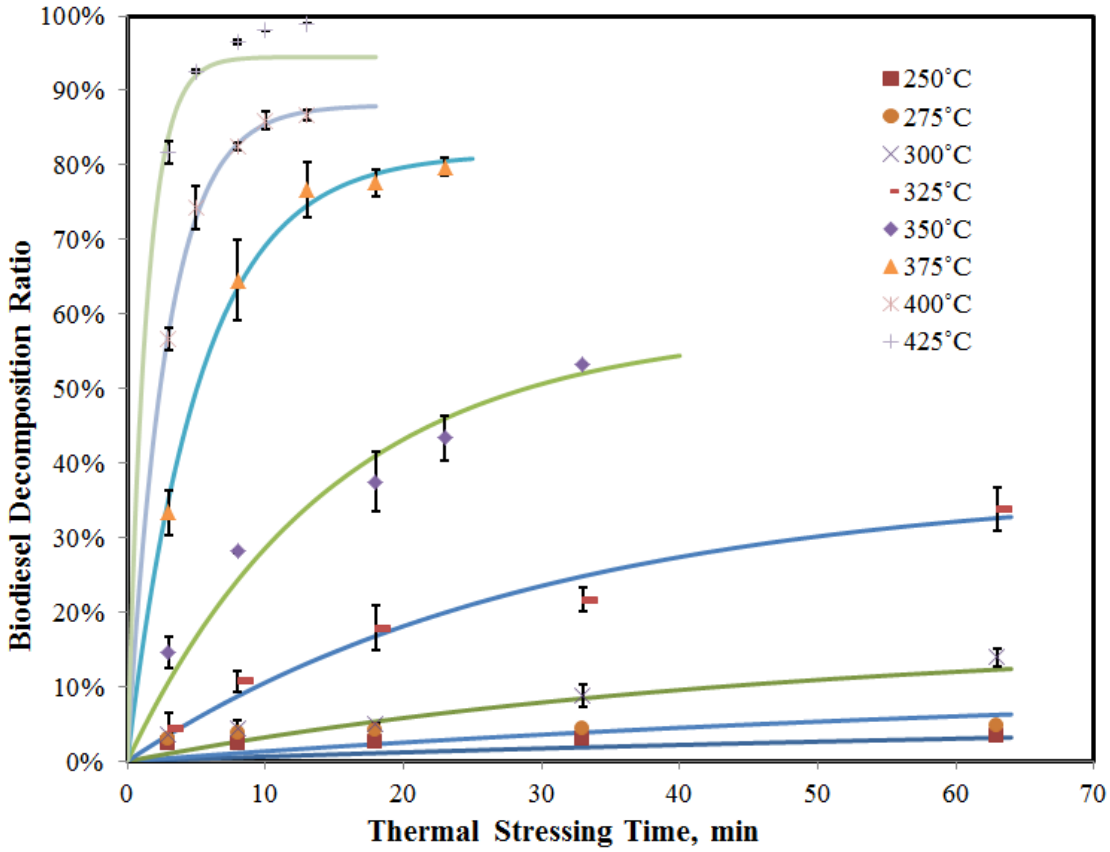

Fig. 24 Plot of fitting curves with experimental data using the first-order reversible reaction model.

Table 8 Reaction rate constant (k_3) for the first-order irreversible reaction model

T/ ˚C	k_3/ min^{-1}
250	0.0006
275	0.0011
300	0.0033
325	0.0074
350	0.0260
375	0.1065
400	0.2424
425	0.4823

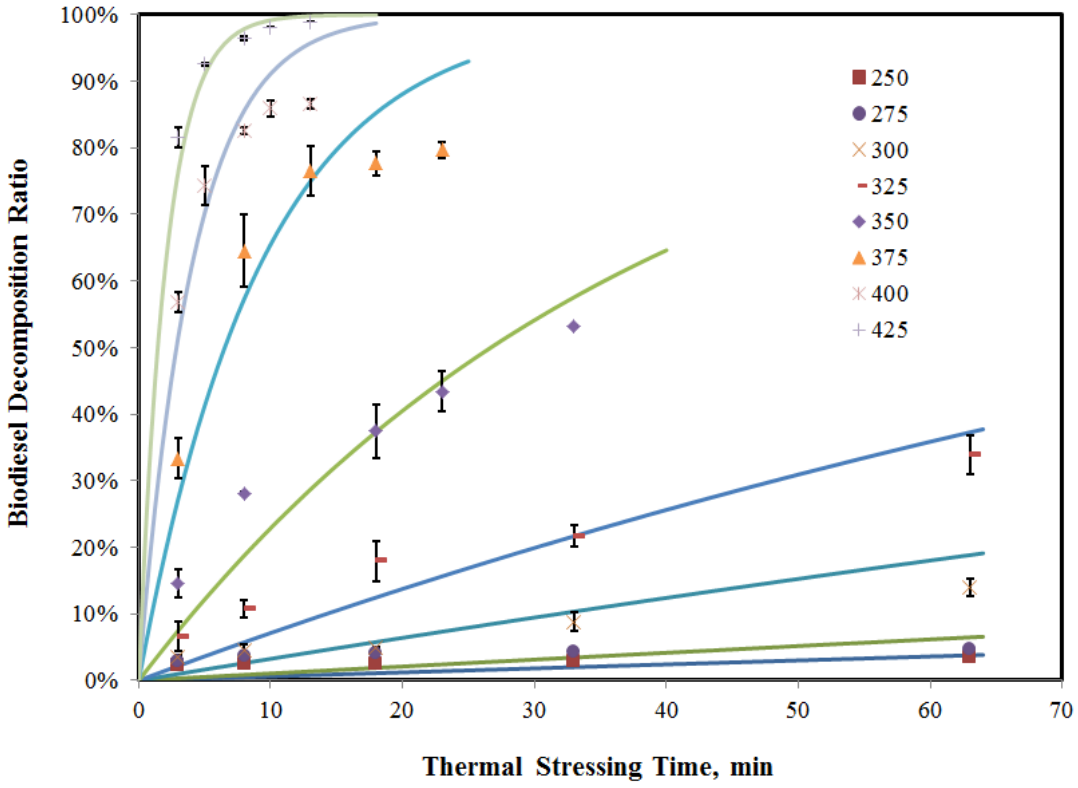

Fig. 25 Plot of fitting curves with experimental data using the first-order irreversible reaction model.

where, B is pure FAEE biodiesel, P represents all the products after thermal decomposition, k_1 and k_2 are reaction rate constants. Therefore, all the thermal decomposition reactions are simplified to this one step reaction and all the calculations can be simplified.

According to this reaction, the reaction rate of thermal decomposition is shown below:

$$-\frac{dC_B}{dt} = k_1 C_B - k_2 C_p \tag{6}$$

Assuming that $C_p=C_{B0}-C_B$ (C_{B0} represents the concentration of FAEE biodiesel before thermal stressing experiments) and using Equation 5 in Section 4.5.1, the differential equation of thermal decomposition ratio and time can be obtained as the following one:

$$\frac{d\omega}{dt} = k_1(1-\omega) - k_2\omega \tag{7}$$

Then with the help of software *Micromath Scientist*, k_1 and k_2 can be simulated to best fit the experimental data. Table 7 shows the reaction rate constants obtained by the software, and K here is k_1 divide by k_2, which is also known as equilibrium constant. It can be found that k_1 increases much faster than k_2, this may be due to the occurrence of pyrolysis reactions. Fig. 24 shows the experimental data compared with simulated data at different thermal stressing temperature. Those eight curves represent the fitting curve obtained by software and there are five points on each curve which are the experimental data at the same temperature. When using the first-order reversible reaction model, it is found that from 250 ˚C to 400 ˚C, the fitting curves fit the experimental data very well. This suggests that at 400 ˚C and below 400 ˚C, this first-order reversible reaction model can well represent the reactions in the thermal decomposition of

biodiesel. It is also known that isomerization and polymerization reactions are reversible reactions, so this kinetic model proves the importance of these two kinds of reactions.

However, at 425 ˚C, the simulated data is lower than the experimental data. Table 7 shows that k_1 increased with the increasing temperature, but k_2 decreased from 400 ˚C to 425 ˚C. These results indicate that at 425 ˚C, reactions in the thermal decomposition are very different from the reactions at other temperatures, the first-order reversible reaction model is not suitable at 425 ˚C. Therefore, another model is needed to explain this phenomenon, a first-order irreversible reaction model is tested in the following section.

4.5.2.2 First-order irreversible kinetic model

While choosing first-order irreversible reaction model, a similar method was used. But it was even simpler, only one reaction rate constant (k_3) needed to be estimated. This model can be represented by the following reaction:

$$B \xrightarrow{k_3} P$$

Here, the reaction is irreversible, it goes forward to make biodiesel break down.

The reaction rate is given by the following equation:

$$-\frac{dC_B}{dt} = k_3 C_B \qquad (8)$$

Using Equation 5 in Section 4.5.1 again, the differential equation of thermal decomposition ratio and time can be obtained as the following one:

$$\frac{d\omega}{dt} = k_3(1-\omega) \tag{9}$$

Then the software *Micromath Scientist* is used to simulate a proper k_3 to fit the experimental data. The results of simulated k_3 are shown in Table 8. Here, k_3 increases when temperature becomes higher. In Fig. 25, it shows fitting curves compared with experimental data, each point represents an experimental condition. From Fig. 25, it is observed that it is opposite to Fig. 24, all the fitting curves do not fit well with the experimental data, except at 425 ˚C. At 425 ˚C, the first-order irreversible reaction model fits the experimental data very well, which suggests that the main reactions are irreversible reactions when the temperature is 425 ˚C. Furthermore, it is mentioned in the previous chapters that pyrolysis reactions are irreversible reactions, so it may be concluded that the thermal decomposition reactions of biodiesel at 425 ˚C are mainly pyrolysis reactions. The GC-FID and GC-MSD plots also support this conclusion, because these plots show that the main decomposed products are small molecular weight compounds and almost all the C16 and C18 peaks disappeared at 425 ˚C, which are also indication of pyrolysis reactions.

However, due to experimental limits, the details of the concentrations of all compounds under each experimental condition were not able to be determined, more work needs to be done. In this work, simple models have been built. The first-order reversible reaction model can well represent the thermal decomposition of biodiesel at the temperature from 250 to 400 ˚C, but at 425 ˚C, the first-order irreversible reaction model is a better fit of the experimental data.

4.5.3 Calculations of kinetic parameters

Besides simulating the reaction rate constants and equilibrium constants, the results are further analyzed to obtain more kinetic data in the thermal decomposition of biodiesel.

The Arrhenius equation is use to express the relationship between temperature and reaction rate constant. The equation is shown below:

$$k = A\exp(-\mathrm{E}_a / \mathrm{RT}) \tag{10}$$

where A is the pre-exponential factor, E_a is the activation energy, R is the universal gas constant, which is 8.314 J mol^{-1} K^{-1}. Taking natural logarithms to both sides, Equation 10 can be changed into:

$$\ln k = \ln A - \frac{\mathrm{E}_a}{RT} \tag{11}$$

So the Arrhenius equation becomes a linear equation here, E_a and A can be easily obtained from the plots of lnk versus 1/T.

The Arrhenius plots are shown in Fig. 26 and Fig 27, for the forward and reverse reaction rate constants, repectively.

Van't Hoff equation is also used here. It expresses reaction equilibrium constant as a function of temperature and is shown below:

$$\frac{d\ln K}{d(1/T)} = -\frac{\Delta H^0}{R} \tag{12}$$

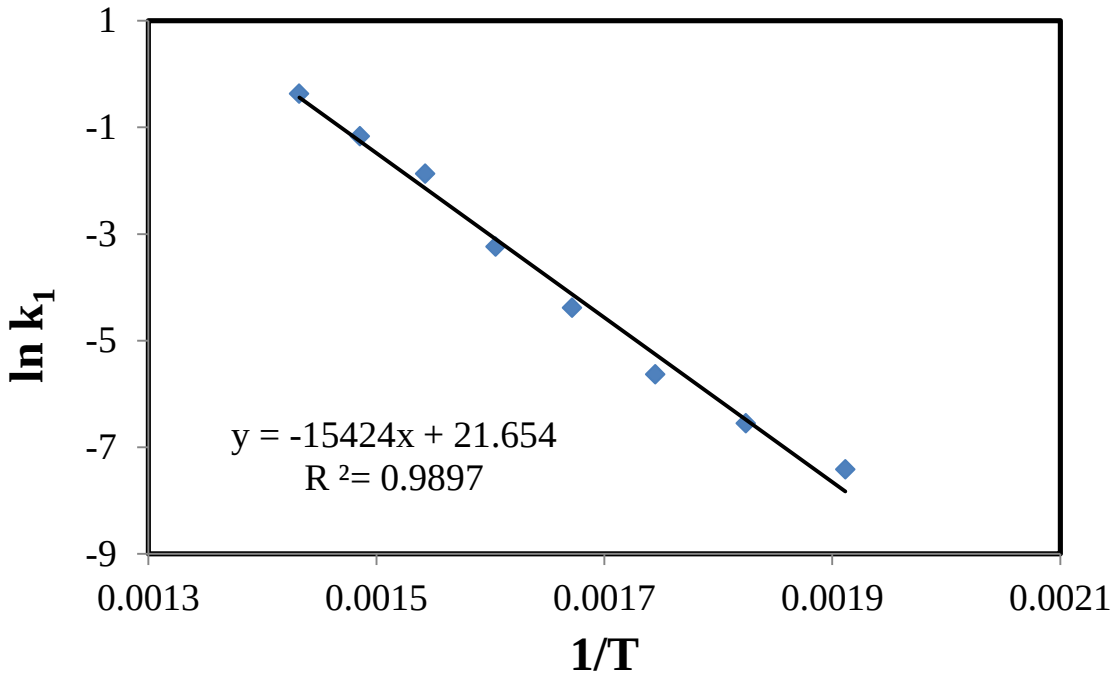

Fig. 26 Arrhenius plot of first-order reversible reaction model (forward reaction).

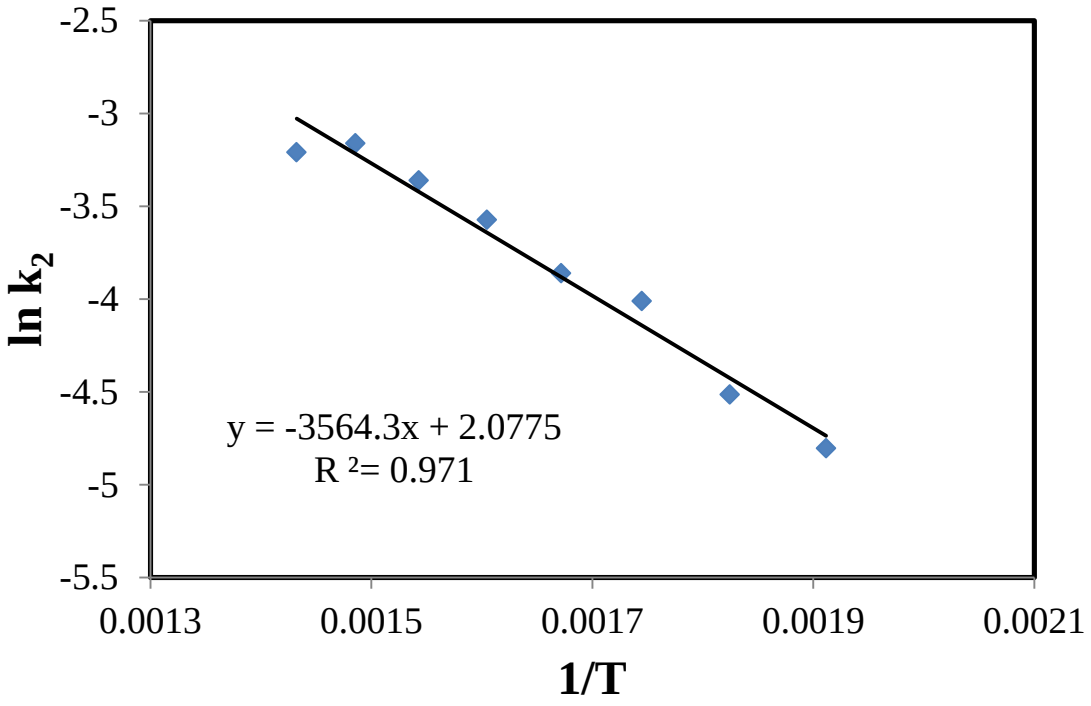

Fig. 27 Arrhenius plot of first-order reversible reaction model (backward reaction).

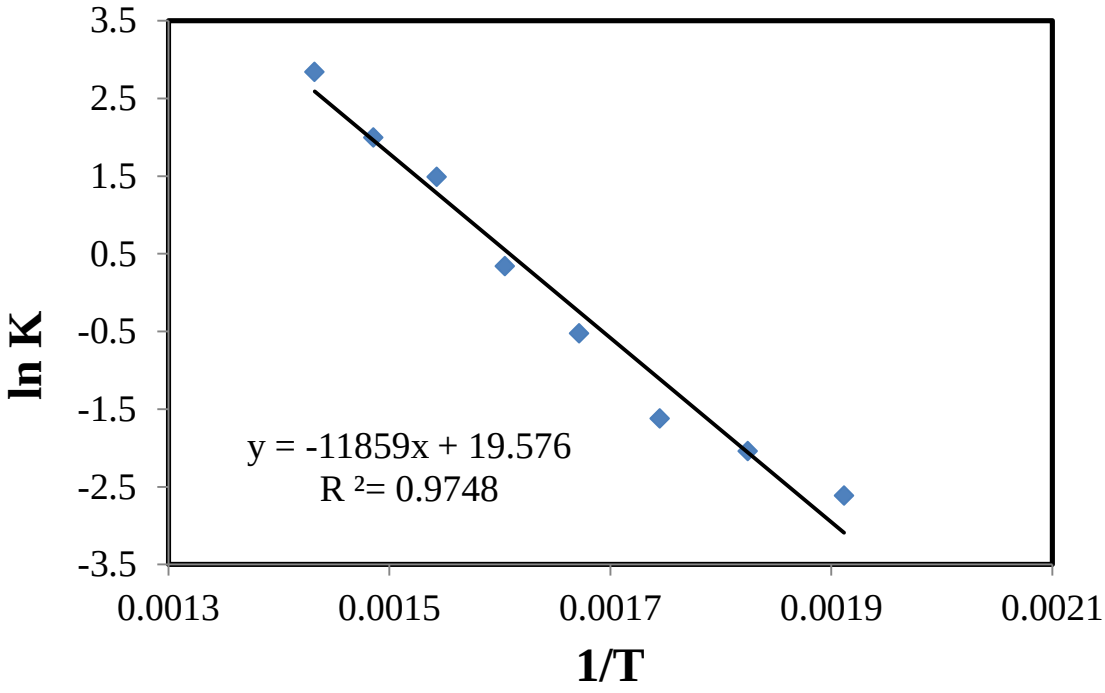

Fig. 28 Van't Hoff plot of first-order reversible reaction model.

where K is the reaction equilibrium constant, $K=k_1/k_2$, and ΔH^0 is the standard enthalpy of reaction. Similar to the Arrhenius plots, ln K versus 1/T is plotted, so ΔH^0 can be calculated. The van't Hoff plot is shown in Fig. 28.

In Fig. 26, 27 and 28, R^2 is found above 0.95 which suggests that the experimental data fit Arrhenius equation and van't Hoff equation very well, and it also suggests that the assumption of first-order reversible reaction model is reasonable.

Using the expression of each curve below, the kinetic parameters can be calculated by the gradient and intercept.

$$\ln k_1 = -15424 / T + 21.654 \tag{13}$$

$$\ln k_2 = -3564.3 / T + 2.0775 \tag{14}$$

$$\ln K = -11859 / T + 19.576 \tag{15}$$

For the forward reaction, the pre-exponential factor (A) is 2.54×10^9 min^{-1} and the activation energy (E_a) is 128.2 kJ/mol. For the reverse reaction, A is 7.98 min^{-1} and E_a is 29.6 kJ/mol. For the entire reaction, the standard enthalpy (ΔH^0) is 98.6 kJ/mol, which indicates that the thermal decomposition of biodiesel is an endothermic process.

Chapter 5: Conclusions

In this study, FAEE biodiesel was produced using vegetable oil and ethanol as feedstock. The vegetable oil used was soybean oil. Three kinds of catalysts were tested and KOH showed the best performance. In producing biodiesel, the molar ratio of oil to ethanol was 1:9, the weight of KOH was 1.5 wt% of vegetable oil. The reaction was kept at 75 ˚C for 2 hours, and then ethanol and catalyst was added again to repeat the whole procedure (this time, the molar ratio of oil to ethanol was reduced to 1:5, the weight percent of catalyst was kept the same), so the yield can be improved. Using GC-MSD, the composition of synthesized biodiesel can be obtained, the results showed that nearly 100 % FAEE biodiesel was produced.

In the thermal stressing experiments, the above biodiesel was mixed with ethanol at the volume ratio of 1:1 and was heated in stainless steel coils. The experiments were carried out at the temperature range from 250 to 425 ˚C for 3 to 63 min. At high temperature, residence time was reduced due to the occurrence of gases. Final products were analyzed using GC-FID and GC-MSD to determine product compositions. It is found that FAEE biodiesel is very stable below 275 ˚C. In the thermal decomposition of biodiesel, there are 3 main reactions and their temperature range shows below: isomerization reactions (≥275 ˚C), polymerization reactions (≥300 ˚C) and pyrolysis reactions (≥350 ˚C).

In isomerization reactions, cis-type C18:2 FAEE was converted into trans-type C18:2 FAEE. In polymerization reactions, the production of dimers and polymers was detected, which are a result of the Diels-Alder reactions. In pyrolysis reactions, gases and small molecular weight compounds were observed in the experiments, these were two indications of pyrolysis reactions.

The decomposition ratio under each experimental condition was calculated using the peak area in the GC-FID plots.

Due to the complicated reactions in the thermal decomposition of biodiesel, a simplified model is considered. In this work, two kinetic models (first-order reversible reaction model and first-order irreversible reaction model) were proposed to fit the experimental data using the software *Micromath Scientist*. The results show that the reversible reaction model fits the data from 250 to 400 ˚C and the irreversible reaction model fits the data at 425 ˚C, which indicates that the main reaction is pyrolysis at 425 ˚C. Therefore, the first-order reversible reaction model is used to calculate basic kinetic parameters in the thermal decomposition of biodiesel.

Using the reaction rate constants and Arrhenius equation, pre-exponential factor (A) and activation energy (E_a) in the first-order reversible reaction model were determined by plotting ln k versus 1/T. For the forward reaction, A and E_a are 2.54×10^9 min^{-1} and 128.2 kJ/mol, respectively. For the backward reaction, A and E_a are 7.98 min^{-1} and 29.6 kJ/mol, respectively. Furthermore, the standard enthalpy (ΔH^0) can be obtained by the equilibrium constant and van't Hoff equation. The standard enthalpy is 98.6 kJ/mol for the thermal decomposition of biodiesel, which indicates that the thermal decomposition of biodiesel is an endothermic process.

Chapter 6: Future work

In this study, the main purpose is to analyze the thermal stability of FAEE biodiesel mixed with ethanol, thermal stability of FAEE biodiesel itself has not been explored. Once the latter experiment is done, the effect of ethanol can be known, whether it is promoting or restraining the thermal decomposition of biodiesel. The viscosity and cold flow properties of thermal stressed biodiesel should also be tested in the future, which will reveal the effect of high temperature on the quality of biodiesel fuels.

As mentioned in the experimental section, the temperature gap was 25 ˚C, so it only showed the approximate starting temperature of each reaction. Therefore, the temperature gap should be decreased and more experiments should be done, especially around reaction starting temperature, so that more accurate data can be obtained.

Appendix Supplementary information

In this section, more detailed information is provided.

Fig.A-1 is the GC-FID plot of heptane, which shows that solvent peak only appears at the beginning of the chromatogram and it has no effect on the biodiesel peaks.

Fig.A-2 to Fig.A-6 show the GC-FID plots of pure FAEE biodiesel at different concentrations. Table A-1 shows the total peak area at different concentrations. Using the concentration and its total peak area, the calibration curve of FAEE biodiesel can be obtained in Fig A-7.

Fig.A-8 to Fig.A-31 record the GC-FID plots of thermal stressed FAEE biodiesel under different conditions. By comparing the peaks, the mechanism in thermal decomposition of biodiesel can be studied.

Table A-2 shows the GC-FID peak area of pure FAEE biodiesel, which can be used to establish the calibration curve. The total peak area represents the peak area of C16:0, C18:0 and C18:1-3, which are the main components in pure FAEE biodiesel.

Table A-3 is the GC-FID peak area of thermal stressed samples, using the calibration curve equation (Equation 4 in Section 4.3), the concentration of undecomposed biodiesel can be calculated. The total peak area here has the same meaning as that in Table A-2.

Table A-4 shows the concentration of undecomposed biodiesel under different experimental conditions, which can be used to calculate some kinetic parameters.

At the end, two examples were also provided. E1- example calculation shows the calculation of how decomposition ratio was obtained. E2- isomerization reaction shows how isomers were determined in GC-FID plots.

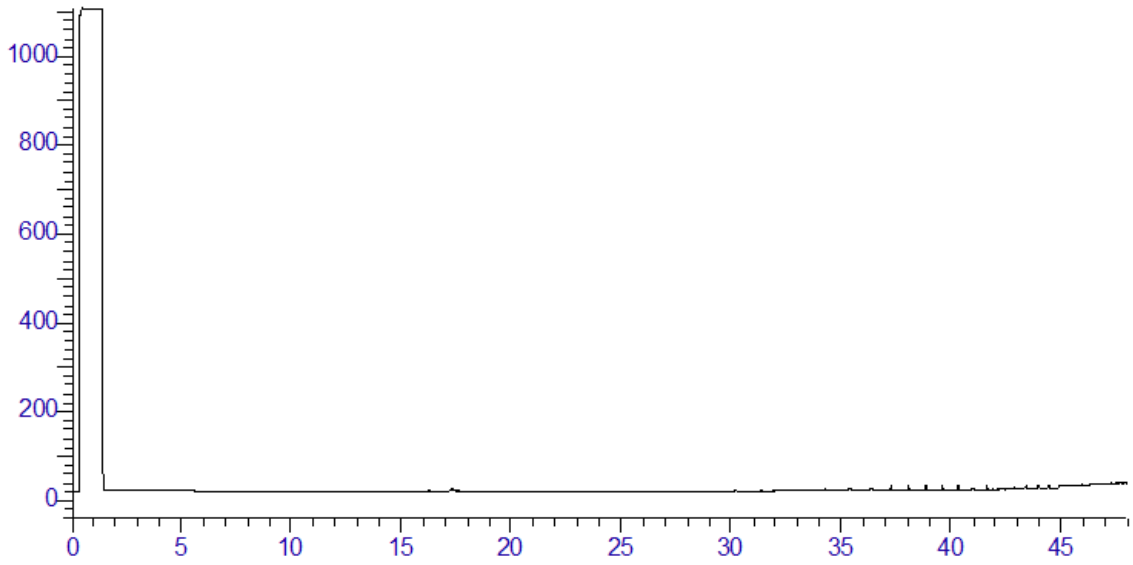

Fig.A- 1 GC-FID plot of pure heptane.

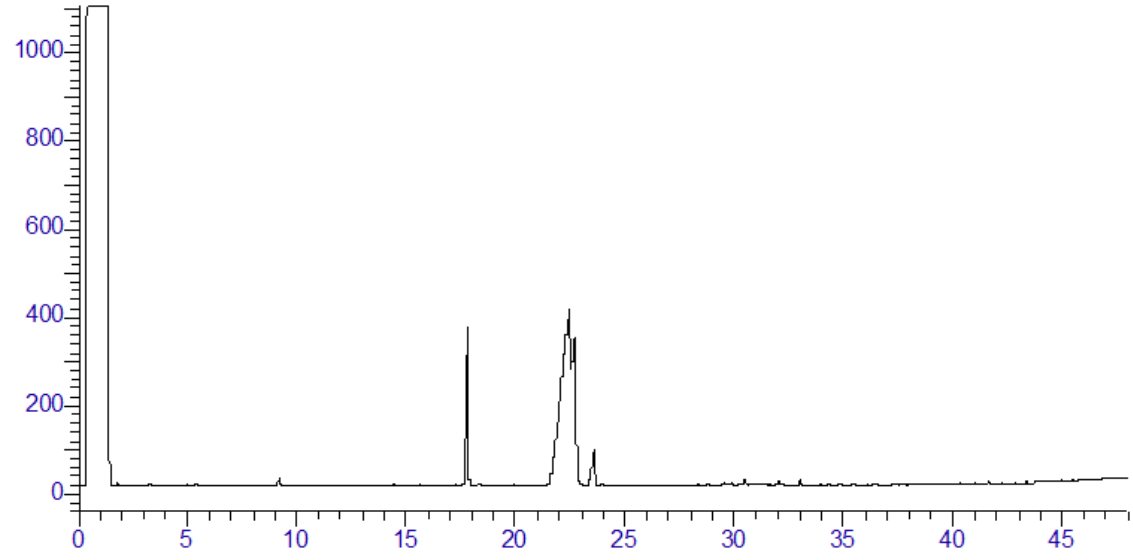

Fig.A- 2 GC-FID plot of 500 ppm FAEE biodiesel (volume ratio).

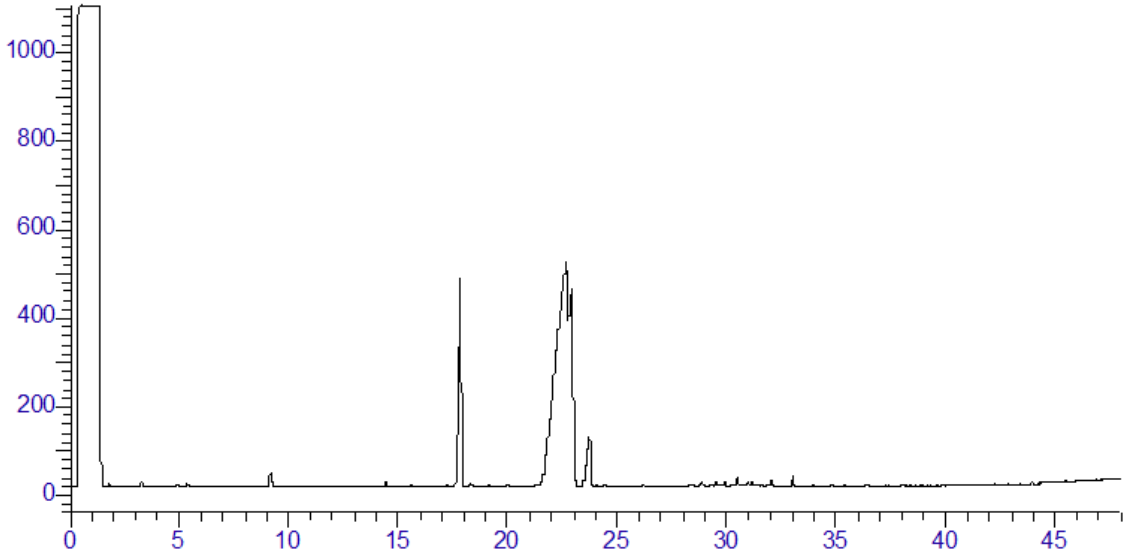

Fig.A- 3 GC-FID plot of 1000 ppm FAEE biodiesel (volume ratio).

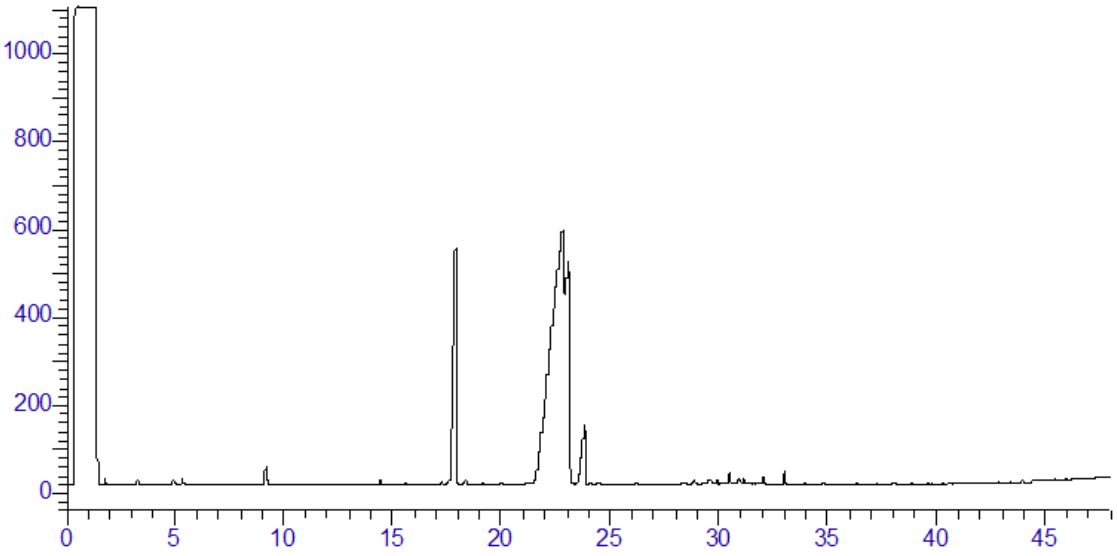

Fig.A- 4 GC-FID plot of 1500 ppm FAEE biodiesel (volume ratio).

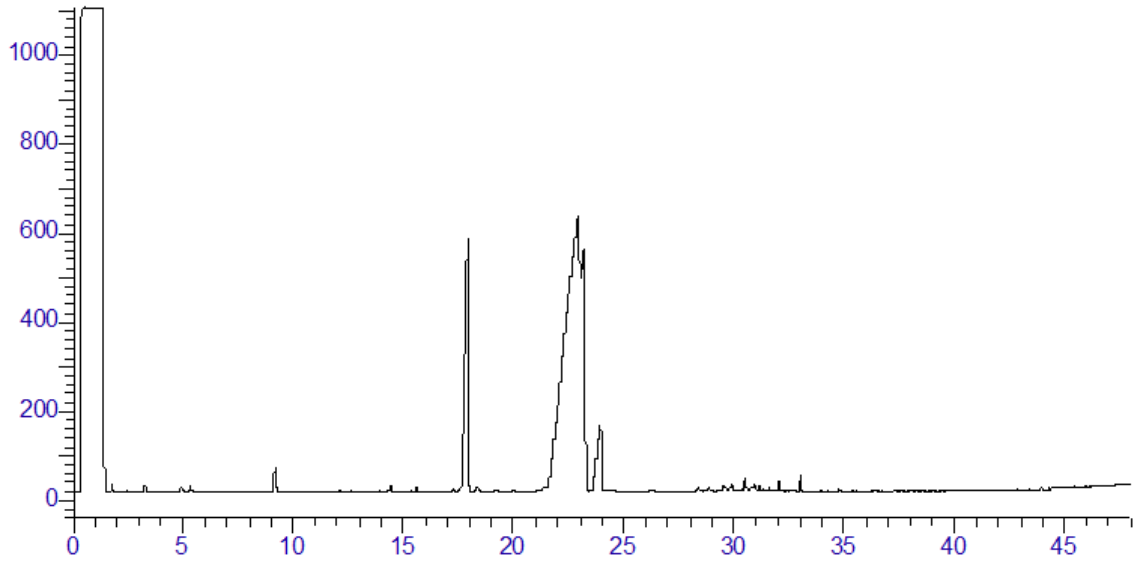

Fig.A- 5 GC-FID plot of 2000 ppm FAEE biodiesel (volume ratio).

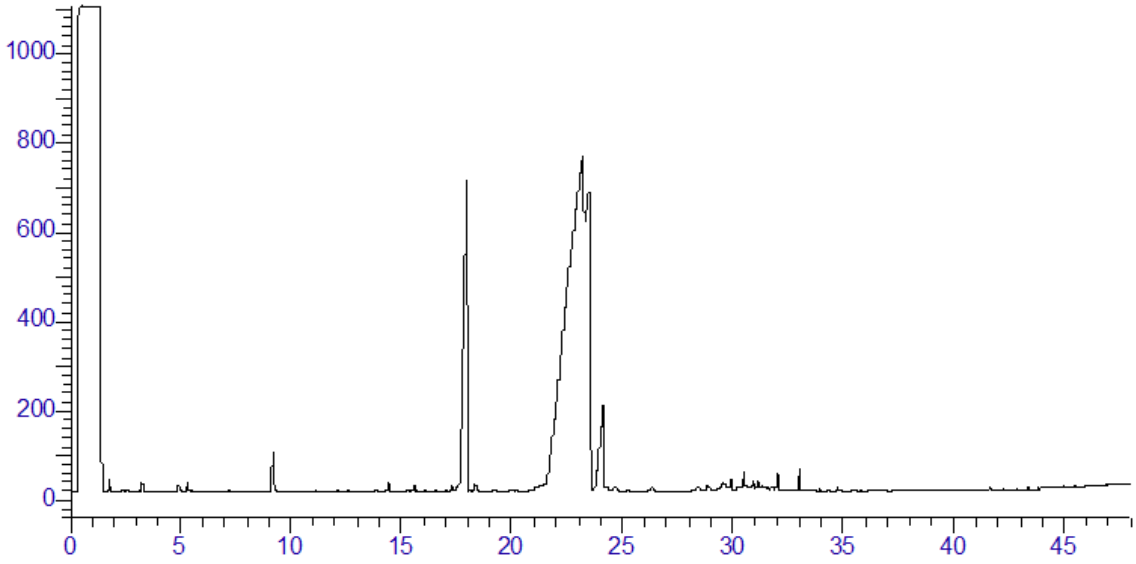

Fig.A- 6 GC-FID plot of 3000 ppm FAEE biodiesel (volume ratio).

Table A- 1 Peak area of pure FAEE biodiesel at different concentration

Concentration (ppm)	Peak area ($\times 10^6$)	
	C16:0	Total
500	2.61	20.13
500 R*	2.61	20.36
1000	4.00	29.99
1000 R*	4.11	30.80
1500	5.08	38.23
1500 R*	5.21	38.83
2000	6.21	47.61
2000 R*	5.81	43.75
3000	8.10	62.02
3000 R*	8.10	62.33

R*-Replicate experiments

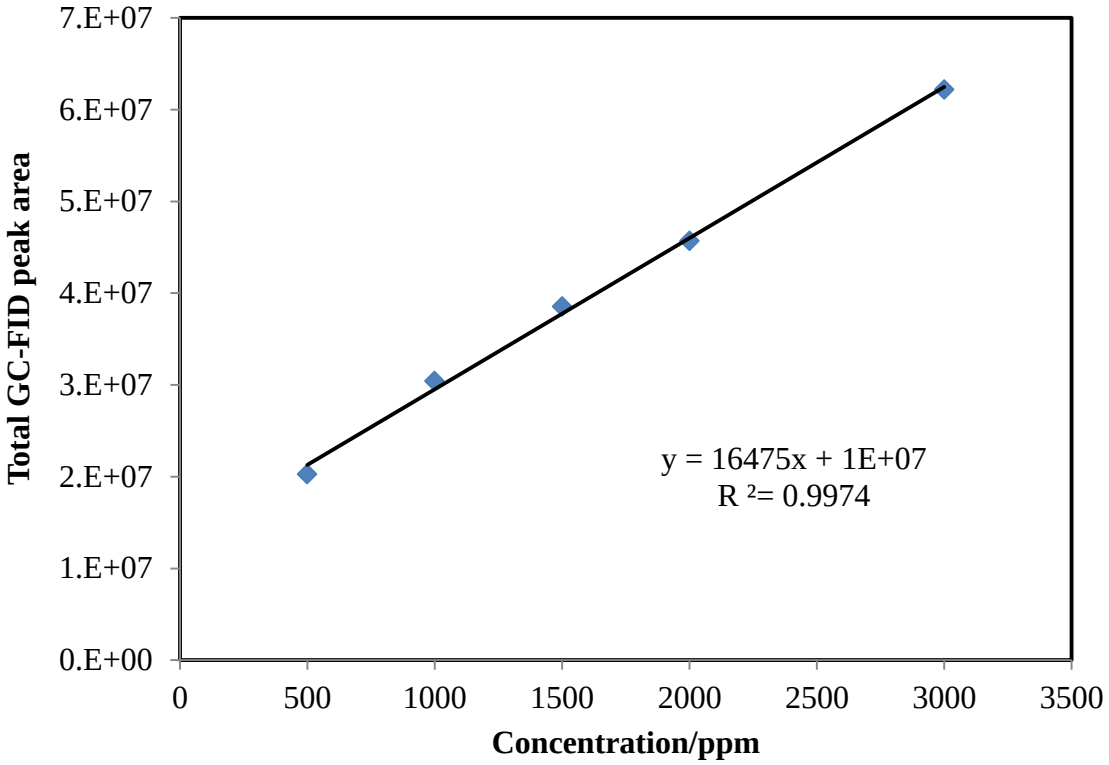

Fig.A- 7 GC-FID calibration curve of pure FAEE biodiesel

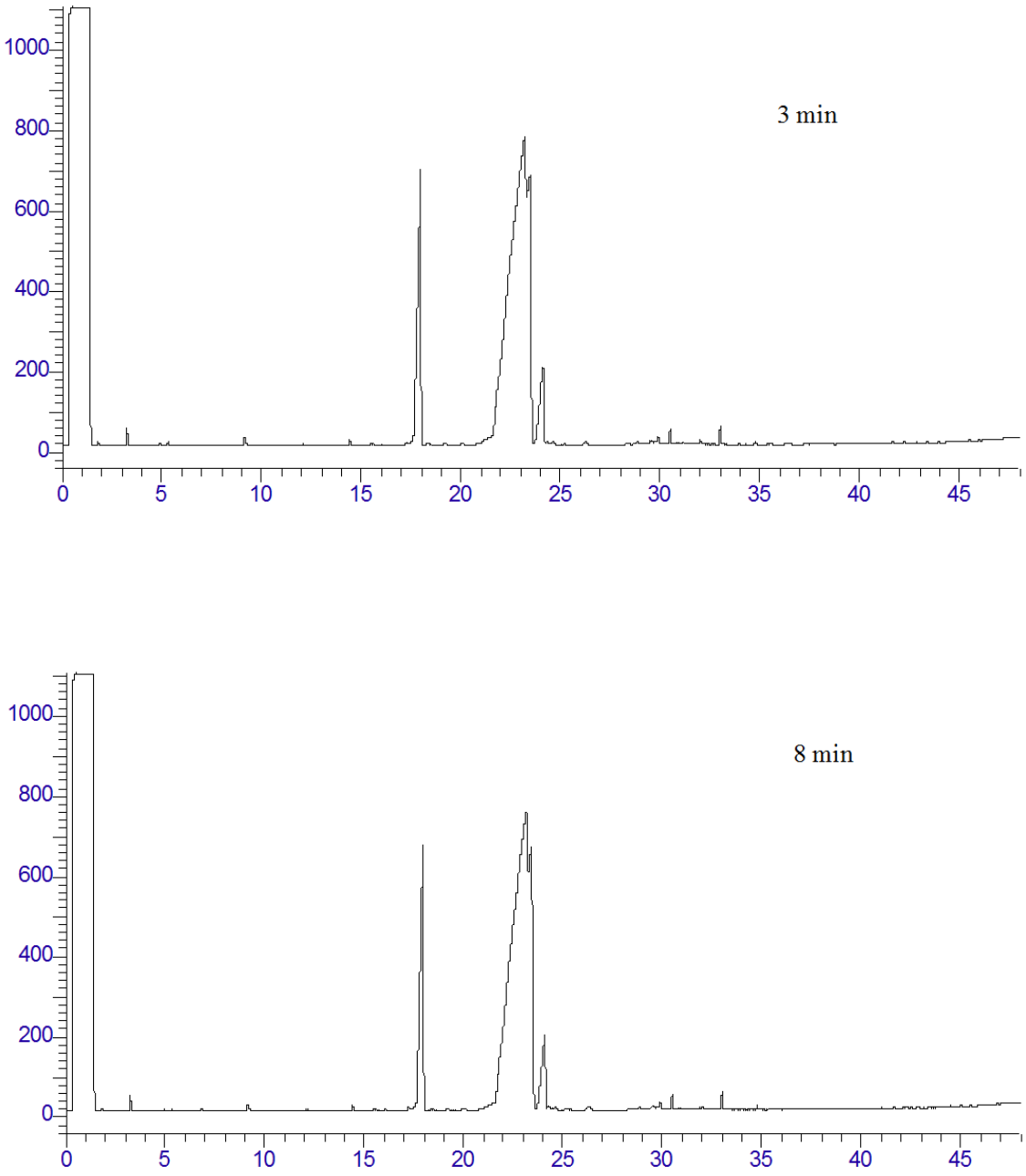

Fig.A- 8 GC-FID plot of FAEE biodiesel thermal stressed at 250 ˚C for 3 and 8 min.

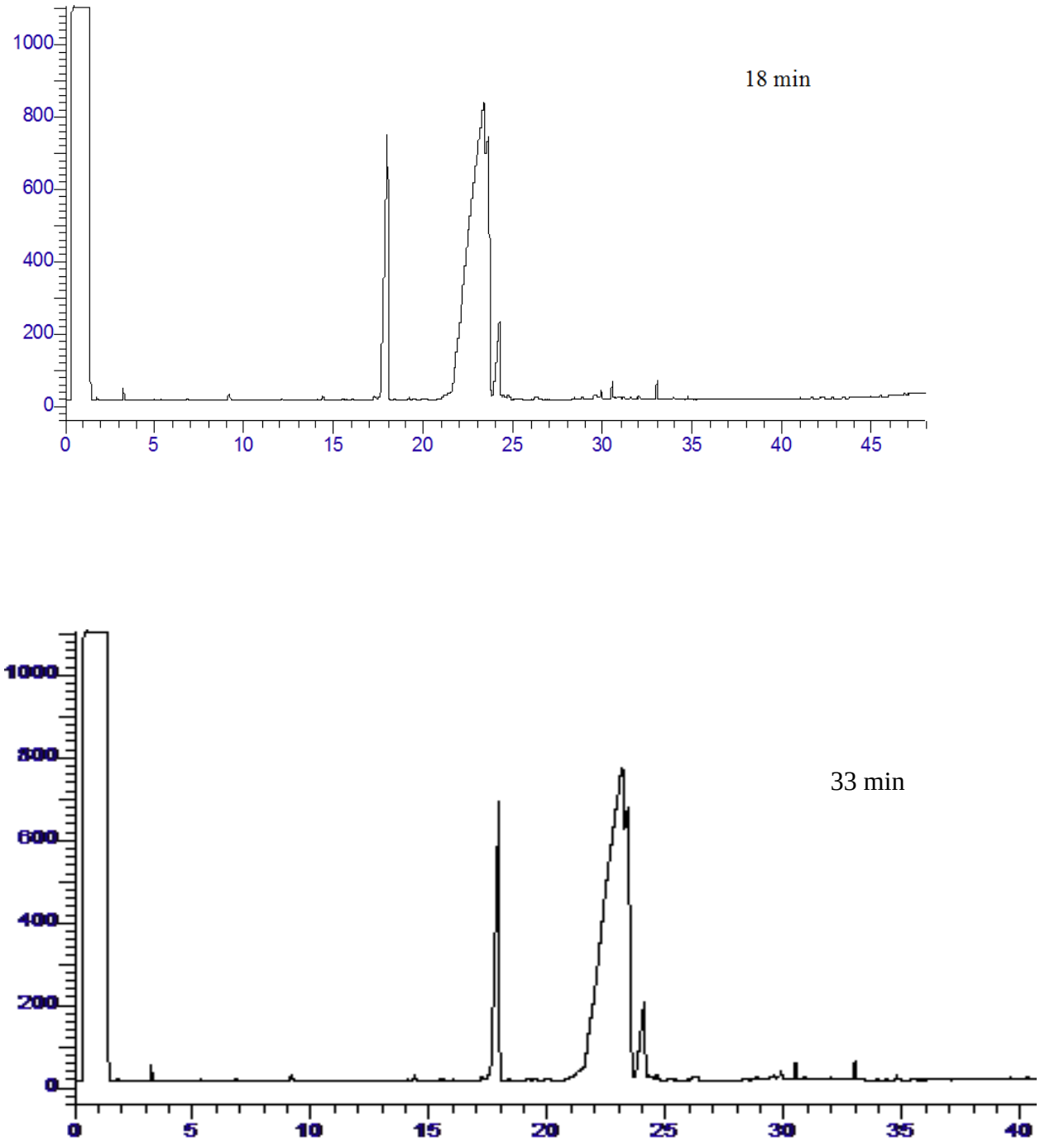

Fig.A- 9 GC-FID plot of FAEE biodiesel thermal stressed at 250 ˚C for 18 and 33 min.

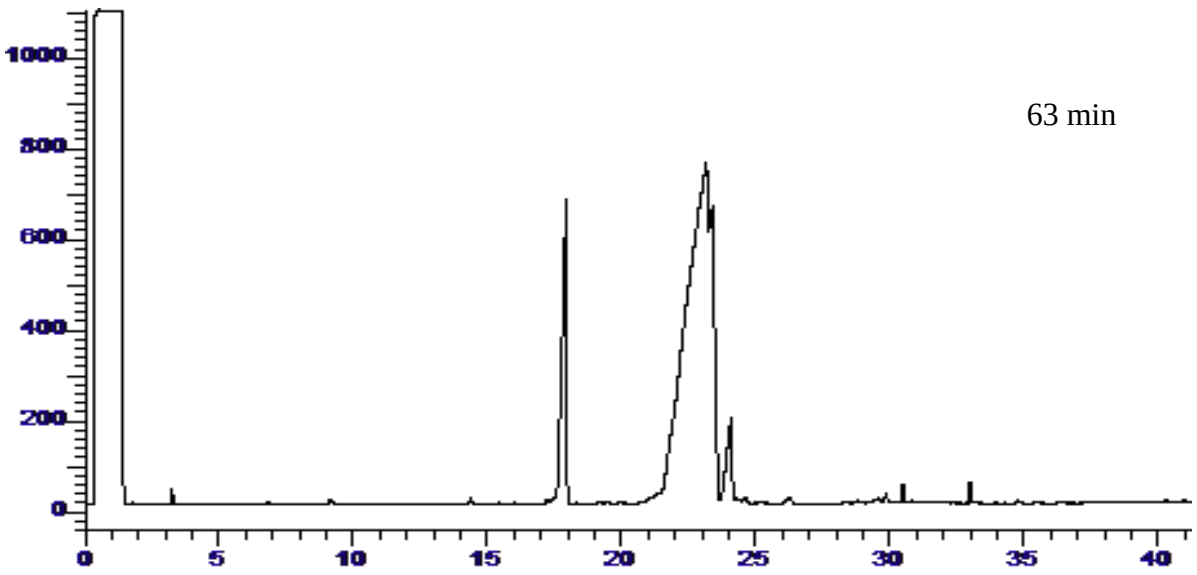

Fig.A- 10 GC-FID plot of FAEE biodiesel thermal stressed at 250 ˚C for 63 min.

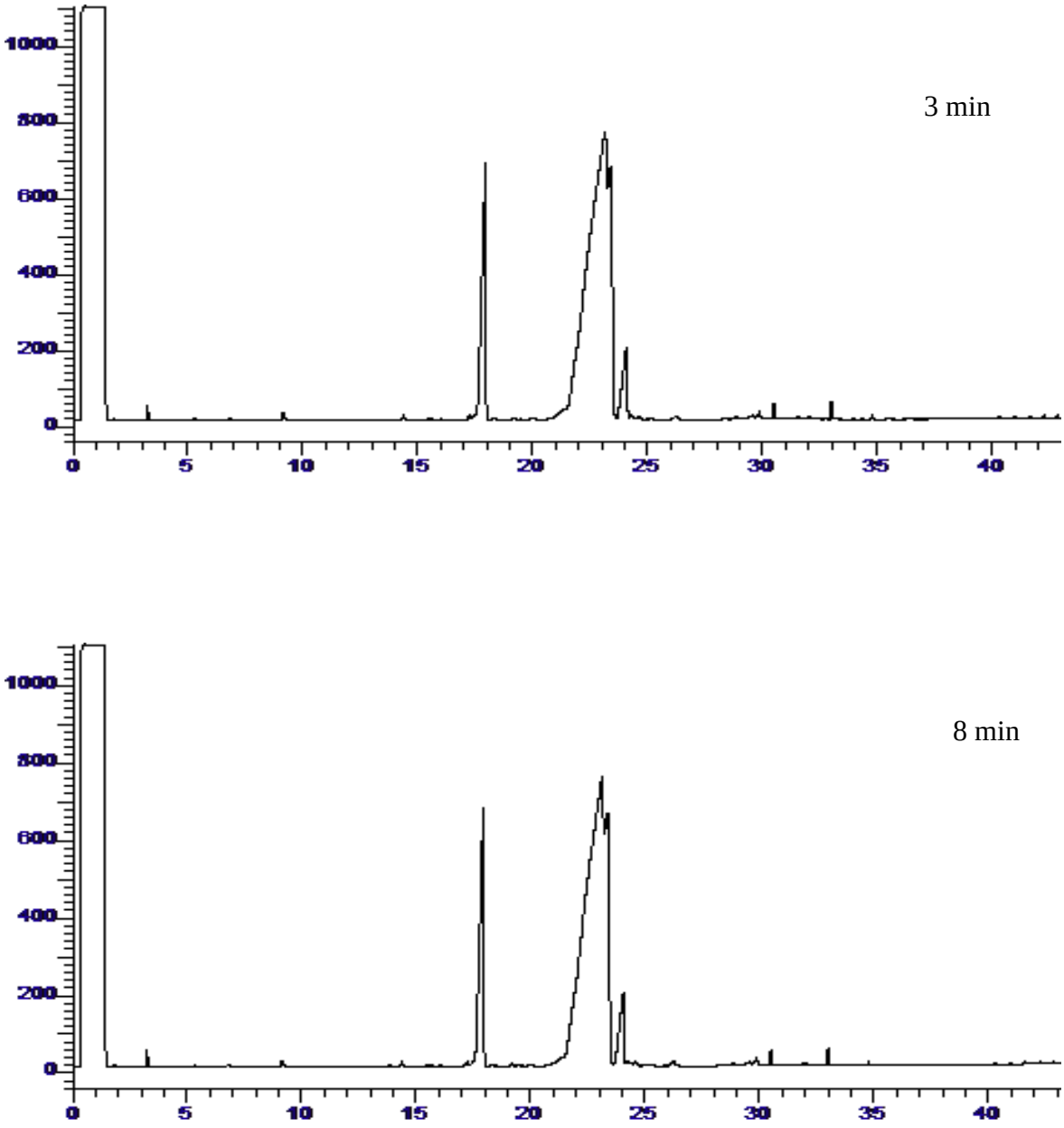

Fig.A- 11 GC-FID plot of FAEE biodiesel thermal stressed at 275 ˚C for 3 and 8 min.

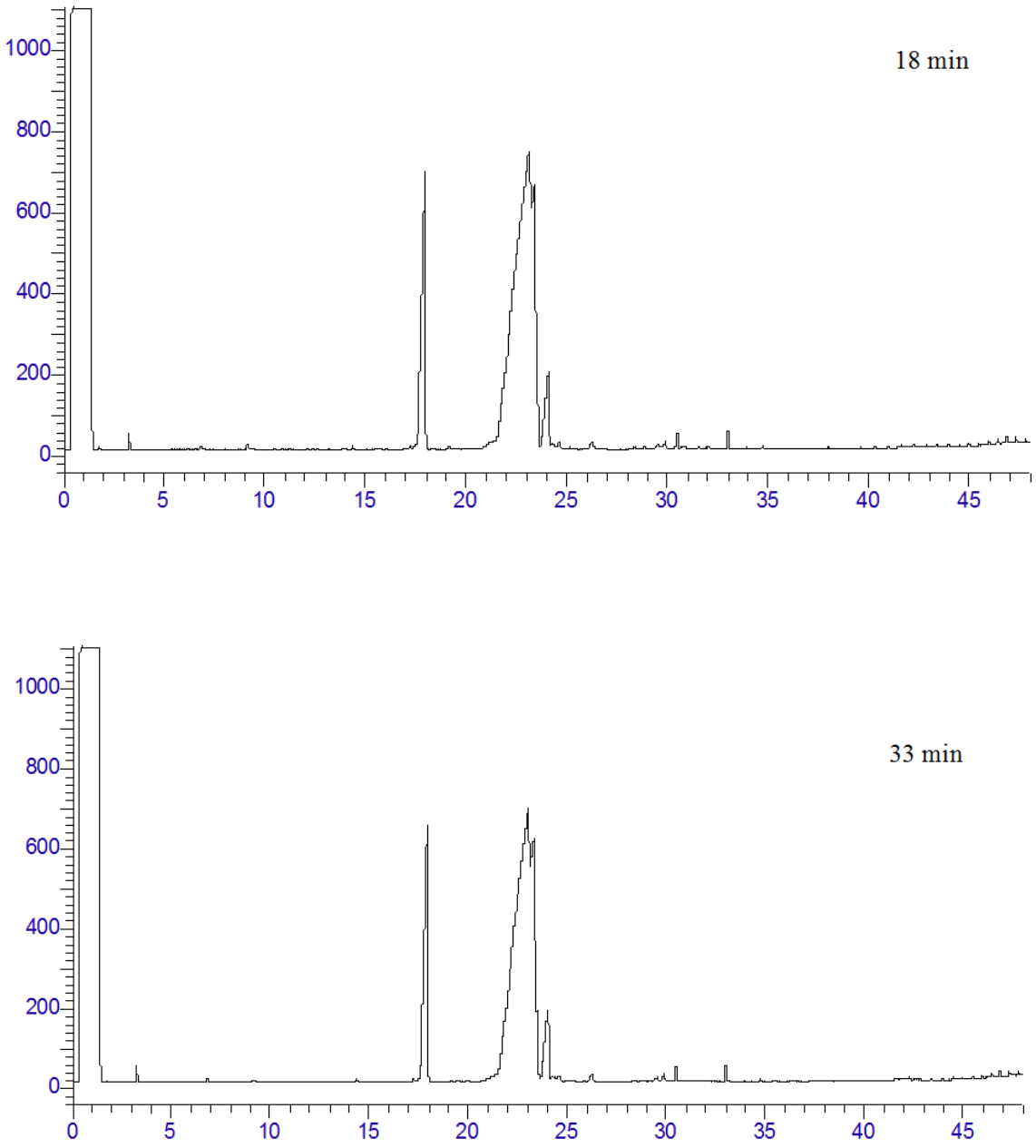

Fig.A- 12 GC-FID plot of FAEE biodiesel thermal stressed at 275 ˚C for 18 and 33 min.

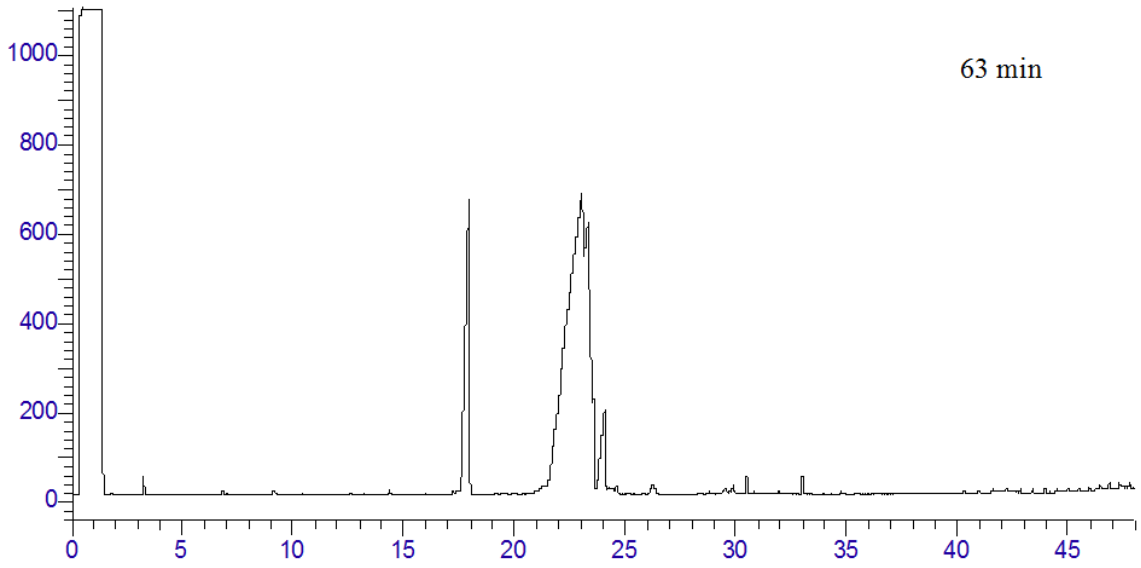

Fig.A- 13 GC-FID plot of FAEE biodiesel thermal stressed at 275 ˚C for 63 min.

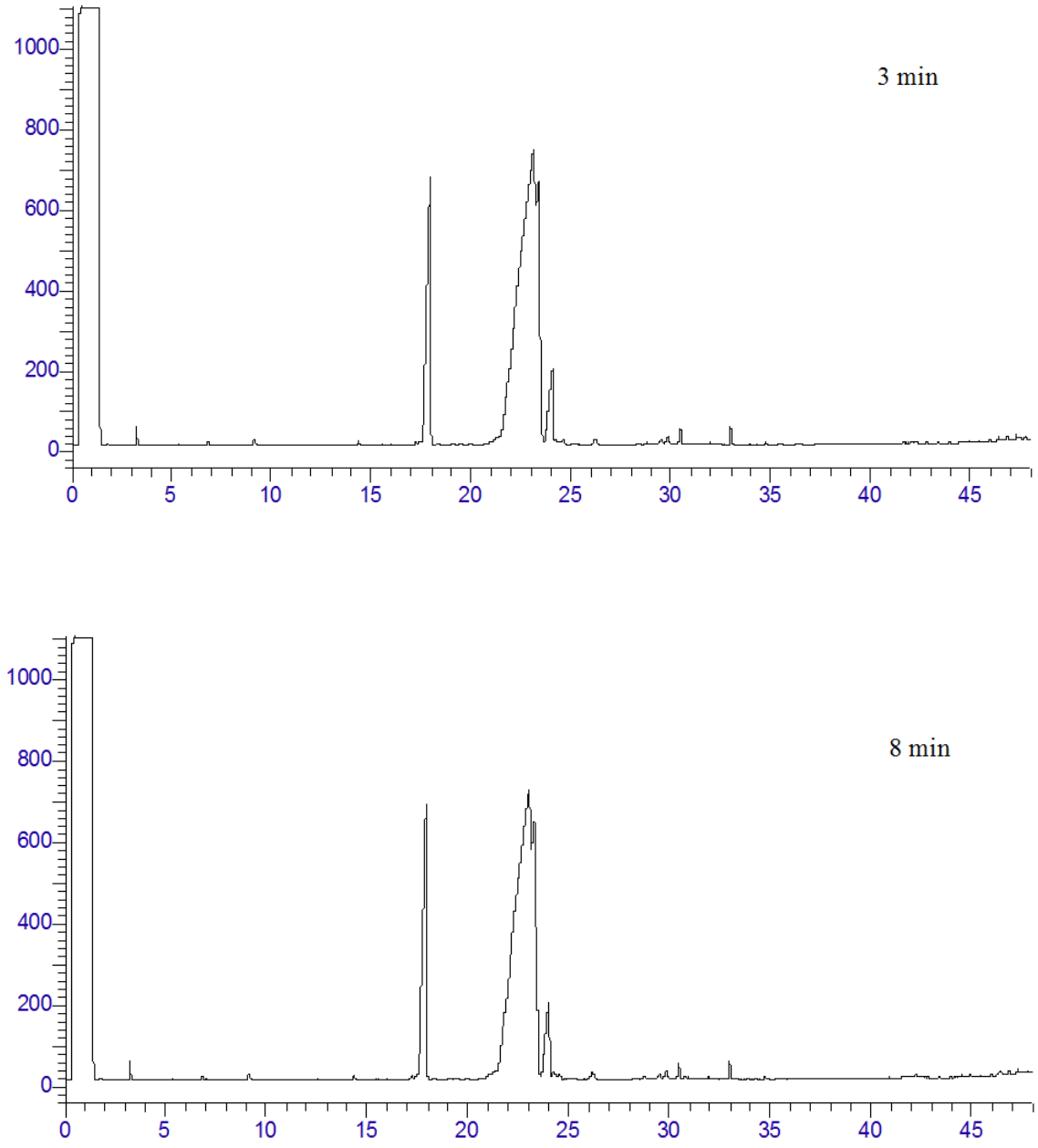

Fig.A- 14 GC-FID plot of FAEE biodiesel thermal stressed at 300 ˚C for 3 and 8 min.

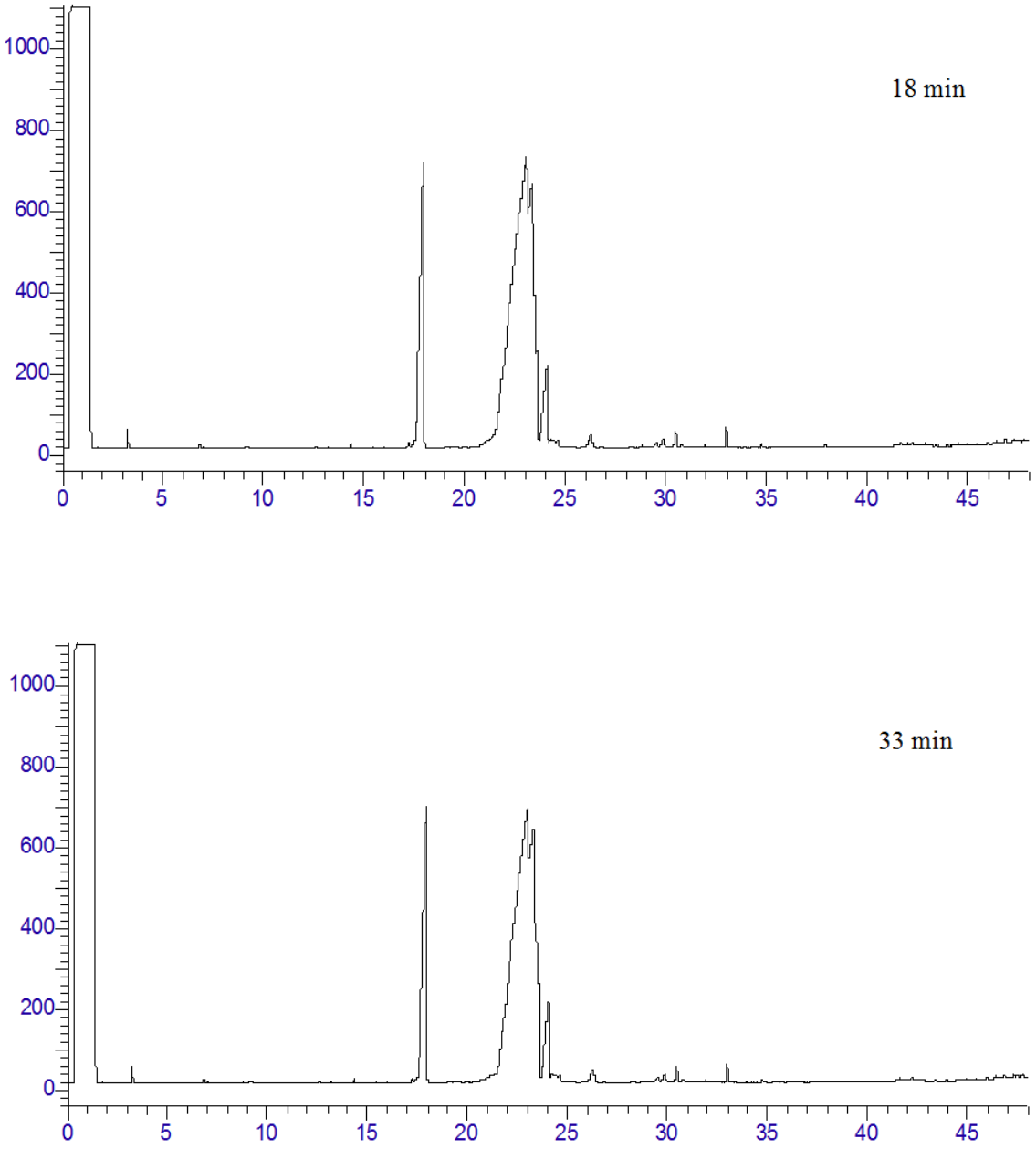

Fig.A- 15 GC-FID plot of FAEE biodiesel thermal stressed at 300 ˚C for 18 and 33 min.

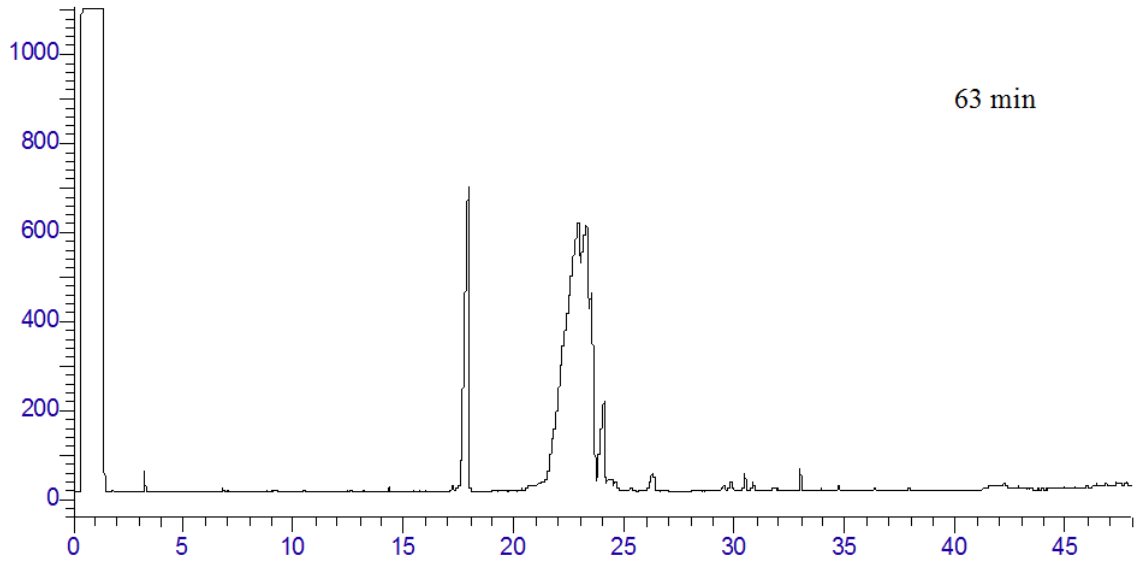

Fig.A- 16 GC-FID plot of FAEE biodiesel thermal stressed at 300 ˚C for 63 min.

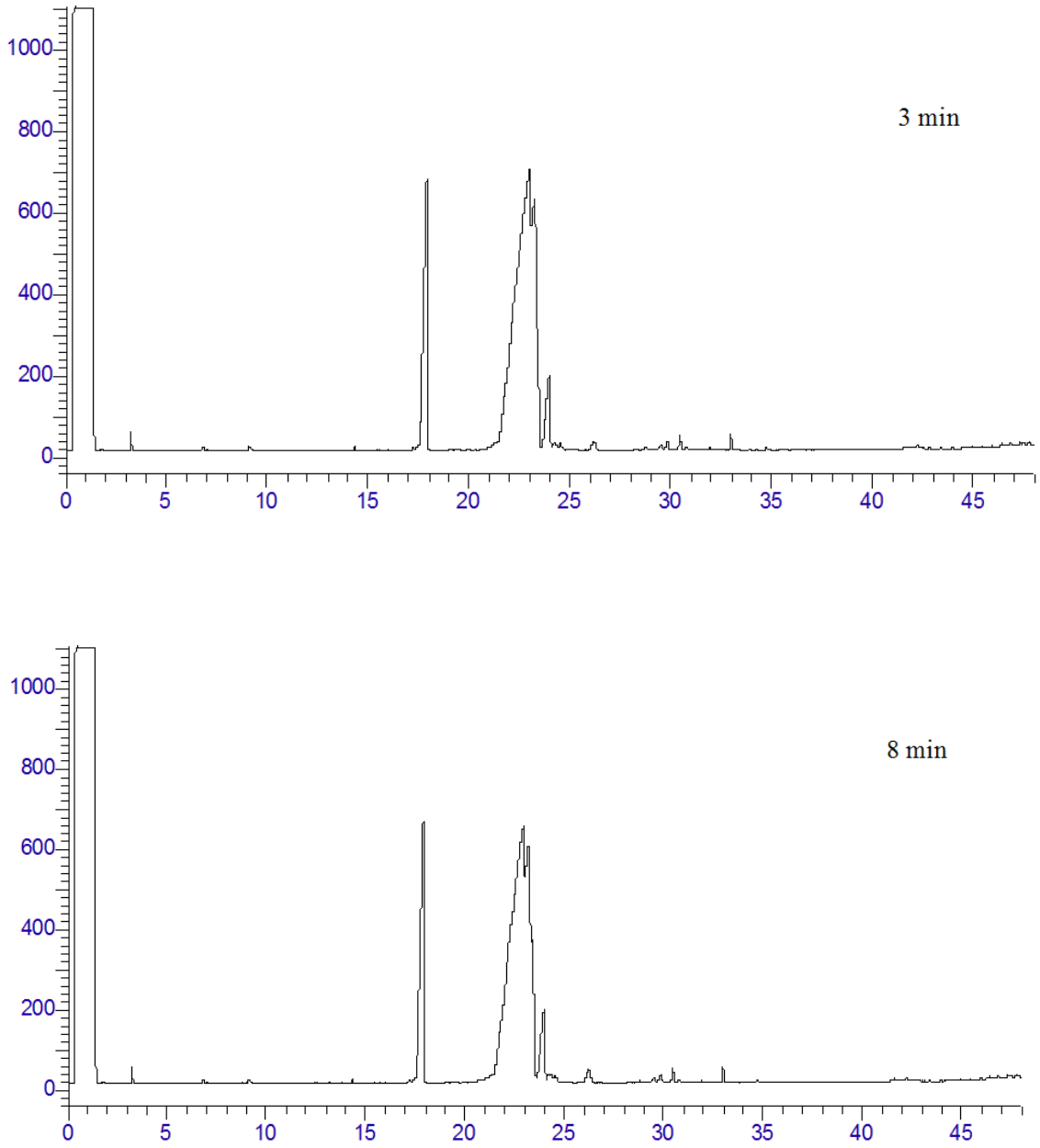

Fig.A- 17 GC-FID plot of FAEE biodiesel thermal stressed at 325 ˚C for 3 and 8 min.

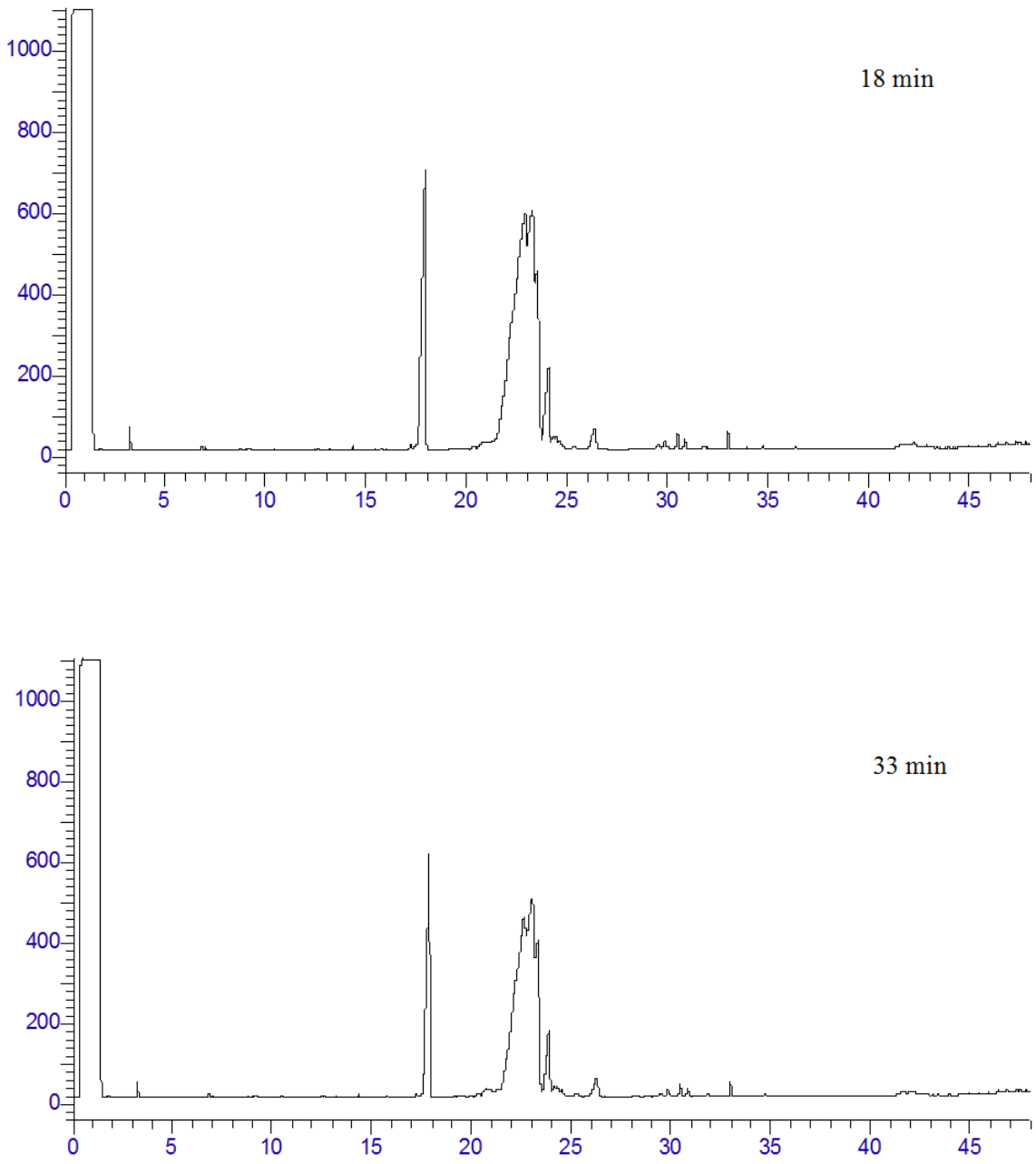

Fig.A- 18 GC-FID plot of FAEE biodiesel thermal stressed at 325 ˚C for 18 and 33 min.

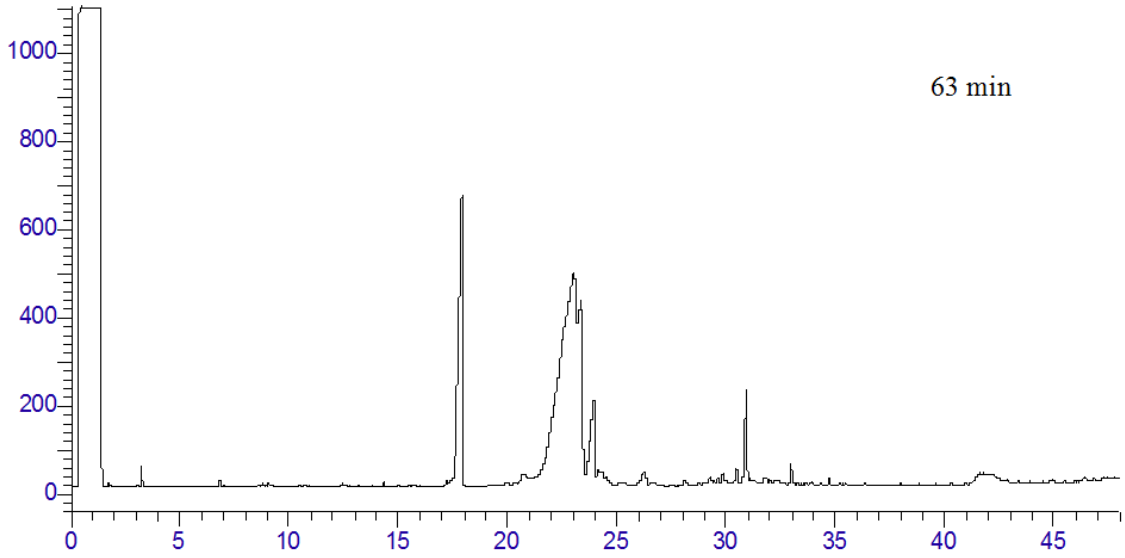

Fig.A- 19 GC-FID plot of FAEE biodiesel thermal stressed at 325 ˚C for 63 min.

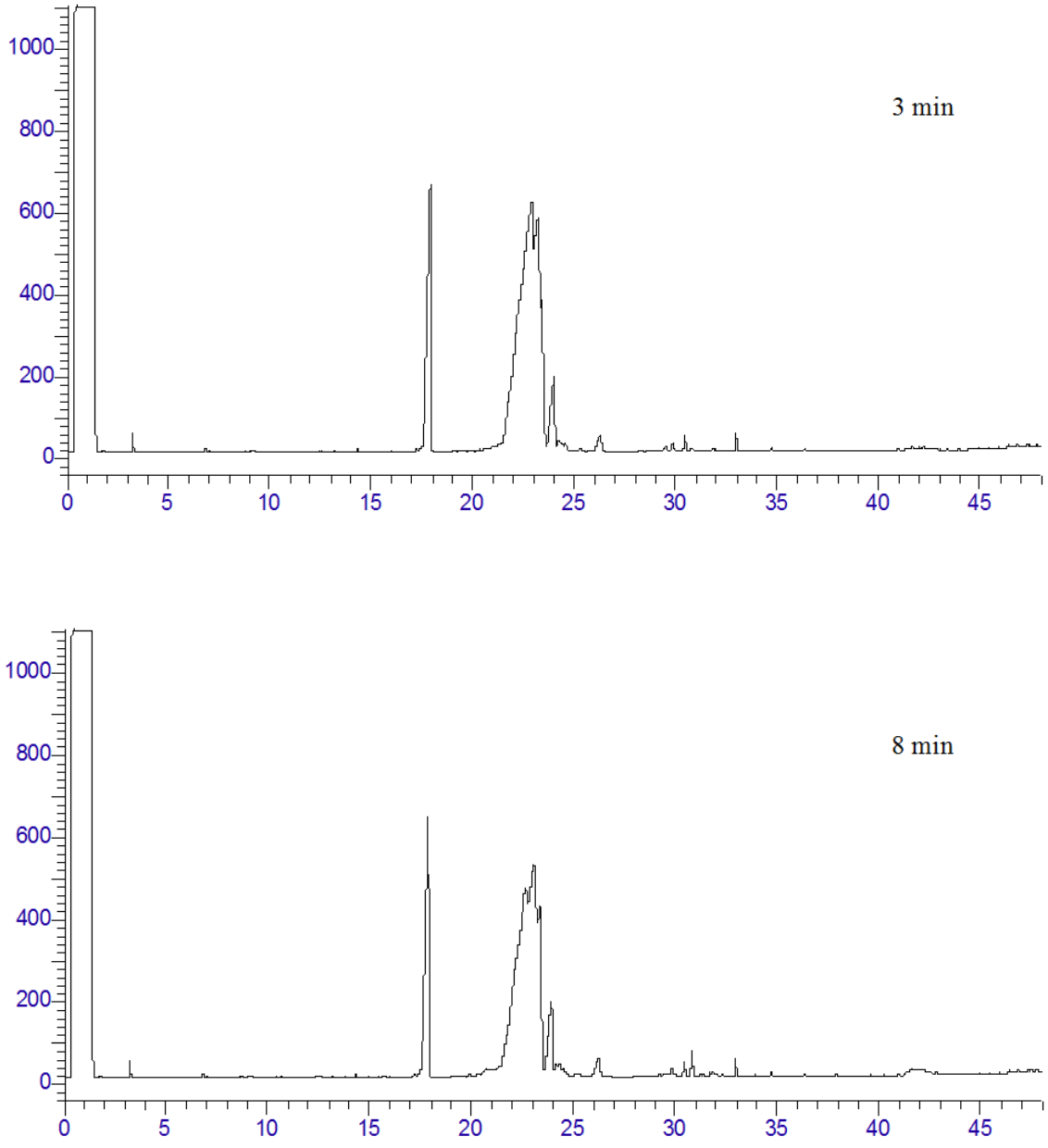

Fig.A- 20 GC-FID plot of FAEE biodiesel thermal stressed at 350 ˚C for 3 and 8 min.

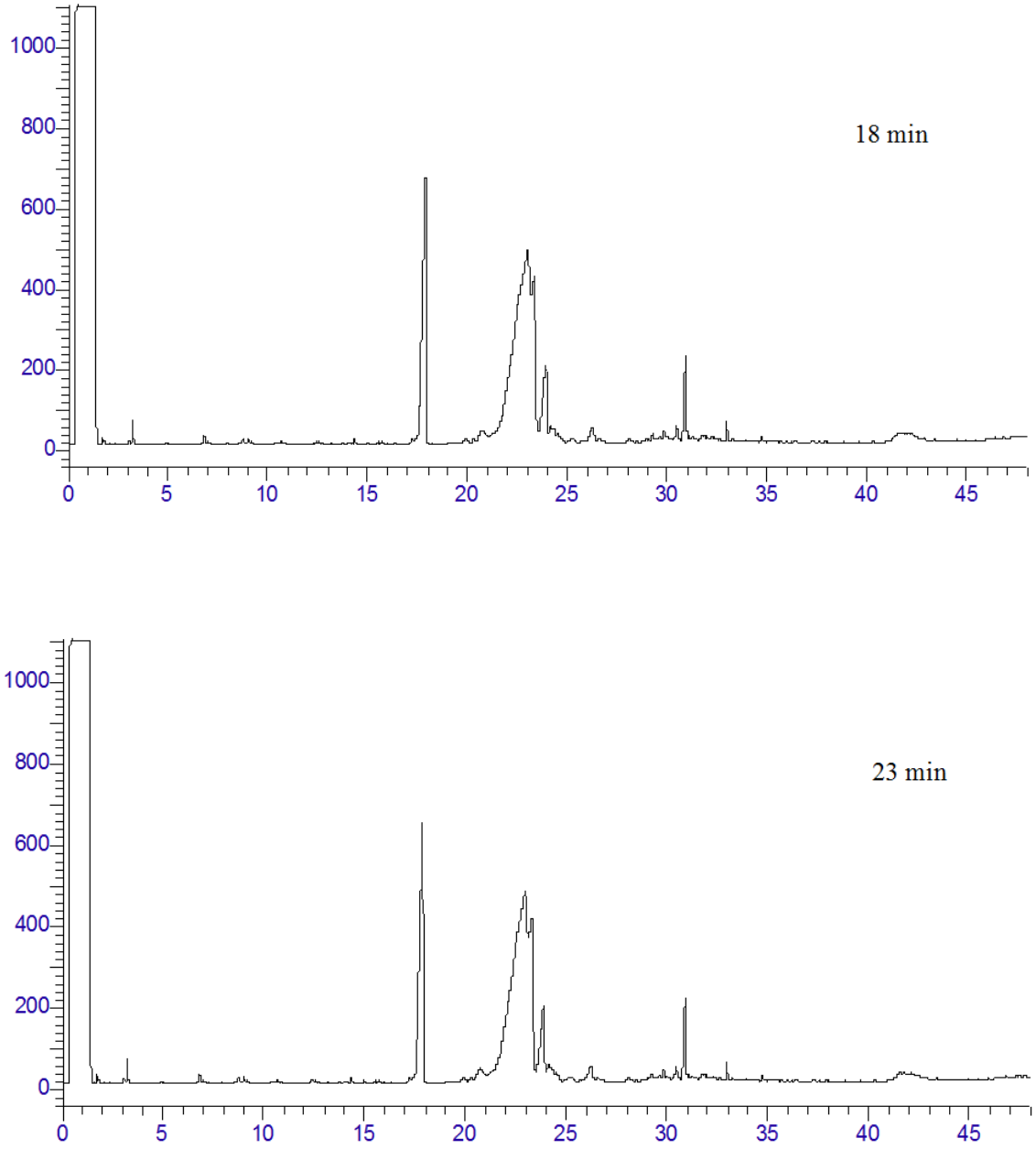

Fig.A- 21 GC-FID plot of FAEE biodiesel thermal stressed at 350 ˚C for 18 and 23 min.

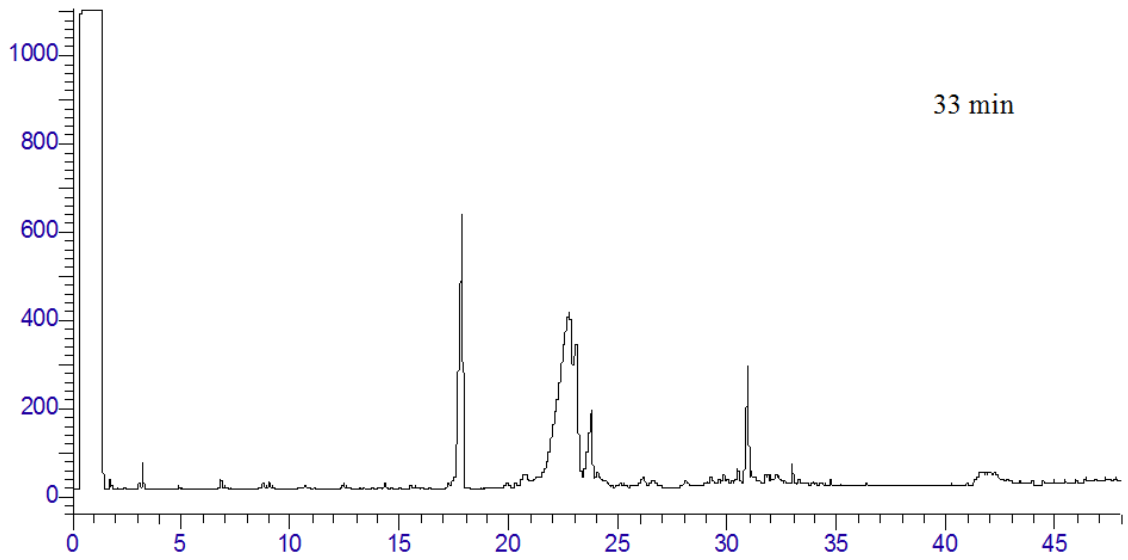

Fig.A- 22 GC-FID plot of FAEE biodiesel thermal stressed at 350 ˚C for 33 min.

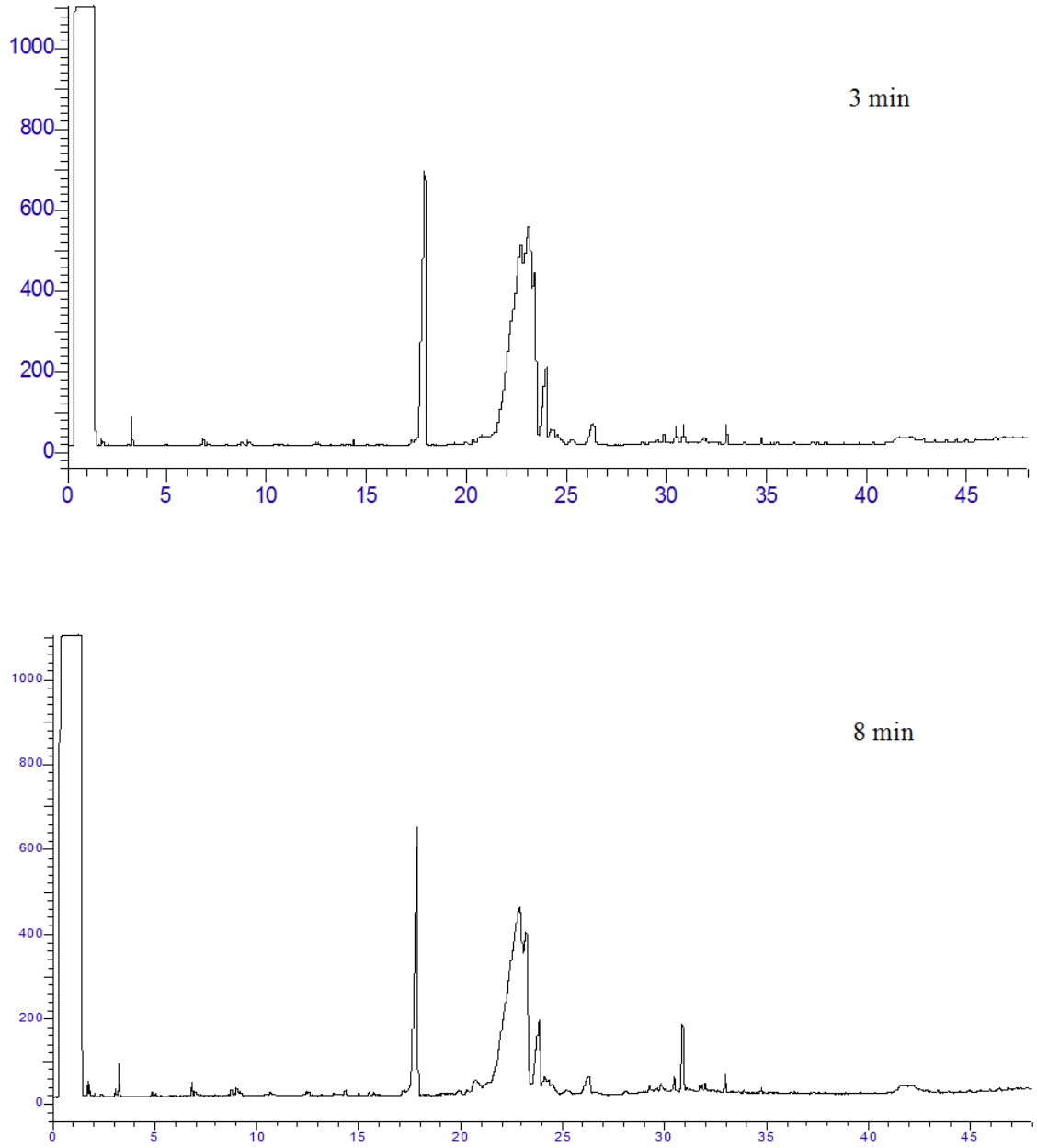

Fig.A- 23 GC-FID plot of FAEE biodiesel thermal stressed at 375 ˚C for 3 and 8 min.

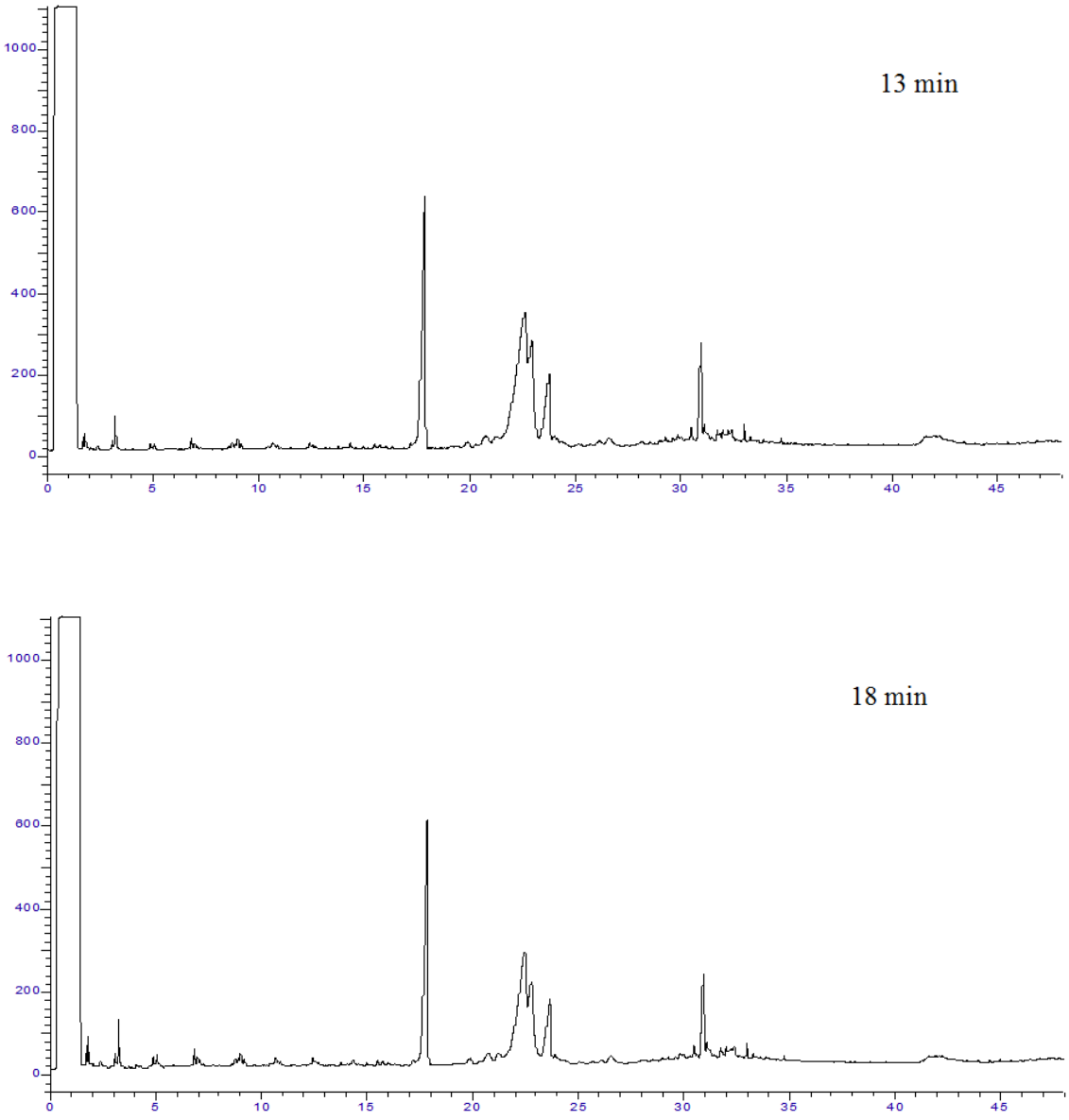

Fig.A- 24 GC-FID plot of FAEE biodiesel thermal stressed at 375 ˚C for 13 and 18 min.

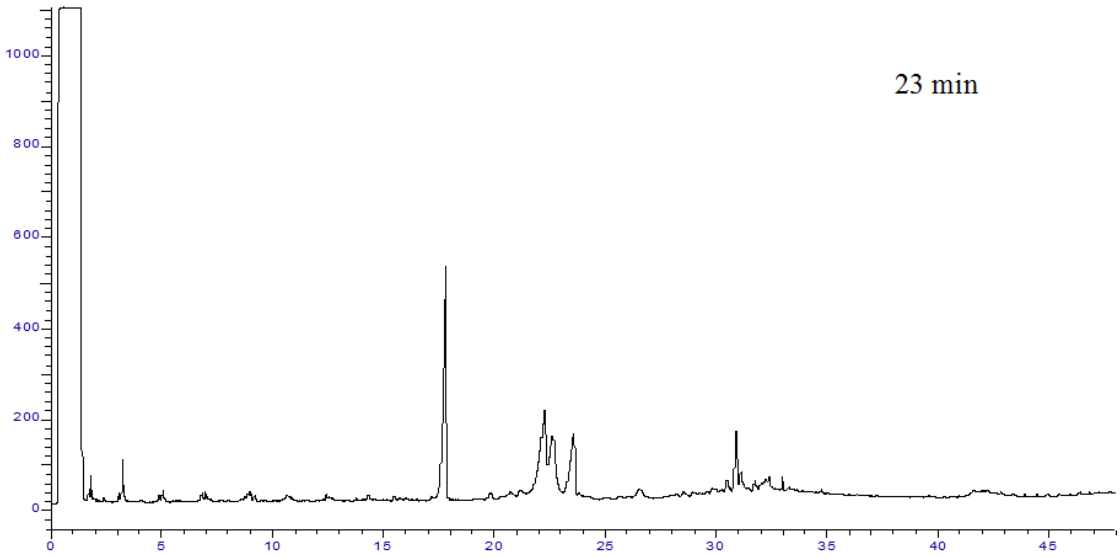

Fig.A- 25 GC-FID plot of FAEE biodiesel thermal stressed at 375 ˚C for 23 min.

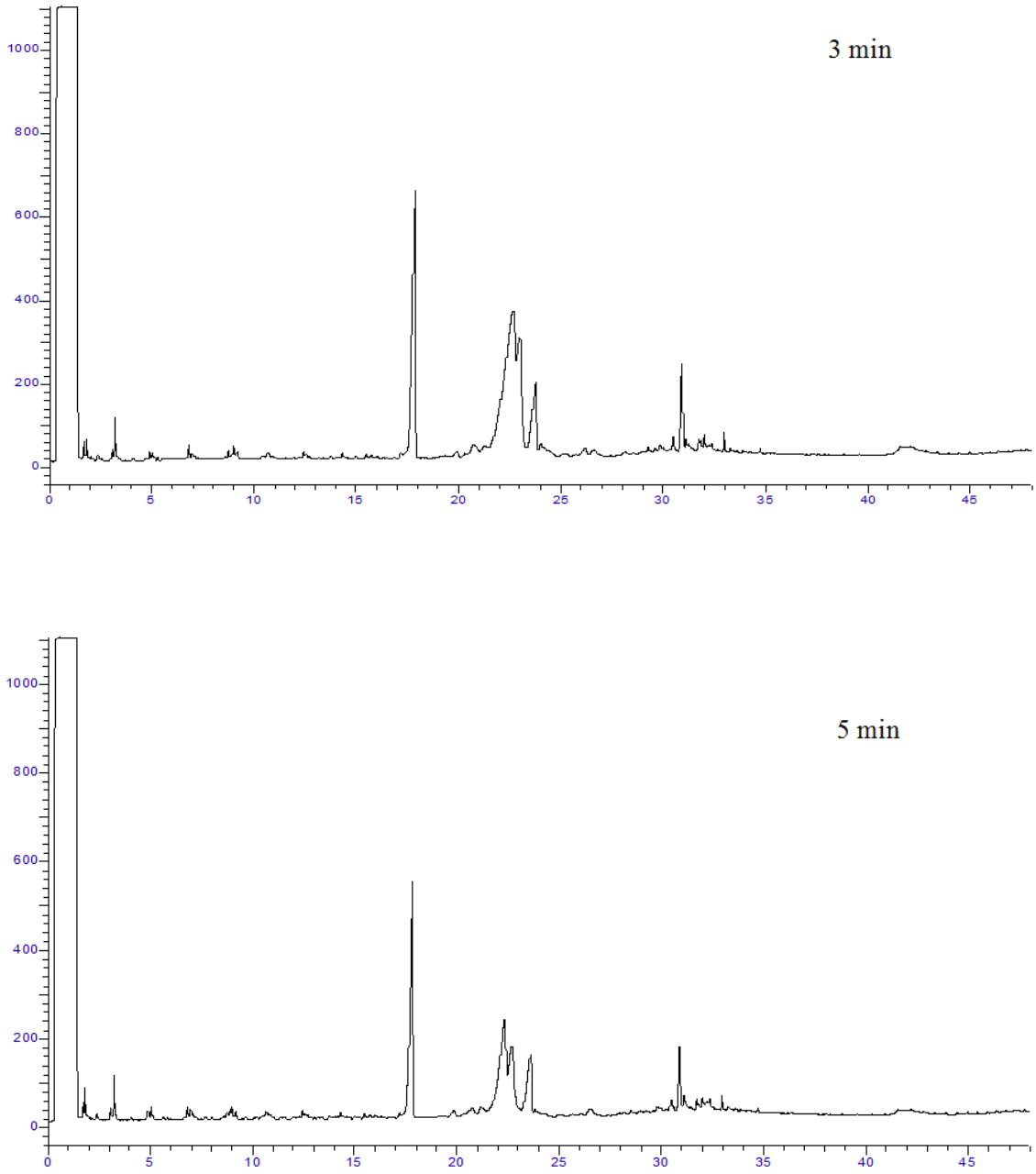

Fig.A- 26 GC-FID plot of FAEE biodiesel thermal stressed at 400 ˚C for 3 and 5 min.

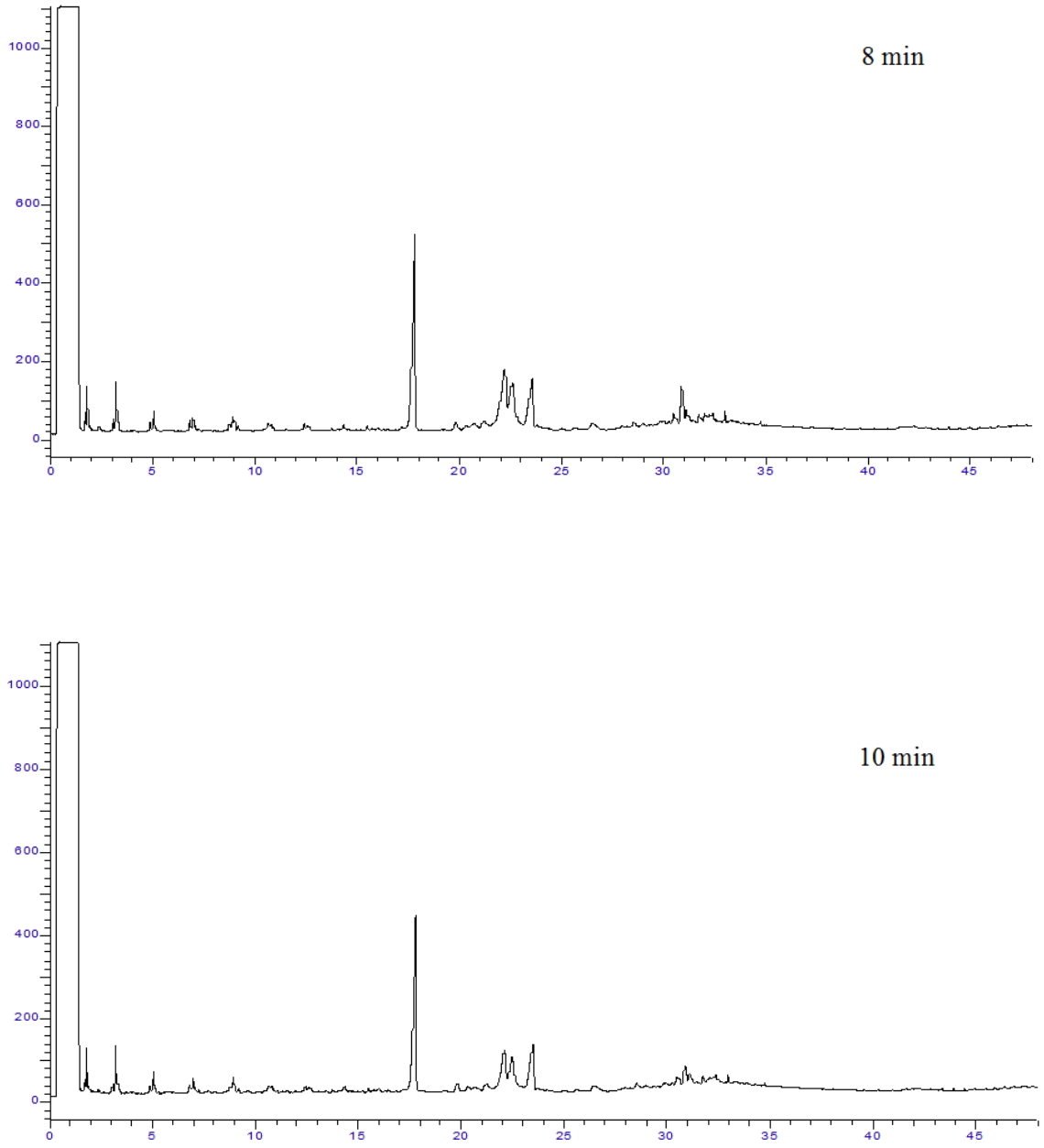

Fig.A- 27 GC-FID plot of FAEE biodiesel thermal stressed at 400 ˚C for 8 and 10 min.

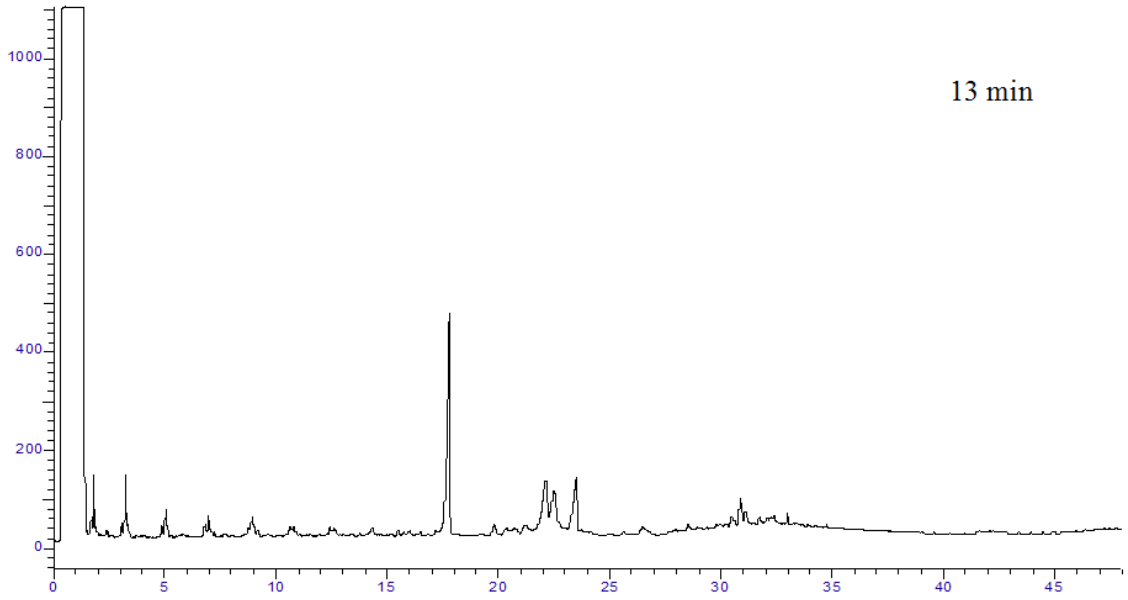

Fig.A- 28 GC-FID plot of FAEE biodiesel thermal stressed at 400 ˚C for 13 min.

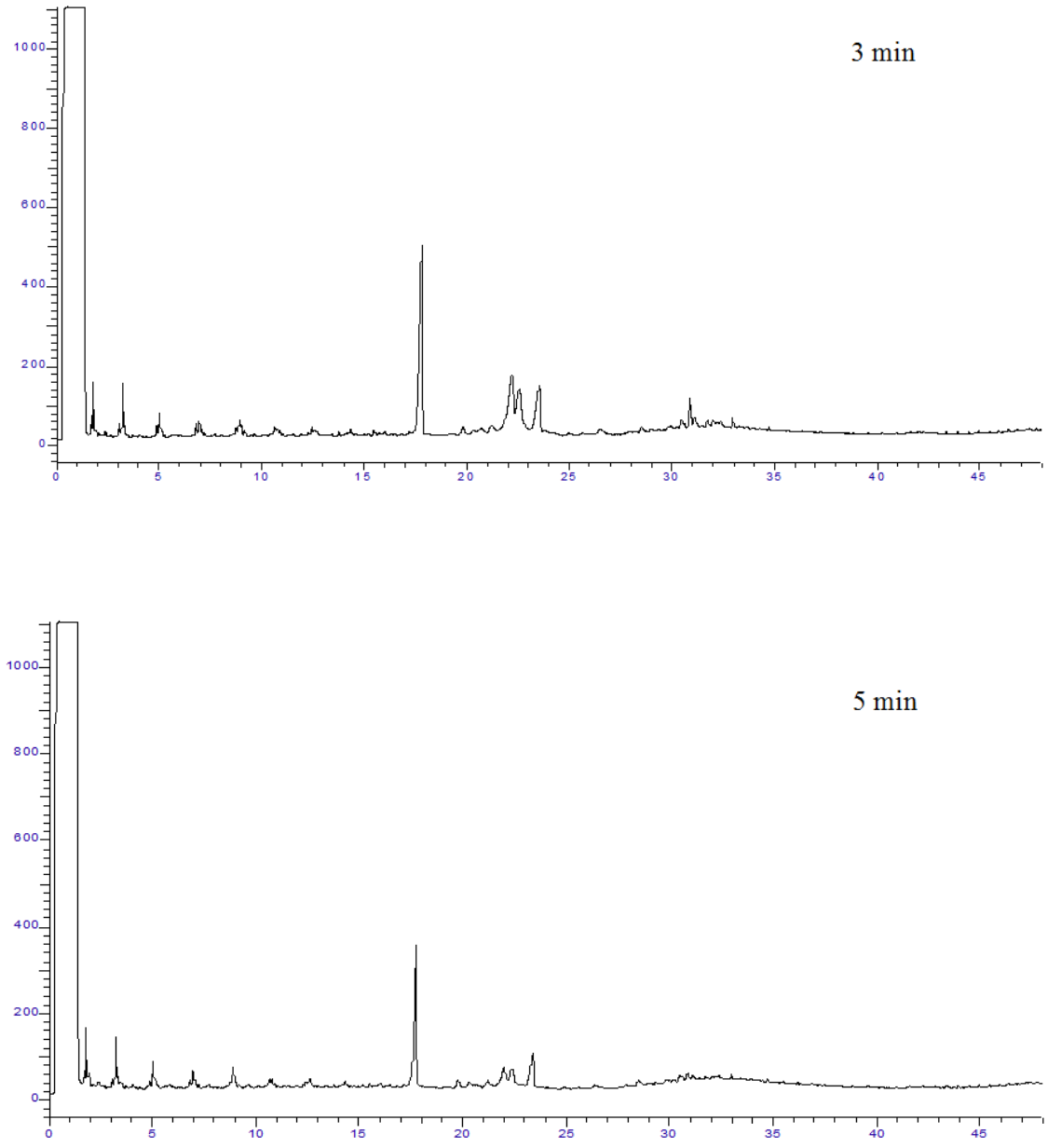

Fig.A- 29 GC-FID plot of FAEE biodiesel thermal stressed at 425 ˚C for 3 and 5 min.

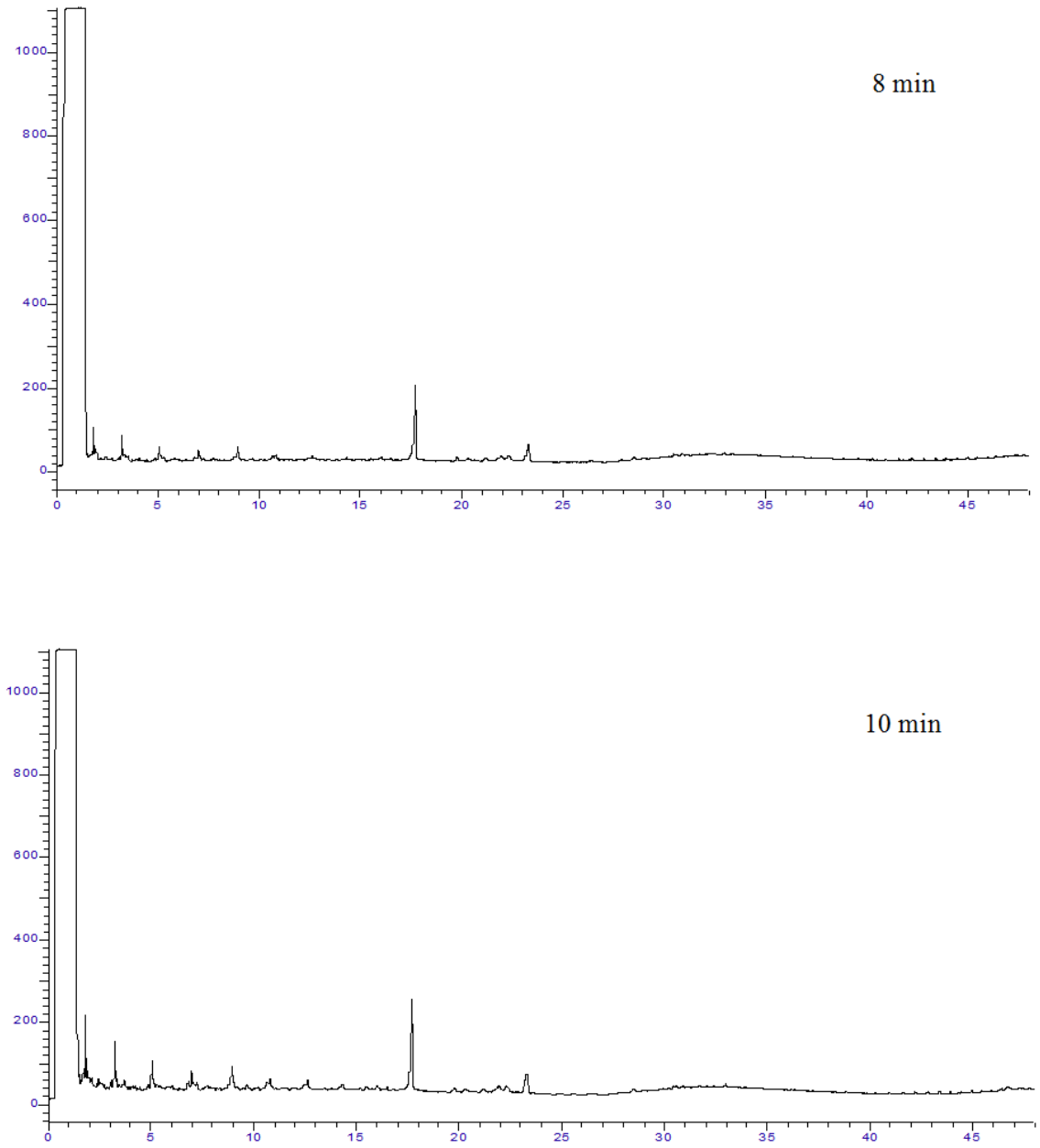

Fig.A- 30 GC-FID plot of FAEE biodiesel thermal stressed at 425 ˚C for 8 and 10 min.

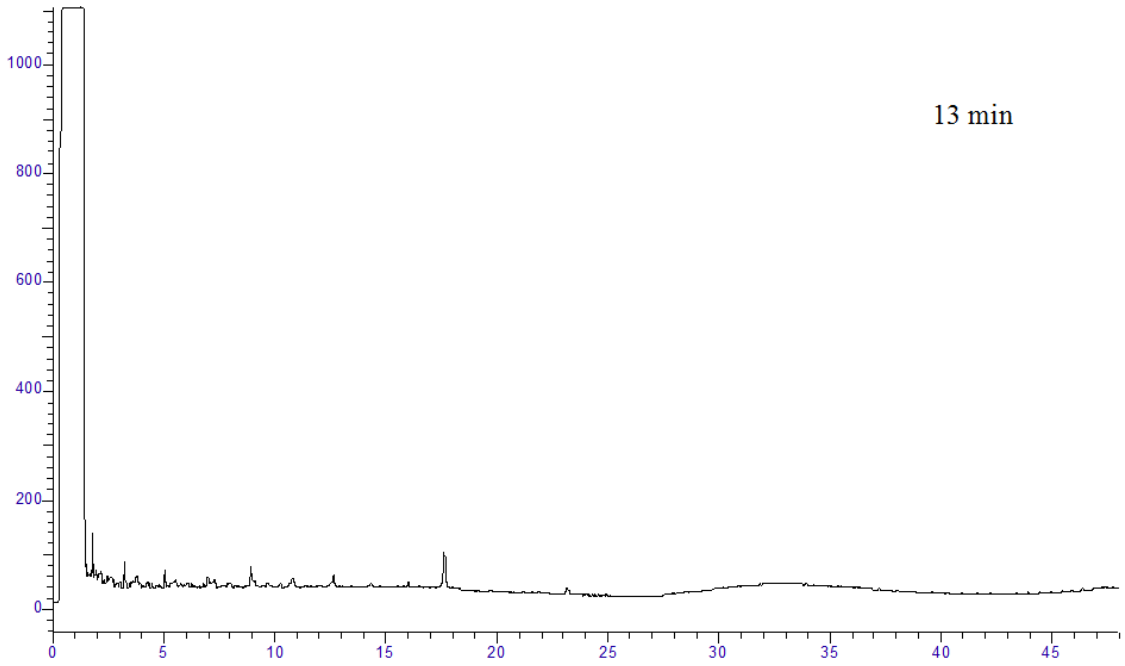

Fig.A- 31 GC-FID plot of FAEE biodiesel thermal stressed at 425 ˚C for 13 min.

Table A- 2 GC-FID peak area of pure FAEE biodiesel at different concentration

Biodiesel concentration (ppm by volume)	C16:0 peak area ($\times 10^6$)	Total peak area ($\times 10^6$)
500	2.61	20.24
1000	4.05	30.40
1500	5.14	38.53
2000	6.01	45.68
3000	8.10	62.17

Table A- 3 GC-FID peak area of thermal stressed biodiesel under different experimental conditions

Temperature (˚C)	Residence time (min)	Peak area ($\times 10^6$)	
		C16:0	Total
250	3	7.80	60.96
	8	6.96	58.04
	18	7.13	60.62
	33	7.72	58.67
	63	7.12	61.89
250 R*	3	8.06	61.31
	8	7.89	60.60
	18	7.39	60.02
	33	7.56	61.27
	63	7.59	58.47
275	3	7.67	58.34
	8	7.36	55.95
	18	7.95	60.44
	33	6.83	51.98
	63	7.32	55.67
275 R*	3	7.23	55.01
	8	7.51	57.11
	18	7.46	56.72
	33	7.04	53.54
	63	7.74	58.87

Table A- 3 (Continued) GC-FID peak area of thermal stressed biodiesel under different experimental conditions

Temperature (˚C)	Residence time (min)	Peak area ($\times 10^6$)	
		C16:0	Total
300	3	7.46	60.59
	8	7.48	60.26
	18	7.30	59.03
	33	7.87	59.62
	63	7.62	57.93
300 R*	3	7.66	60.81
	8	7.35	59.04
	18	8.03	61.04
	33	8.25	59.83
	63	7.23	54.99
325	3	7.16	56.71
	8	7.23	56.37
	18	7.77	55.15
	33	8.05	59.55
	63	7.20	42.93
325 R*	3	7.38	59.47
	8	6.90	54.62
	18	7.35	52.10
	33	5.98	43.74
	63	7.24	39.33

Table A- 3 (Continued) GC-FID peak area of thermal stressed biodiesel under different experimental conditions

Temperature (˚C)	Residence time (min)	Peak area ($\times 10^6$)	
		C16:0	Total
350	3	7.43	54.40
	8	7.11	44.81
	18	7.44	38.90
	23	7.03	37.43
	33	6.58	29.01
350 R*	3	7.02	51.80
	8	6.79	44.54
	18	7.18	44.33
	23	6.57	32.97
	33	6.98	29.20
375	3	7.60	47.52
	8	6.77	28.44
	13	6.49	23.51
	18	6.36	12.74
	23	5.04	13.35
375 R*	3	7.67	44.59
	8	6.54	33.81
	13	7.54	27.20
	18	5.63	15.04
	23	4.54	11.84

Table A- 3 (Continued) GC-FID peak area of thermal stressed biodiesel under different experimental conditions

Temperature (˚C)	Residence time (min)	Peak area ($\times 10^6$)	
		C16:0	Total
400	3	6.95	25.99
	5	5.57	17.84
	8	4.59	10.54
	10	3.71	7.99
	13	3.61	7.87
400 R*	3	6.76	27.82
	5	5.08	14.19
	8	4.69	11.21
	10	4.10	9.50
	13	4.03	8.74
425	3	4.85	12.40
	5	2.50	4.74
	8	1.17	2.04
	10	0.80	1.19
	13	0.52	0.65
425 R*	3	4.34	10.45
	5	2.47	4.54
	8	1.61	2.40
	10	1.49	2.53
	13	0.49	0.67

*R-Replicate experiments

Table A- 4 Concentration of undecomposed biodiesel under different experimental conditions

Temperature (˚C)	Residence time (min)	Concentration of undecomposed biodiesel (ppm in volume)
Untreated		3000
250	3	2929.70
	8	2912.87
	18	2925.71
	33	2913.75
	63	2861.00
250 R*	3	2908.32
	8	2901.36
	18	2851.41
	33	2927.55
	63	2905.8
275	3	2982.48
	8	2889.03
	18	2917.23
	33	2840.42
	63	2937.75
275 R*	3	2841.25
	8	2872.52
	18	2876.76
	33	2861.26
	63	2817.95

Table A- 4 (Continued) Concentration of undecomposed biodiesel under different experimental conditions

Temperature (˚C)	Residence time (min)	Concentration of undecomposed biodiesel (ppm in volume)
300	3	2885.96
	8	2866.06
	18	2791.34
	33	2717.45
	63	2687.64
300 R*	3	2899.20
	8	2791.64
	18	2852.32
	33	2791.52
	63	2581.71
325	3	2650.26
	8	2629.47
	18	2555.93
	33	2522.74
	63	1813.96
325 R*	3	2818.14
	8	2523.79
	18	2370.61
	33	2063.12
	63	1595.36

Table A- 4 (Continued) Concentration of undecomposed biodiesel under different experimental conditions

Temperature (˚C)	Residence time (min)	Concentration of undecomposed biodiesel (ppm in volume)
350	3	2510.01
	8	1928.23
	18	1569.00
	23	1479.89
	33	969.24
350 R*	3	2352.19
	8	1911.57
	18	1898.89
	23	1209.17
	33	980.27
375	3	2092.81
	8	934.22
	13	635.30
	18	614.88
	23	644.1
375 R*	3	1914.67
	8	1260.60
	13	858.83
	18	725.9
	23	517.29

Table A- 4 (Continued) Concentration of undecomposed biodiesel under different experimental conditions

Temperature (˚C)	Residence time (min)	Concentration of undecomposed biodiesel (ppm in volume)
400	3	1253.94
	5	861.03
	8	508.38
	10	385.95
	13	379.8
400 R*	3	1342.44
	5	684.51
	8	540.77
	10	458.58
	13	421.86
425	3	598.20
	5	228.72
	8	98.17
	10	57.28
	13	32.52
425 R*	3	504.46
	5	219.20
	8	115.97
	10	55.93
	13	31.57

R*-Replicate experiments

E1 - Example calculation

This example can help to explain how Fig. 23 is obtained.

Take the experimental data at 350 ˚C for 18 min as an example.

The experiments were done twice, so the total peak area measured by the software was 38.90×10^6 and 44.33×10^6, respectively. Using the calibration curve equation in Section 4.3,

$$A=1.65\times10^4C+1.31\times10^7$$

the concentration of remaining biodiesel in each experiment can be calculated as 1898.89 and 1569.00ppm. Then, the decomposition ratio of biodiesel under this experimental condition can be obtained as 36.70% and 47.70%.

Next, the average number for the decomposition ratio was used to draw Fig. 23, and the two points were used as the error bar in that figure.

Finally, the software was used to fit the data in Fig. 23, the results were shown in Fig. 24 and Fig. 25.

E2- Isomerization reactions

This example shows how isomers were determined in GC-FID plots.

First, in the GC-FID analysis, a new peak was observed when the thermal stressing temperature was 275 ˚C (Fig. 11). This peak has a very similar shape and appearance time with Ronghong Lin's work (Lin, Zhu, & Tavlarides, 2013). In their work, they showed that this peak was the isomer peak.

Second, GC-MSD was used to show more details about this peak. When comparing Fig. 18 and Fig. 6, a new peak appeared, and this new peak is determined as C18:2 9-cis, 11-trans FAEE by the GC-MSD. However, GC-FID and GC-MSD were equipped with different columns and different heating programs were used, so, subsequently, more samples were tested in this work.

Third, Fig. 19 shows that in GC-MSD plots, the peak area of this new peak increased with residence time (8, 18 and 33 min) at 275 ˚C. This tendency is the same as what was observed in the GC-FID plot of Fig. 11. The new peak also increased with the residence time.

In summary, according to these results, it can be concluded that the new peak that appeared in the GC-FID plots at 275 ˚C around 26.5 min is the C18:2 9-cis, 11-trans FAEE.

REFERENCES

Anitescu, G., Deshpande, A., & Tavlarides, L. L. (2008). Integrated technology for supercritical biodiesel production and power cogeneration. *Energy & Fuels, 22*(2), 1391-1399.

Bajpai, D., & Tyagi, V. K. (2006). Biodiesel: Source, Production, Composition, Properties and Its Benefits. *Journal of Oleo Science, 55*(10), 487-502.

Bertoldi, C., da Silva, C., Bernardon, J. P., Corazza, M. L., Cardozo, L., Oliveira, J. V., & Corazza, F. C. (2009). Continuous Production of Biodiesel from Soybean Oil in Supercritical Ethanol and Carbon Dioxide as Cosolvent. *Energy & Fuels, 23*, 5165-5172.

Bournay, L., Casanave, D., Delfort, B., Hillion, G., & Chodorge, J. A. (2005). New heterogeneous process for biodiesel production: A way to improve the quality and the value of the crude glycerin produced by biodiesel plants. *Catalysis Today, 106*(1-4), 190-192.

Bozbas, K. (2008). Biodiesel as an alternative motor fuel: Production and policies in the European Union. *Renewable and Sustainable Energy Reviews, 12*(2), 542-552.

Canakci, M., & Van Gerpen, J. (1999). Biodiesel production via acid catalysis. *Transactions Of the Asae, 42*(5), 1203-1210.

Cao, W., Han, H., & Zhang, J. (2005). Preparation of biodiesel from soybean oil using supercritical methanol and co-solvent. *Fuel, 84*(4), 347-351.

Carraretto, C. (2004). Biodiesel as alternative fuel: Experimental analysis and energetic evaluations. *Energy, 29*(12-15), 2195-2211.

Chang, C. C., & Wan, S. W. (1947). China's motor fuels form tung oil. *Industrial and Engineering Chemistry, 39*, 1543-1548.

Dantas Neto, A. A., Fernandes, M. R., Barros Neto, E. L., Castro Dantas, T. N., & Moura, M. C. P. A. (2014). Effect Of Biodiesel/Diesel-Based Microemulsions on the Exhaust Emissions Of a Diesel Engine. *Brazilian Journal of Petroleum and Gas, 7*(4), 141-153.

Demirbas, A. (2002). Biodiesel from vegetable oils via transesterification in supercritical methanol. *Energy Conversion and Management, 43*(17), 2349-2356.

Demirbaş, A. (2003). Biodiesel fuels from vegetable oils via catalytic and non-catalytic supercritical alcohol transesterifications and other methods: a survey. *Energy Conversion and Management, 44*(13), 2093-2109.

Encinar, J. M., Gonzalez, J. F., Rodriguez, J. J., & Tejedor, A. (2002). Biodiesel fuels from vegetable oils: Transesterification of Cynara cardunculus L. oils with ethanol. *Energy & Fuels, 16*(2), 443-450.

Fukuda, H., Kondo, A., & Noda, H. (2001). Biodiesel fuel production by transesterification of oils. *Journal of Bioscience and Bioengineering, 92*(5), 405-416.

Gude, M., & Teja, A. S. (1995). Vapor-Liquid Critical Properties Of Elements And Compounds .4. Aliphatic Alkanols. *Journal of Chemical and Engineering Data, 40*(5), 1025-1036.

He, H., Wang, T., & Zhu, S. (2007). Continuous production of biodiesel fuel from vegetable oil using supercritical methanol process. *Fuel, 86*(3), 442-447.

Huang, G., Chen, F., Wei, D., Zhang, X., & Chen, G. (2010). Biodiesel production by microalgal biotechnology. *Applied Energy, 87*(1), 38-46.

Huynh, L. K., & Violi, A. (2008). Thermal decomposition of methyl butanoate: ab initio study of a biodiesel fuel surrogate. *The Journal of Organic Chemistry, 73*(1), 94-101.

Imahara, H., Minami, E., Hari, S., & Saka, S. (2008). Thermal stability of biodiesel in supercritical methanol. *Fuel, 87*(1), 1-6.

Jain, S., & Sharma, M. P. (2011). Thermal stability of biodiesel and its blends: A review. *Renewable and Sustainable Energy Reviews, 15*(1), 438-448.

Ladommatos, N., Parsi, M., & Knowles, A. (1996). The effect of fuel cetane improver on diesel pollutant emissions. *Fuel, 75*(1), 8-14.

Leung, D. Y. C., & Guo, Y. (2006). Transesterification of neat and used frying oil: Optimization for biodiesel production. *Fuel Processing Technology, 87*(10), 883-890.

Lin, R., Zhu, Y., & Tavlarides, L. L. (2013). Mechanism and kinetics of thermal decomposition of biodiesel fuel. *Fuel, 106,* 593-604.

Lin, R., Zhu, Y., & Tavlarides, L. L. (2014). Effect of thermal decomposition on biodiesel viscosity and cold flow property. *Fuel, 117,* 981-988.

Liu, J., Lin, R., Nan, Y., & Tavlarides, L. L. (2015). Production of biodiesel from microalgae oil (Chlorella protothecoides) by non-catalytic transesterification: Evaluation of reaction kinetic models and phase behavior. *The Journal of Supercritical Fluids, 99,* 38-50.

Lotero, E., Liu, Y. J., Lopez, D. E., Suwannakarn, K., Bruce, D. A., & Goodwin, J. G. (2005). Synthesis of biodiesel via acid catalysis. *Industrial & Engineering Chemistry Research, 44*(14), 5353-5363.

Luo, Y., Ahmed, I., Kubátová, A., Šťávová, J., Aulich, T., Sadrameli, S. M., & Seames, W. S. (2010). The thermal cracking of soybean/canola oils and their methyl esters. *Fuel Processing Technology, 91*(6), 613-617.

Ma, F. R., & Hanna, M. A. (1999). Biodiesel production: a review. *Bioresource Technology, 70*(1), 1-15.

Marchetti, J. M., & Errazu, A. F. (2008). Esterification of free fatty acids using sulfuric acid as catalyst in the presence of triglycerides. *Biomass and Bioenergy, 32*(9), 892-895.

Miao, X., & Wu, Q. (2006). Biodiesel production from heterotrophic microalgal oil. *Bioresource Technology, 97*(6), 841-846.

Nan, Y., Liu, J., Lin, R., & Tavlarides, L. L. (2015). Production of biodiesel from microalgae oil (Chlorella protothecoides) by non-catalytic transesterification in supercritical methanol and ethanol: Process optimization. *The Journal of Supercritical Fluids, 97*, 174-182.

Olivares-Carrillo, P., & Quesada-Medina, J. (2012). Thermal decomposition of fatty acid chains during the supercritical methanol transesterification of soybean oil to biodiesel. *The Journal of Supercritical Fluids, 72*, 52-58.

Prado, C. M. R., & Antoniosi Filho, N. R. (2009). Production and characterization of the biofuels obtained by thermal cracking and thermal catalytic cracking of vegetable oils. *Journal of Analytical and Applied Pyrolysis, 86*(2), 338-347.

Predojević, Z. J. (2008). The production of biodiesel from waste frying oils: A comparison of different purification steps. *Fuel, 87*(17-18), 3522-3528.

Pryde, E. H. (1983). Vegetable-Oils as Diesel Fuels - Overview. *Journal Of the American Oil Chemists Society, 60*(8), 1557-1558.

Pryde, E. H. (1984). Vegetable-Oils as Fuel Alternatives - Symposium Overview. *Journal Of the American Oil Chemists Society, 61*(10), 1609-1610.

Qi, D. H., Chen, H., Matthews, R. D., & Bian, Y. Z. (2010). Combustion and emission characteristics of ethanol–biodiesel–water micro-emulsions used in a direct injection compression ignition engine. *Fuel, 89*(5), 958-964.

Quesada-Medina, J., & Olivares-Carrillo, P. (2011). Evidence of thermal decomposition of fatty acid methyl esters during the synthesis of biodiesel with supercritical methanol. *The Journal of Supercritical Fluids, 56*(1), 56-63.

Saka, S., & Kusdiana, D. (2001). Biodiesel fuel from rapeseed oil as prepared in supercritical methanol. *Fuel, 80*(2), 225-231.

Shin, H. Y., Lim, S. M., Bae, S. Y., & Oh, S. C. (2011). Thermal decomposition and stability of fatty acid methyl esters in supercritical methanol. *Journal of Analytical and Applied Pyrolysis, 92*(2), 332-338.

Sun, Y., Reddy, H. K., Muppaneni, T., Ponnusamy, S., Patil, P. D., Li, C., Deng, S. (2014). A comparative study of direct transesterification of camelina oil under supercritical methanol, ethanol and 1-butanol conditions. *Fuel, 135*, 530-536.

Widegren, J. A., & Bruno, T. J. (2008). Thermal decomposition kinetics of the aviation turbine fuel Jet A. *Industrial & Engineering Chemistry Research, 47*(13), 4342-4348.

Zhang, Y. (2003). Biodiesel production from waste cooking oil: 1. Process design and technological assessment. *Bioresource Technology, 89*(1), 1-16.

Vita

Yujie Shen was born in Zhejiang Province, China on June 11, 1991. After graduating from high school in 2009, he entered Harbin Institute of Technology in Shandong, China. He studied Chemical Engineering there, and later he received his Bachelor's degree in 2013. In the same year, he attended Syracuse University in Syracuse, USA to continue his study on Chemical Engineering as a graduate student. In 2015, he received his Master's degree from Syracuse University.